

# **INTERACTIONS BETWEEN THE PRE-FRONTAL CORTEX AND TEMPORAL LOBE IN VISUAL WORKING MEMORY: AN EEG STUDY**

Sonia Mitchell

**MSc Bioengineering**

**Neurophysiology Lab**

**2012**

# Declaration

This thesis is the result of the author's original research. It has been composed by the author and has not been previously submitted for examination which has led to the award of a degree.

The copyright of this thesis belongs to the author under the terms of the United Kingdom Copyright Acts as qualified by University of Strathclyde Regulation 3.50. Due acknowledgement must always be made of the use of any material contained in, or derived from, this thesis.

Signed:

Date:

Project supervisors:

Dr. Campbell Reid

Prof. Bernard Conway

# Abstract

*This study considered visual working memory and the brain's ability to encode and store an internal representation of an external visual stimulus for comparison to other visual stimuli. Visual working memory relies on interactions between the visual association area of the pre-frontal cortex and the inferior temporal lobe. The primary focus of this research was to collect electrophysiological evidence of communication between these regions whilst determining the upload and download mechanisms involved in temporo-frontal interactions.*

*The experimental protocol utilised a modified sequential matching task, whereby a subject was asked to attend to a series of view-invariant fractal images, each followed by a fixation cross, the colour of which signalled the subject to either 'store' or 'ignore' the image. The participant then had to determine if subsequent images matched the stored image. This method forced the subject to give each image the same level of concentration. It was proposed that the 'store' and 'match' processes would require temporo-frontal interactions with information flowing in opposite directions, whilst the 'ignore' process would be restricted to the temporal lobe.*

*Using the standard 10/20 setup, a 64-channel electroencephalographic (EEG) system was used to record brain activity whilst the subject was engaged in the task. A classification algorithm was developed to select an optimal distribution of electrodes across the scalp. Time domain event-related potentials (ERPs) associated with the 'store', 'ignore' and 'match' processes were then calculated and compared.*

*Results confirmed the original hypothesis in that interaction between the temporal lobe and pre-frontal cortex was identified. A statistical analysis revealed differential activity within the temporal lobe indicative of the temporary storage of visual information. Synchronous activity between the temporal lobe and pre-frontal cortex was observed during image recall and match recognition processes. Finally, an ERP analysis revealed further evidence of transient activity associated with visual working memory processes.*

# Acknowledgements

I would like to extend my thanks to everyone who has helped me throughout this project. Most worthy of this gratitude is Dr. Guy Wallis of the University of Queensland, without whom, it would not have been possible to begin this work. The effort which went into the design of this project is both remarkable and comprehensive, providing the experimental paradigm on which this work was based.

Deserving of equally high praise is my project supervisor, Dr. Campbell Reid, who was also involved in its original creation. His generosity in proposing this project and facilitating its inclusion into the MSc Bioengineering degree allowed me the opportunity to pursue my passion and gain experience within the field. His support throughout this work has been admirable, providing valuable encouragement above and beyond his duty. Without his knowledge, expertise, and persistent guidance, this dissertation would not have been possible.

Of course thanks must also be given to Prof. Bernard Conway, the ubiquitous head of department, for allowing me the opportunity to conduct this work. His contributions within the department itself are indispensable, both inspiring and motivating the completion of this project.

Appreciation goes to, Evangelos Filippidis (soon to be MSc) for his invaluable assistance in the lab. Special mention should go to Choi Lau (soon to be MSc) for continuously being online, supporting and motivating the writing of this thesis. Thank you also, to all my friends within the department who have supported me and generously volunteered as participants during this study.

Finally, I am perhaps indebted to my loving boyfriend, Gavin Lawson, and equally delightful flatmate, Kit Mei Tan, for providing me with tea, wine, and encouragement.

# Table of Contents

Declaration.....	i
Abstract.....	ii
Acknowledgements.....	iii
Table of Contents.....	iv
List of Figures.....	vi
List of Tables.....	x
Chapter 1 Introduction.....	1
1.1    Behavioural Studies in Working Memory.....	2
1.1.1    The Atkinson-Shiffrin Model.....	3
1.1.2    The Baddeley and Hitch Model.....	4
1.1.3    Visual Working Memory.....	9
1.2    The Neurophysiology of Visual Processing.....	10
1.3    Electrophysiological Theory.....	13
1.3.1    Neural Origins of EEG.....	13
1.3.2    Event Related Potentials.....	16
1.4    Current Aims.....	20
Chapter 2 Review of Literature.....	21
2.1    Delay Activity in Non-Human Primates.....	22
2.2    Contextual Influence and Object Recognition.....	26
2.3    Wallis' Paradigm.....	29
2.4    Event-related Potentials.....	31
Chapter 3 Methodology.....	33
3.1    Experimental Paradigm.....	33
3.2    Participants.....	33
3.3    Experimental Design.....	34
3.4    Experimental Setup.....	36
3.5    Data Processing.....	40
3.5.1    NeuroScan.....	41
3.5.1    EEGLab.....	42

Chapter 4 Results .....	44
4.1 Subject Selection .....	44
4.2 Electrode Selection .....	46
4.3 Grand Averaged ERPs.....	55
Chapter 5 Discussion.....	66
5.1 T-score Analysis.....	66
5.2 ERP Analysis .....	70
5.3 Additional Results .....	76
5.4 Limitations of Study .....	80
5.5 Further Study .....	82
5.6 Final Note .....	88
Chapter 6 Conclusion .....	89
References .....	90
Appendix A MATLAB Script .....	96
Appendix B Electrode Selection (Cross Analysis) .....	97
Appendix C Participant Information Sheet .....	98
Appendix D Participant Consent Form.....	101

# List of Figures

Figure 1: Diagrammatic representation of Broadbent’s model of short-term memory, whereby multiple sensory inputs are stored in parallel in the S system before being transferred to the P system (Broadbent 1958).....	3
Figure 2: The Atkinson-Shiffrin memory model, comprising a range of environmental inputs feeding into unitary short-term and long-term memory stores (Atkinson & Shiffrin, 1971). .....	4
Figure 3: The original three-component working memory model, comprising of one supervisory and two subsidiary systems capable of storing information from sensory input or the central executive (Baddeley 2000). .....	5
Figure 4: An updated, multi-component model of working memory, expanded to include the episodic buffer; LTM- long-term memory (Baddeley 2000). .....	7
Figure 5: The relationship between components leading to the episodic buffer in visual working memory (Baddeley et al. 2011).....	8
Figure 6: The current multi-component model of working memory, consisting of the central executive, the episodic buffer, and subsidiary visuo-spatial sketchpad and phonological loop, with articulatory rehearsal component (Baddeley et al. 2011).....	9
Figure 7: Schematic of the visual pathways within the human brain (Martini et al. 2011)...	12
Figure 8: Representation of the flow of visual information in the ventral and dorsal streams. MST- medial superior temporal area; LO- lateral occipital, FFA- fusiform face area, PPA- parahippocampal place area (Prasad & Galetta 2011). .....	13
Figure 9: The first recording of a human EEG by Hans Berger in 1924. The lower trace indicates a time base frequency of 10 Hz and the upper trace is an EEG recording of his 15 year old son, Klaus (Berger 1929). .....	14
Figure 10: Electrical activity of a pyramidal neuron. a) Excitatory postsynaptic potentials (EPSPs) cause a flow of charged ions between positive and negative points in the cell. b) Positive ions enter the cell, causing a potential difference across the membrane. c) Charged ions flow through the cell, following electrical and chemical gradients. d) Charge flows towards the cell body, whilst outside the cell, ions flow towards the synaptic region. e) The flow of current produces a magnetic field orthogonal to the current (Zani & Proverbio 2003, p.14). .....	14
Figure 11: Standard representation of a grand averaged ERP waveform. Early components are marked green, middle ones are red, the purple P300 component typically occurs between 300 - 500 ms, followed by a late positive potential (Lithari et al. 2010). .....	16
Figure 12: Visual ERP C1 component and polarity reversal effect (Rauss et al. 2011). .....	17
Figure 13: Schematic representation of the human brain showing regions of importance and the major anatomical landmarks of the left cerebral hemisphere (adapted from Martini et al. 2011, p.473). .....	21

Figure 14: Peri-stimulus rastergrams showing neuronal activity in response to face stimulus. a) Unmasked trial - stimulus observed from 0 – 16 ms, causing activation at approximately 75 ms, which then continues for 200 – 300 ms. b) Masked trial - stimulus observed from 0 – 16 ms, causing activation, which is inhibited by a masking image from 20 – 320 ms (Rolls & Tovee 1994). .....	23
Figure 15: Sakai and Miyashita’s paired association task. Monkeys are trained to retrieve the other member of the pair associated with a cue. a) 12 sets of paired-associate fractal stimuli. b) Trials for cue 12 – note the strength of response to the cue. c) Trials for cue 12’- note the increase in delay period activity greater than the cue (Sakai & Miyashita 1991). .....	24
Figure 16: Flow diagram showing the processes involved in the recognition of objects by the ITC (Bar 2004); PFC- pre-frontal cortex, PHC- parahippocampal (within the medial temporal cortex), ITC- inferior temporal cortex, V2 & V4- regions of the visual cortex, LF- low frequency, ‘lightning symbol’- activation of representations. ....	27
Figure 17: Diagrammatic representation of the major components of visual working memory and corresponding neuroanatomy (Zimmer 2008). .....	28
Figure 18: Examples of randomly generated fractal images. a) Original stimuli used in Miyashita’s experiments (Miyashita 1988). b) Randomly generated fractal images used in Wallis’ paradigm, produced using methods described by Miyashita (Wallis 1998). .	29
Figure 19: Results of Wallis’ simulated trials. a) Average auto-correlation function showing response of cells to trained and novel image sets, indicative of the trace rule. b) Average auto-correlation function showing response of cells to trained and novel image sets, using Hebbian learning. ....	31
Figure 20: Examples of randomly generated fractal images used in the current paradigm, produced by Wallis (Wallis 1998). .....	34
Figure 21: Example sequence of trial events consisting of randomly generated images followed by fixation crosses. Corresponding event labels are illustrated below each image / cross, indicating the sequence of events; where each event lasts 750 ms and the black arrow represents the passage of time. ....	35
Figure 22: SynAmps <sup>2</sup> Quick-Cap 64-channel montage, in accordance with the International 10/20 System. ....	37
Figure 23: Location of electrode placement according to the International 10-20 System (Sanei & Chambers, 2008, pg.7).....	37
Figure 24: NeuroScan Acquire screen capture showing EEG montage with colour-coded legend corresponding to electrode impedance level. ....	39
Figure 25: Subject 9 attending to visual stimuli during the working memory task. ....	40



Figure 26: Screen capture of NeuroScan Acquire software showing continuous EEG waveform of a drowsy subject (large amplitude, slow waveform visible in the middle channels) creating a blink artefact; evidenced by a large peak in the vertical eye channel (at the bottom of the screen) and corresponding artefact in frontal channels (at the top of the screen). .....	41
Figure 27: NeuroScan Edit capture of grand averaged ERP data of event type '10'. (a) Raw data (b) 70 Hz low pass FIR filter, zero phase shifted, 96 dB/oct. ....	43
Figure 28: 64-channel montage displaying electrodes exhibiting the most significant differential activity in response to events per region (calculated by summing differential activity over all image events). ....	51
Figure 29: 64-channel montage displaying electrodes exhibiting the most significant differential activity in response to events, per region (calculated as the relative proportion of activity per region, summed over all events). ....	52
Figure 30: 64-channel montage displaying electrodes exhibiting the most significant differential activity in response to events per region (calculated as the relative proportion of activity per region, summed over all cross events). ....	54
Figure 31: Grand averaged ERP comparison of event 10 (red) against event 20 (green). ....	57
Figure 32: Grand averaged ERP comparison of event 10 (red) against event 30 (green). ....	58
Figure 33: Grand averaged ERP comparison of event 10 (red) against event 40 (green). ....	59
Figure 34: Grand averaged ERP comparison of event 10 (red) against event 50 (green). ....	60
Figure 35: Grand averaged ERP comparison of event 110 (red) against event 120 (green). ....	61
Figure 36: Grand averaged ERP comparison of event 110 (red) against event 130 (green). ....	62
Figure 37: Grand averaged ERP comparison of event 110 (red) against event 140 (green). ....	63
Figure 38 Grand averaged ERP comparison of event 110 (red) against event 150 (green). .	64
Figure 39: Comparative analysis of the PFC, electrode Fc5. a) Events 10 and 20. b) Events 10 and 30. c) Events 10 and 40. d) Events 10 and 50; with grey bars indicating regions of interest as calculated from paired t-test results.....	71
Figure 40: Comparative analysis of the centro-parietal region, electrode Cp5. a) Events 10 and 20. b) Events 10 and 30. c) Events 10 and 40. d) Events 10 and 50; with grey bars indicating regions of interest as calculated from paired t-test results.....	72
Figure 41: Comparative analysis of the temporal lobe, electrode T7. a) Events 10 and 20. b) Events 10 and 30. c) Events 10 and 40. d) Events 10 and 50; with grey bars indicating regions of interest as calculated from paired t-test results.....	73
Figure 42: Comparative study of ERP components C1 and P1 during image perception recorded from electrode O2. a) Events 10 and 20. b) Events 10 and 30. c) Events 10 and 40. d) Events 10 and 50; with grey bars indicating regions of interest as calculated from paired t-test results.....	74

Figure 43: Comparative study of ERP component N2 during image perception, with grey bars indicating regions of interest as calculated from paired t-test results. ....	75
Figure 44: Comparative study of ERP component P3a during image perception recorded from electrode Fc5. a) Events 10 and 20. b) Events 10 and 30. c) Events 10 and 40. d) Events 10 and 50; with grey bars indicating regions of interest as calculated from paired t-test results.....	75
Figure 45: Comparison of 10-40 ERP waveforms over the central and parietal regions, with grey bars indicating regions of interest as calculated from paired t-test results. ....	77
Figure 46: An idealized ERP waveform illustrating the three proposed correlates of consciousness, P1, VAN, and LP. VAN- visual awareness negativity, LP- late positivity (Adapted from Railo et al. 2011).....	78
Figure 47: Grand averaged ERPs reflecting activity over the primary visual cortex, electrode O2. a) Events 10 and 20. b) Events 10 and 30. c) Events 10 and 40. d) Events 10 and 50; with grey bars indicating regions of interest as calculated from paired t-test results..	79
Figure 48: Grand averaged ERPs reflecting activity over the centro-parietal region, electrode Cp5. a) Events 10 and 20. b) Events 10 and 30. c) Events 10 and 40. d) Events 10 and 50; with grey bars indicating regions of interest as calculated from paired t-test results. ....	80
Figure 49: Randomly generated fractal image number 109, the ‘evil Mexican god’. ....	82
Figure 50: Experimental paradigm of Kessler and Keifers visual working memory task (Kessler & Kiefer 2005).....	85
Figure 51: Time course of activation under electrodes F10 and O10 across trials, showing ERP modulation associated with various cognitive processing (Kessler & Kiefer 2005). ....	85
Figure 52: Regions of the brain implicated in the functionality of visual working memory. a) Neural substrates of visual working memory. b) Processes involved in the maintenance of internal visual representations and associated regional interaction. (Ranganath & D’Esposito 2005). ....	87
Figure 54: MATLAB script automating the filtering process within EEGLab.....	96

# List of Tables

Table 1: List of events (triggers) per trial; event labels and corresponding descriptions relative to the stimulus (blue fixation cross) and matching image.....	36
Table 2: Total number of accepted sweeps for each subject, relative to event type; subjects 3 and 9 (highlighted) were rejected due to the low number of accepted sweeps during event 40. ....	44
Table 3: Number of correct and incorrect matching and non-matching trials for each subject; subjects 8 and 12 (highlighted) were excluded due to their low accuracy during matching trials. ....	45
Table 4: Listing of event types and associated behaviour. ....	46
Table 5: Ordered listing of t-test results with the largest number of significantly different data points for each image event. ....	48
Table 6: Comparison of electrodes exhibiting the greatest significant difference with respect to event 10, including the number of standard deviations from the mean. ....	49
Table 7: Total number of electrodes for each event comparison presenting an absolute t-score greater than the absolute mean value. ....	49
Table 8: Electrode categorization with associated anatomical locations and relevant nomenclature.....	50
Table 9: Listing of the most significant electrodes per region, per image event.....	50
Table 10: Most significant electrodes, per region (calculated by summing differential activity over all image events). ....	51
Table 11: The most significant electrodes per region (calculated as the relative proportion of activity per region, summed over all image events). ....	52
Table 12: Listing of the most significant electrodes per region, per cross event. ....	53
Table 13: The most significant electrodes per region (calculated as the relative proportion of activity per region, summed over all cross events). ....	54
Table 14: Extracted from Section 4.2 (Table 9): Listing of the most significant electrodes per region, per image event. ....	67
Table 15: Extract from Section 4.2 (Table 12): Listing of the most significant electrodes per region, per cross event. ....	69
Table 16: Extracted from Section 4.2 (Table 5): The t-test results listing electrodes with the largest number of significantly different data points for each image event. ....	76
Table 17: Ordered listing of t-test results with the largest number of significantly different data points for each cross event.....	97

# Chapter 1

## Introduction

The concept of working memory has intrigued researchers for many years, with the most extensive work in this area carried out during the last few decades. Initially, research focused primarily on cognitive psychology, attempting to define and understand underlying processes involved in cognitive function by means of psychometric theory. In recent years, the field has expanded to include a neuroanatomical component, in an effort to identify specific regions of the brain associated with these functions. As a result of this, the relatively new field of neuropsychology has developed to describe psychological behaviours and processes as they relate to neuroanatomical substrates. Clinically, this is of overwhelming importance since it is now possible to assess patients who may be suffering as a result of neurological or psychiatric illness. The understanding of cognitive and perceptual abnormalities associated with visual working memory in schizophrenia may contribute to an understanding of deficits at higher levels (Haenschel & Linden 2011; Neuhaus et al. 2011). Degenerative disorders such as Parkinson's and Alzheimer's disease (Chapman et al. 2011) that may cause levels of cognitive decline are of particular relevance as in June of this year, the Scottish government reported that the number of Scots affected by dementia is expected to double over the next 25 years (Sturgeon 2012). From a sociological stand point, differences in working memory capacity have been found to vary greatly within the healthy population, and have been used as measures of predicting and improving (N. Jaušovec & K. Jaušovec 2012) general intelligence and reasoning ability.

The first chapter of this report will attempt to describe the cognitive processes involved in visual working memory, whilst presenting relevant information regarding its corresponding neuroanatomy.

## 1.1 Behavioural Studies in Working Memory

A large amount of research has been conducted over the last hundred years regarding the storage and processing of memory. Working memory originated in theories distinguishing short-term and long-term memory. In 1891, William James defined the term *primary memory* to distinguish the part of memory related to attention, conscious inspection, and introspection of the "*specious present*" (James 1891); active representations which have not yet left the consciousness are retained for a short period of time, allowing real-time awareness of a continuous experience. The remaining component, *secondary memory* was described as a permanent store of information which may be recalled to the conscious mind at any time.

It was not until the 1950's that work specifically pertaining to short-term memory began to achieve popularity and experimental data was collected. In 1956, Miller conducted experimental studies on short-term memory capacity (G. Miller 1956). During this study, he suggested a memory span of around seven active memory items, with the possibility of expanding this capacity limit by means of recoding procedures such as grouping items into "*chunks*". In 1958, a series of experiments conducted by John Brown presented a 'trace-decay hypothesis'; defining memory-span to be exceeded if the length of time between presentation and recall of a stimulus exceeds a minimum length of time required for accurate recall (Brown 1958). He proposed that the forgetting of short term memories occurs from the spontaneously decay of a *memory trace*, a neural substrate associated with retention. His subjects were asked to retain sample stimuli whilst attending and responding to subsequent stimuli. Results verified his hypothesis by showing that forgetting occurred with the addition of new stimuli. Given that the sequence of sample stimuli were well below the memory span, he suggested that trace decay was due to a lack of rehearsal and delayed recall.

A similar conclusion was reached by Donald Broadbent in a study of the effects of selective attention on immediate memory (Broadbent 1957). In 1958, Broadbent incorporated these results in the first information processing model of short-term memory (Broadbent 1958). His model showed a dichotomy whereby sensory information from multiple sources is simultaneously stored in the *S system* before being transferred to the *P system*, a limited capacity processor (Figure 1). He assumed that as the processing-capacity of the *S system* was reached, information stored in the

P system would stagnate and trace decay would occur, thus implying long-term forgetting to result as a consequence of this interference.

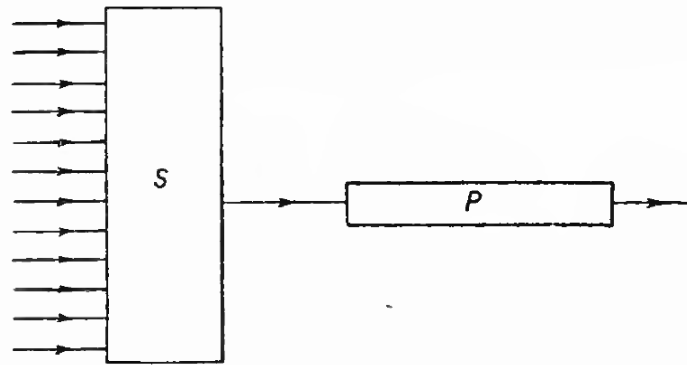


Figure 1: Diagrammatic representation of Broadbent's model of short-term memory, whereby multiple sensory inputs are stored in parallel in the S system before being transferred to the P system (Broadbent 1958).

The term “*working memory*” was coined by Miller et al. in 1960 (G. Miller et al. 1960) and was frequently referenced in works throughout the 1960's likening the mind's cognitive processes to those of a computer. What we now call working memory has recently been described by Baddeley et al. as, “... a broad framework of interacting processes that involve the temporary storage and manipulation of information in the service of performing complex cognitive activities” (Baddeley et al. 2011).

### 1.1.1 The Atkinson-Shiffrin Model

In 1968, Atkinson and Shiffrin created a model of memory known as the *modal model* (also known as the multi-memory model, multi-store model, or Atkinson-Shiffrin memory model). This three-stage memory model (Figure 2) shows information entering the system by way of the sensory register before reaching the short-term memory store (STS), and finally being transferred to the long-term memory store (LTS) (Atkinson & Shiffrin 1968). They assumed that the STS was a unitary memory store, limited in capacity and functioning as a working memory, able to utilize a variety of control processes whilst temporarily storing items for cognitive processing. Whereas, the LTS was suggested to be a relatively permanent and unlimited-capacity store, receiving information from the STS only after repeated rehearsal of the memory items. It was presumed that the longer an item was held in the STS, the more likely it would be transferred to the LTS, and a greater degree of learning achieved.

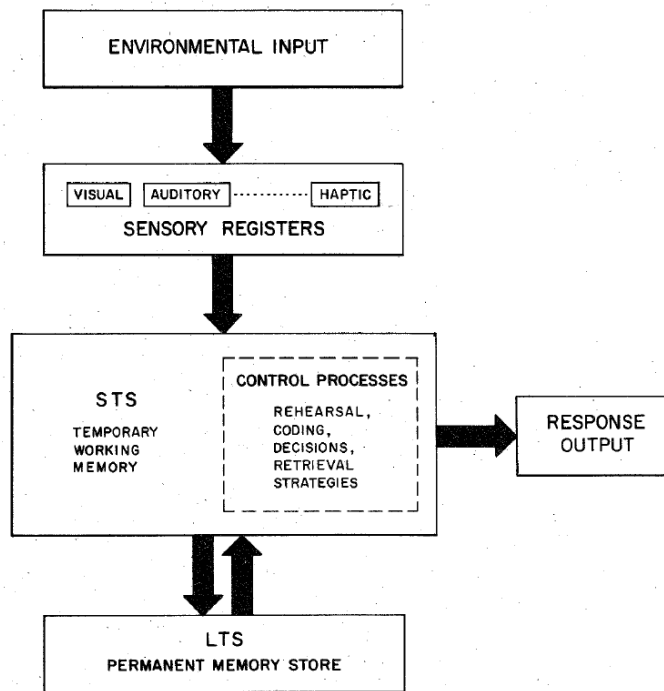


Figure 2: The Atkinson-Shiffrin memory model, comprising a range of environmental inputs feeding into unitary short-term and long-term memory stores (Atkinson & Shiffrin, 1971).

Unfortunately, little empirical evidence was collected to support these theories until 1974, when Baddeley and Hitch conducted empirical testing in an effort to directly link the STS to functional working memory (Baddeley & Hitch 1974).

### 1.1.2 The Baddeley and Hitch Model

Experimental studies focusing primarily on verbal recall showed that tasks designed to load working memory, such as reasoning, comprehension, and retrieval from the LTS had minimal effect on memory span. Considering the STS to be a limited-capacity memory store, Baddeley and Hitch concluded that working memory consists of a *workspace*, whereby the capacity is separated between storage, the *phonemic loop*, and *central executive* processing areas (Baddeley 1983): meaning that, memory span occupies a fixed area in the working memory workspace and once capacity is exceeded, space is taken up in the flexible processing areas and cognitive function impaired. Further work carried out in 1974 prompted Baddeley to expand the working memory model to include the *visuo-spatial sketchpad* (Figure 3).

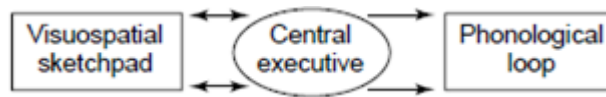


Figure 3: The original three-component working memory model, comprising of one supervisory and two subsidiary systems capable of storing information from sensory input or the central executive (Baddeley 2000).

This revised model defined working memory as consisting of subsidiary systems served by a passive sensory input store where information is maintained by active control feedback processes (Baddeley 1986). The phonemic loop (also known as the phonemic buffer, articulatory loop, or phonological loop) is a form of active memory responsible for maintaining verbal and acoustic information by repeated articulatory rehearsal, whilst the visuo-spatial sketchpad (originally known as the visuo-spatial scratchpad) is an active subsidiary system capable of retaining and manipulating representations of spatial and visual information, as well as any imagery not processed by the phonological loop (Atwood 1971). The existence of visual working memory was consistent with Philips work, in which he defined a two part system: a limited-capacity short-term memory store which is not tied to spatial position and not affected by interference; and a relatively brief, high-capacity, sensory memory store capable of retaining multiple items and spatial locations but is sensitive to interference (Philips 1974). The least understood part of working memory is the central executive, originally assumed to be an all-powerful homunculus, Baddeley's model defined it as a limited-capacity attentional control system tasked with extracting information from the subsidiary systems; signalling rehearsal of memory items, recoding and *chunking* strategies, and applying various retrieval strategies.

Unfortunately, this model is not fully comprehensive. The world around us consists of an immeasurable array of objects each differing in their constituent elements. Each object is presented to us in its own context, connected to other objects in its environment. The problem here is how the visual system binds together individual features of an object, such as shape, brightness, orientation, and movement, to form a complete image. Similar issues arise in phonological memory, how sequences of words can be bound together into chunks, by meaning, grammar, or common phrases. In 1997, Luck and Vogel attempted to tackle this problem by conducting studies on visual working memory capacity. They concluded that it was possible to retain around four items of feature-based information before threshold was reached (Luck & Vogel 1997).



Likewise, these features could be combined with four additional features when distributed across four objects, confirming Miller's earlier chunking theory whilst improving his numerical estimate (G. Miller 1956). From this, they concluded that visual working memory must be constrained by the number of integrated objects and not individual features. However, increasing the stimulus complexity to a point which exceeds a maximum limit of visual informational load decreases the number of items which can be retained in memory. Alvarez and Cavanagh postulated that this result may be due to features being encoded into separate visual memory stores, or the existence of a minimum number of fundamental features which may be increased, without increasing load, so long as the number of objects remains below four or five (Alvarez & Cavanagh 2004). Allowing additional time for encoding to take place, diminishes the effect experienced by images of high complexity, but does not remove it completely (Eng et al. 2005). Awh et al. later insisted on a return to unconstrained feature limitations, claiming that capacity limits for simple objects were equivalent to those of feature-rich conjugations, so long as test-samples were of low similarity (Awh et al. 2007). As this debate continues (Fukuda et al. 2010), there is little conclusive evidence to allow any definitive theory to be established.

Returning to the working memory model, following the work of Luck and Vogel, the assumption of a limited-capacity central executive was retracted. This was significant in that the subsidiary systems are incapable of providing enough storage for the range of functions required in working memory. The 'binding problem', or how features relating to an object – particularly those which are novel – are integrated and maintained whilst being kept separate from those belonging to other objects in working memory (Treisman 1996), was solved with the addition of a third subsidiary system, termed the *episodic buffer* (Baddeley 2000). The episodic buffer is defined as a passive limited-capacity attentional storage system theoretically capable of the temporary storage of information based on multimodal coding, integrating information into coherent episodes, or conjunctions. This multimodal buffer is hypothesised to form a link between long-term memory and the specialized subsidiary systems; temporarily storing phonological and visuo-spatial information. Binding occurs as information is combined in a unitary episodic representation, where a presumed limitation is imposed on storage capacity of around four memory items. Figure 4 shows an expansion of the tripartite working memory model with the episodic buffer becoming a significant component in the long-term accumulation of knowledge; visual semantics and

language. In this updated model, the visuo-spatial sketchpad and phonological loop remain, as before, temporary limited capacity stores, and are unaffected by learning.

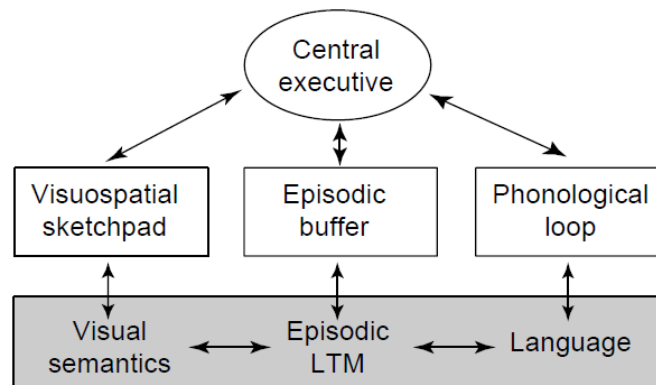


Figure 4: An updated, multi-component model of working memory, expanded to include the episodic buffer; LTM- long-term memory (Baddeley 2000).

Building on previous work conducted by Allen et al. (Allen et al. 2006), a recent study by Baddeley et al. attempted to discern the relationship between the episodic buffer and central executive in the context of binding (Baddeley et al. 2011). First, it was assumed that the buffer is accessible through conscious awareness, via the central executive, which in theory should provide enough processing power to integrate feature configurations during object binding. If this was correct, interference with *executive processes* (referring to tasks performed by the central executive component of working memory) would prevent binding. A series of experiments were carried out both visually and phonologically, disrupting various components of working memory across time, space, and modality. Findings suggested that the original assumptions were incorrect and that binding occurs automatically, independent of the central executive, within the visuo-spatial sketchpad (or phonological loop), before being fed through the episodic buffer (Figure 5). At which point, objects may be consciously retained and manipulated via signals from the central executive.

Figure 5 describes the episodic buffer component in visual working memory. In this model, it is assumed that the episodic buffer is a hierarchical visuo-spatial system containing representations at object and feature levels. Features such as colour and shape are bound within the visuo-spatial sketchpad before reaching the episodic buffer, where multimodal objects are consciously retained and manipulated; consistent with experimental studies conducted by Parra et al. (Parra et al. 2009).

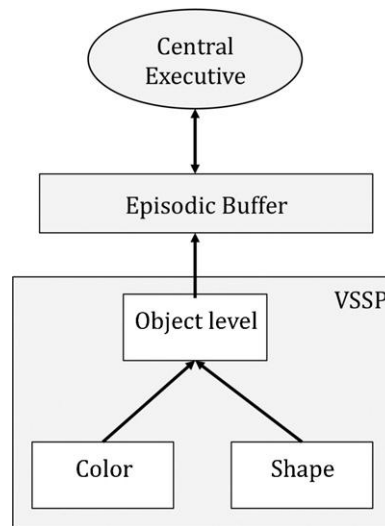


Figure 5: The relationship between components leading to the episodic buffer in visual working memory (Baddeley et al. 2011).

As discussed, the binding of visual features is a passive process occurring in the lower-level buffers with minimal input from executive resources. Although attentional resources are required for the encoding of visual features, no further resources are required during object integration. To retain an object in memory however, attention is required. It has been suggested that objects bound in this way are subject to fragility and replaced in temporary storage on exposure to further feature combinations (Allen et al. 2006). This is not the case with single-feature items such as colour or shape, since these visual properties are coded in distinct regions of the brain and therefore are not subject to feature bindings.

Recent studies by Gorgoraptis et al. (Gorgoraptis et al. 2011) further confirmed these results. Their paradigm consisted of two parts, firstly participants were asked to attend to a series of multi-feature objects, each consisting of a coloured bar presented in a particular orientation. At the end of the trial the computer would select one bar of a particular colour, asking the subject to recall its orientation from the trial. The second part of the experiment displayed each bar simultaneously, after which the computer would again select a colour and require its orientation to be reproduced. Accurate recall required binding each colour to its respective orientation. It was found that as the number of objects was increased, the probability of binding errors increased equally for both trials. Averaging these errors over serial presentation increased relative precision in comparison to trials involving a simultaneous array, showing that these results were likely due to interference caused by subsequent images rather than

temporal decay effects. A dynamic redistribution of memory was postulated, whereby attentional resources are allocated to accommodate the most recent item, increasing interference to items already held in memory.

Figure 6 shows the current version of Baddeley and Hitch's model, contiguous to the episodic buffer. This framework allows individual features to be bound in the lower-level buffers, the visuo-spatial sketchpad and phonological loop. After which, visuo-spatial, phonological, and perhaps also olfactory and gustatory information is passively bound in the episodic buffer.

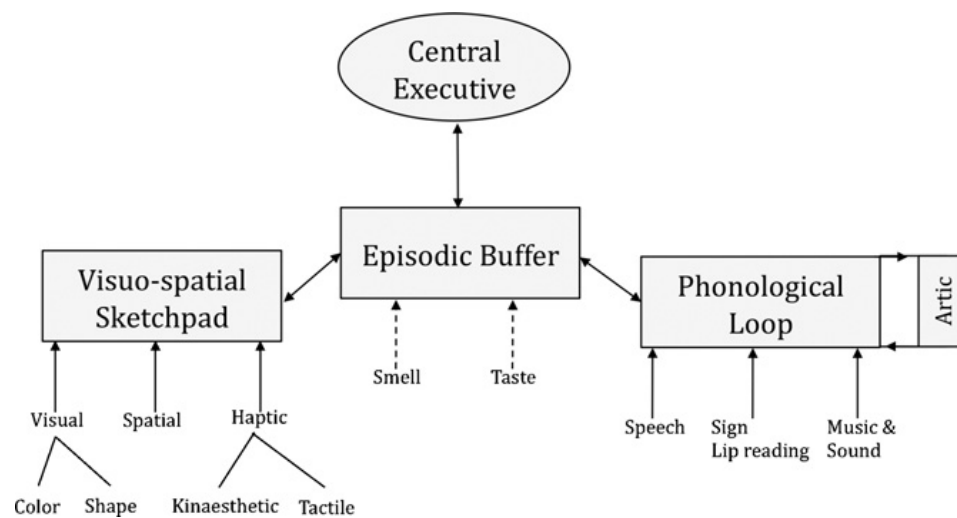


Figure 6: The current multi-component model of working memory, consisting of the central executive, the episodic buffer, and subsidiary visuo-spatial sketchpad and phonological loop, with articulatory rehearsal component (Baddeley et al. 2011).

### 1.1.3 Visual Working Memory

Visual working memory is believed to consist of two distinct subsystems; 'vision for action', the ventral stream, and 'vision for perception', the dorsal stream. The ventral stream corresponds to Baddeley's visual component (Figure 6) and underlies object recognition and features such as shape, size, and colour. Whereas the dorsal stream corresponds to the spatial component, underlying three-dimensional perception and processes required prior to movement. Since this study is concerned specifically with identifying neurological activity associated with the ventral stream, it is important to try to distinguish these processes with those associated with spatial encoding of features.

A further point of clarity would be to distinguish visual working memory from iconic memory which assists in encoding entire visual scenes for considerably shorter periods of time. Two key features of this type of memory are visual persistence and change blindness. Visual persistence depicts the length of time a stimulus remains in memory once removed from view and varies inversely with luminance and duration of exposure. Change blindness describes the inability to detect change between scenes separated by a blank inter-stimulus interval (ISI) of very short duration. Trials conducted by Becker et al. comparing change detection in continuous scenes with those containing brief intervals reaped similar results to those relating to fragility caused by interference in binding (Becker et al. 2000). A probe is either displayed within the ISI, or continuously throughout the trial, indicating which image in the array the subject should consider as having changed. The results suggested that although highly detailed visual representations are possible to maintain, these are quickly over-written by subsequent stimuli if not specifically attended to. Adjusting this paradigm to extend the interval between trials beyond the range of iconic memory, returns us to the working memory theory of binding and interference.

It is known that selective attention provides some level of protection, prolonging the binding of feature conjunctions in objects (Chun 2011). There is general agreement that this limited-capacity memory store has a limit of around four object conjunctions. Studies have shown that outside the limit of what is attended to exists what is known as fragile visual short term memory (VSTM; Sligte et al. 2008). Fragile VSTM is thought to facilitate the retrieval of iconic memory, post-stimuli, accessible from a residual memory trace of the observed scene. Although limited information may be retrieved from this store, it is believed to be of high-capacity, containing visualizations of an entire scene. As the name suggests, fragile VSTM is subject to being overwritten upon exposure to new stimuli.

## 1.2 The Neurophysiology of Visual Processing

Visual processing is a highly complex process which takes place within a series of neural systems in the brain. Visual pathways allow information to be carried to the visual cortex of the cerebral hemisphere, beginning with photoreceptors in the eye. Humans have two types of photoreceptor, rods and cones. Rods are extremely sensitive and become saturated in natural light, unable to distinguish colour. Cones contain special photopigments and can be further separated into three types sensitive to

varying wavelengths; blue, green, and red. These receptors are located on the retina, upon which an inverted visual representation of the focal object is projected. The eye is an incredibly complex sensory organ capable of processing and focusing light before encoding it. Light is focused by changing the shape of the cornea and lens via ciliary muscles through a process called *accommodation*, while the iris controls the pupil aperture to adjust the brightness of the image. Photoreceptors on the retina use the energy received from incident light to inhibit production of neurotransmitters, this electrochemical signal is dependent on the wavelength and intensity of the incident photon. Excitatory and inhibitory inputs are then relayed from photoreceptor neurons to ganglion cells, which emerge from the back of the eye at the optic disc as the optic nerve.

An incredible amount of information is carried from the retina along the 1.1 million neuronal fibres which make an optic nerve (Jonas et al. 1990). Fibres from each eye converge at the optic chiasm, at which point axons from the nasal ganglion (medial side) crossover to join the temporal ganglion (lateral side) axons of the opposing eye, and proceed through the optic tract. A small number of these fibres are redirected to the diencephalon and brain stem where electrochemical signals are utilized in the regulation of autonomic control systems such as involuntary reflex mechanisms and the circadian rhythm. The remaining fibres synapse in the dorsal thalamus, on the lateral geniculate nucleus, a critical relay point which filters information being transmitted to the visual cortex. Due to the crossover in the optic chiasm, each lateral geniculate nucleus receives input from the contralateral field of vision (Figure 7).

In the final stage of the visual pathway, second-order neurons project to the ipsilateral side of the primary visual cortex (also known as the striate cortex, calcarine cortex, or V1) of the occipital lobe. The foveal (central) field of vision is represented in the posterior occipital lobe, proximal to the occipital pole, whereas peripheral vision is represented anteriorly. Accurate spatial representations of retinal inputs are preserved as *retinotopic maps* in regions V1-V4, where the left and right fields of vision of each eye are received by the left and right V1 regions respectively.

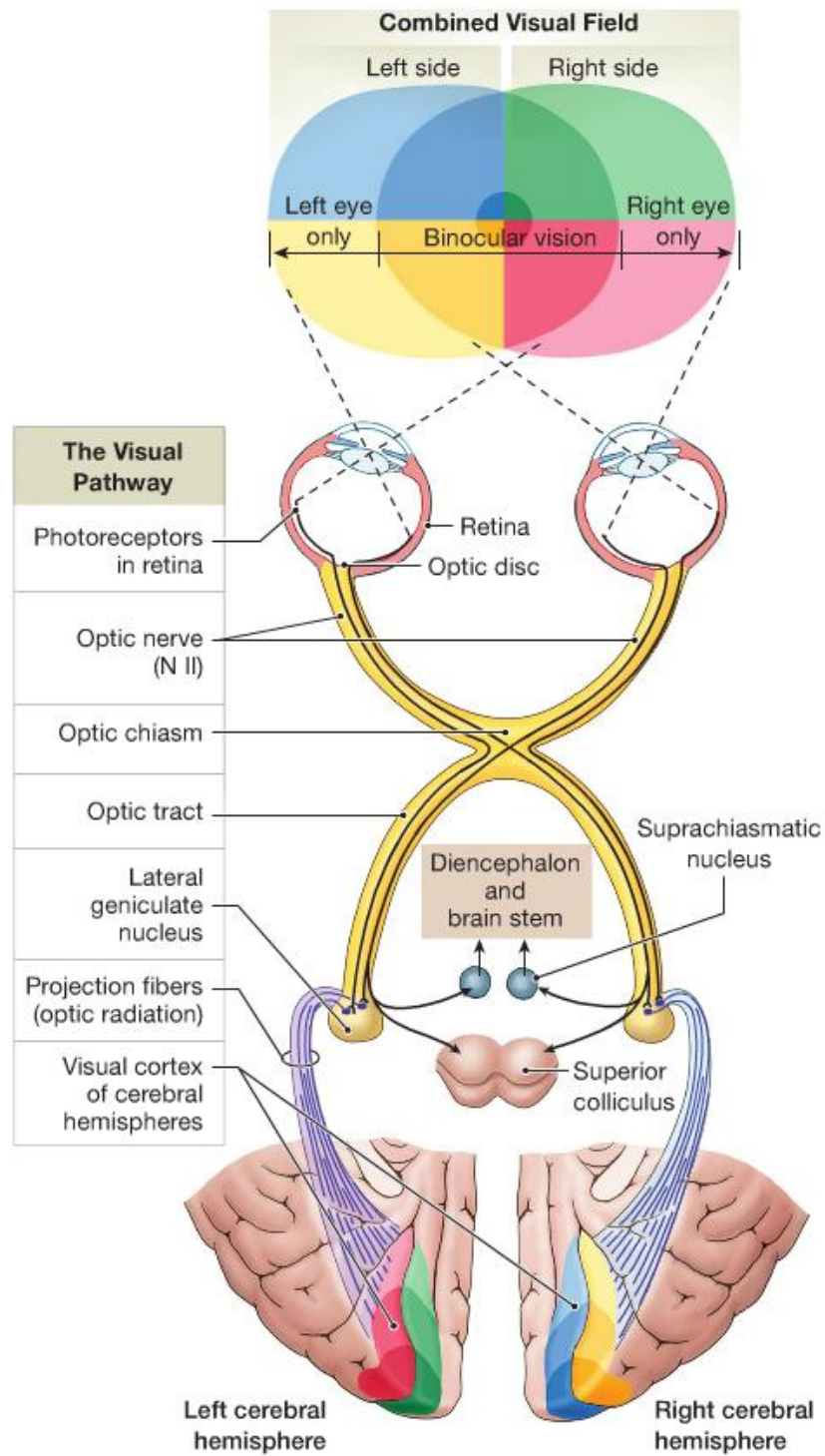


Figure 7: Schematic of the visual pathways within the human brain (Martini et al. 2011).

At this point, neurons are grouped into two major bundles which project temporal and parietal radiations into higher areas in the cortex via the ventral and dorsal streams respectively (Figure 8; Prasad & Galetta 2011). The ventral pathway (also known as the 'what' pathway) is responsible for transmitting information relating to object identify

such as colour, shape, and orientation, whereas the dorsal pathway (also known as the ‘where’ pathway’) is responsible for transmitting information relating to object location such as motion, action, and form.

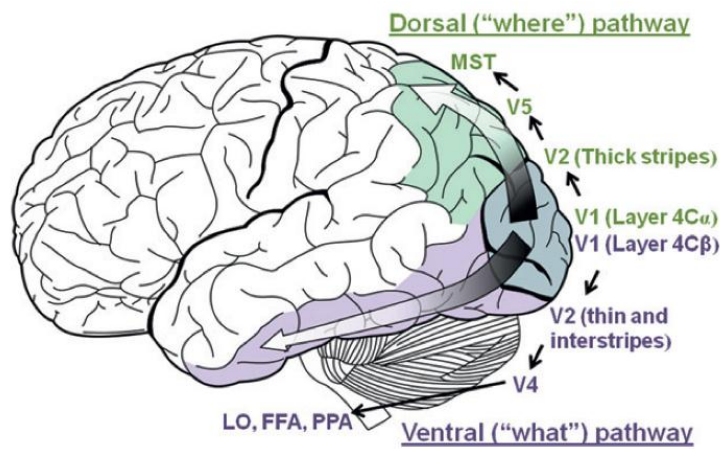


Figure 8: Representation of the flow of visual information in the ventral and dorsal streams. MST- medial superior temporal area; LO- lateral occipital, FFA- fusiform face area, PPA- parahippocampal place area (Prasad & Galetta 2011).

### 1.3 Electrophysiological Theory

In an organ as vastly complex as the brain, it is difficult to comprehend the underlying mechanisms involved in the creation, maintenance, and utilization of memory. As previously discussed, many behavioural studies have enhanced our understanding of the cognitive processes involved during memory formation, maintenance, and retrieval. Without resorting to invasive methods of neuroimaging, functional magnetic resonance imaging (fMRI) is able to provide detailed images of blood flow, allowing researchers to create three-dimensional maps of neural activity within the brain. On the other hand, techniques such as electroencephalography (EEG) are generally used when studying phenomena where a higher level of temporal resolution is desirable.

#### 1.3.1 Neural Origins of EEG

Measures of EEG have been documented as far back as 1875, where British physiologist, Richard Caton produced measurements of electrical signals in the cerebral cortex of animals (Haas 2003). However, it was not until 1924, where German neuropsychiatrist, Hans Berger, hoping to find evidence of psychic phenomena, reported EEG measurements in humans (Figure 9), in a ground-breaking paper entitled, "Über das Elektrenkephalogramm des Menschen" (Berger 1929). In the past



nine decades there have been vast improvements in data processing capabilities and methods of analysis, allowing work to continue at an extraordinary rate.

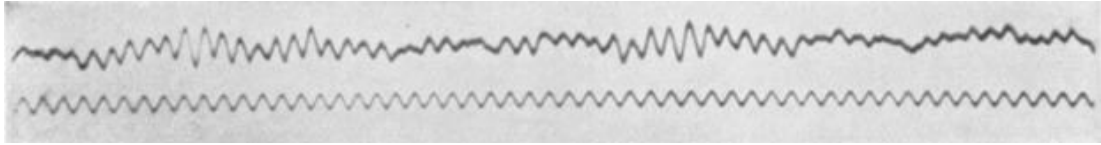


Figure 9: The first recording of a human EEG by Hans Berger in 1924. The lower trace indicates a time base frequency of 10 Hz and the upper trace is an EEG recording of his 15 year old son, Klaus (Berger 1929).

EEG is a way of recording underlying neuronal activity from the scalp. It is represented as a graph of voltage, usually microvolts, against time. Voltage is measured as the difference between two bipolar electrodes. Usually recordings are made over an array of electrodes with a common electrode reference or average reference montage. Local electric fields originating from pyramidal cells (Figure 10) in the underlying cortex generate local electric fields, which may be recorded from the scalp.

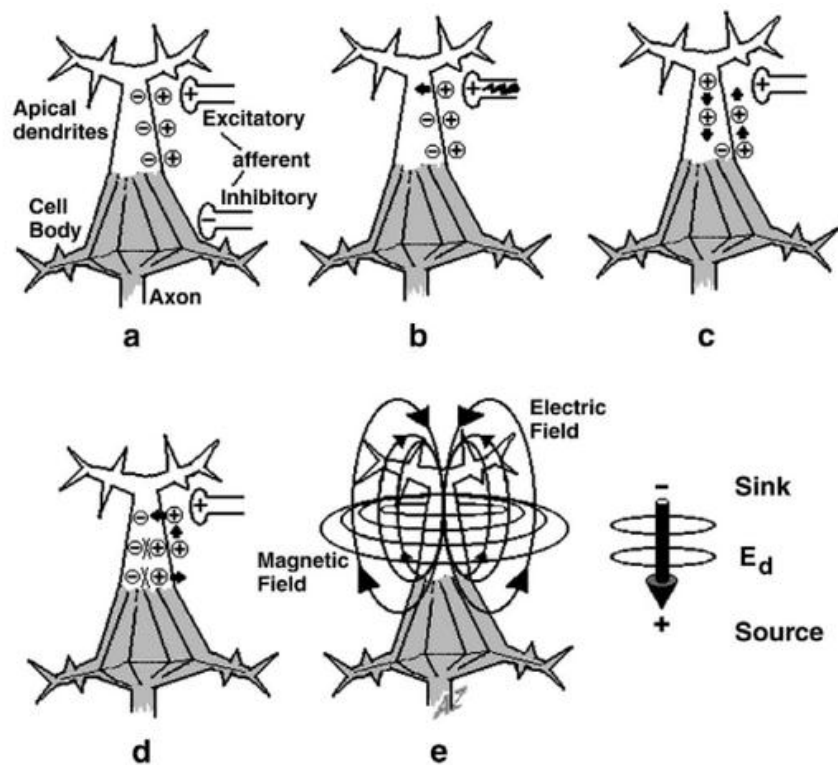


Figure 10: Electrical activity of a pyramidal neuron. a) Excitatory postsynaptic potentials (EPSPs) cause a flow of charged ions between positive and negative points in the cell. b) Positive ions enter the cell, causing a potential difference across the membrane. c) Charged ions flow through the cell, following electrical and chemical gradients. d) Charge flows towards the cell body, whilst outside the cell, ions flow towards the synaptic region. e) The flow of current produces a magnetic field orthogonal to the current (Zani & Proverbio 2003, p.14).

The human brain is made up of grey and white matter. White matter constitutes the main mass of the brain, consisting primarily of glial cells and myelinated axons which allow almost instantaneous transmission of signals between different regions of the hemispheres and lower brain structures. Surrounding this is a highly convoluted layer of grey matter which forms the cerebral cortex. Due to the complex topology of this surface, the population of neuronal constituents is extraordinarily vast with an average neuronal density of approximately 10 neurones per  $0.001 \text{ mm}^3$  (Cooper et al. 1974, p.4). It is also due to this property that EEG encounters its first problem. Surface measurements from the scalp record local electrical current which may be generated within convolutions and fissures on the cortex, making anatomical localization of the source difficult. Although it is not possible to obtain signals from individual neurones with great precision without moving towards more invasive measures, the temporal recordings obtained from online EEG is remarkable.

Originally thought to originate from nerve action potentials, local electrical currents are primarily generated by neuronal inhibitory and excitatory postsynaptic potentials which are relatively long in duration. The summation of postsynaptic potential changes, received from multiple dendritic fibres alters the potential difference across the cell membrane. If the change in potential is great enough, ionic-channels are activated, allowing positively charged sodium ions to enter the cell. An action potential discharges throughout the cell, propagating to other nerve fibres and transmitting information. Action potentials, although much greater in amplitude, are much shorter in duration than the postsynaptic potentials which bear greater resemblance to signals measured using EEG (Fisch 1999, p.3). It is also known that action potentials are less able to penetrate extracellular space and therefore could not contribute to any electrical activity recorded through the scalp.

As mentioned previously, it is difficult to measure neuronal synaptic potentials generated by individual neurones. Instead, local electric currents are measured through the skull, over the scalp. Many factors, including tissue conductivity, orientation of electric fields in relation to receiving electrodes, and the conducting properties of the scalp-electrode interface may have an effect on the EEG signal. It is also necessary to be conscious of any recorded signals which are non-cerebral in origin, as these may cause artefacts and a subsequent loss of data. In order to obtain recordings specific to a neurological process, it is useful to look for evoked potentials relevant to the stimulus. These may be difficult to observe through the vastly complex range of task-irrelevant

noise present in the brain. Through experimental repetition and averaging across trials and individuals, it is possible to increase the signal to noise ratio, producing time-locked waveforms relevant to a task-related event.

### 1.3.2 Event Related Potentials

Event related potentials (ERPs) are continuous, voltage-dependent waveforms seen as positive or negative deflections from a baseline recorded prior to an event. Fluctuations in morphology, latency, duration, and amplitude of the peaks may indicate neuronal activity relative to a particular cognitive process (Zani & Proverbio 2003, p.3). ERPs are a useful means of determining the electrical activity of neuroanatomical substrates triggered by a particular cognitive function, indicating neuronal activity of the brain prior to, during, and immediately after an event. There are a number of well-established ERP components, particularly relating to sensory stimuli, cognitive function, and motor response (Bressler & Ding 2002). Pertinent to this work, various aspects of visual ERP and relevant cognitive ERP will be described henceforth.

It should be noted that auditory ERP components are defined in a similar manner to visual components, using the same notation; where P and N denote a positive or negative voltage deflection and the following number represents the latency of the peak post-stimulus (Figure 11). In the context of this work all nomenclature will relate to visual evoked potentials and ERP only.

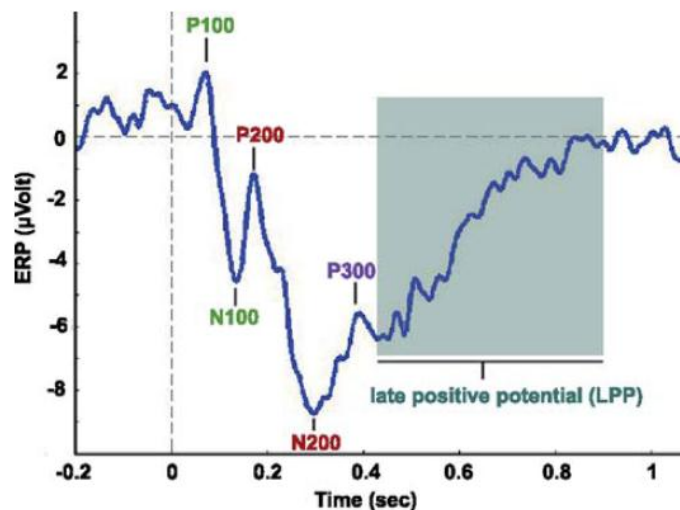


Figure 11: Standard representation of a grand averaged ERP waveform. Early components are marked green, middle ones are red, the purple P300 component typically occurs between 300 - 500 ms, followed by a late positive potential (Lithari et al. 2010).

## Far-field Potentials

The first 25 ms after stimulus onset consists of evoked *far-field* potentials. Originating within the hindbrain, these signals emerge too early to be related to any kind of sensory evaluation, but rather occur as a result of some autonomic visual response, sensitive to psychological parameters associated with the stimulus (Empson 1986, p.37).

## The C1 and P1 Components

Visual stimuli typically evoke an initial component which varies in polarity, termed C1. It is typically observed beginning 60 - 90 ms after the onset of visual stimuli, over the posterior midline sites, peaking between 80 - 100 ms. The C1 (or C100) wave is thought to be generated from the V1 region of the primary visual cortex, surrounding an anatomical landmark known as the calcarine fissure (Luck 2005). Figure 12 describes the mechanisms causing this variation in polarity. As mentioned previously, a retinotopic map characterizing the visual field is represented in V1. This image is inverted, with the lower field encoded superior to the fissure and the upper field coded inferiorly. As a consequence of this, signals recorded above the fissure are characterized by having a positive voltage deflection for the lower field, and negative for the upper field, respectively. Any stimulus horizontal to the midline is difficult to detect as it is much smaller in amplitude and tends to summate with the P1 component.

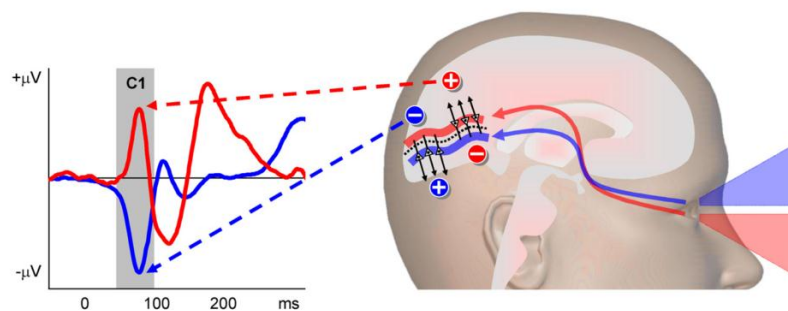


Figure 12: Visual ERP C1 component and polarity reversal effect (Rauss et al. 2011).

Following the C1 wave is the P1 (or P100) component of visual ERP and is in most cases the first observable visually-evoked peak. The P1 wave typically begins 60 - 90 ms post-stimulus, centred over the lateral occipital region, where it peaks at 100 - 130 ms. This region is home to the extrastriate cortical regions such as V2, V3, V4, and V5 (also known as MT; middle temporal), which are responsible for processes such as colour perception, spatial orientation, contour detection, and movement. Within the

first 100 ms as many as thirty distinct visual areas are activated within the cortex, each of which may contribute to the C1 and P1 waves (Luck 2005). For this reason, latency and amplitude may vary substantially, being affected by visual parameters such as contrast and spatiotemporal context (Pollux et al. 2011).

### **The N1 Component**

The N1 (or N100) wave is also related to the sensory processing of low-level features comprising the next part of the positive-negative wave complex. The latency of this component varies according to its location, peaking as early as 100 - 150 ms anteriorly, and 150 - 200 ms in the parietal and lateral occipital cortices. N1 events occurring in the lateral occipital cortices are known to be sensitive to discriminative and are generally associated with object-based spatial-attention processing (E. Vogel & Luck 2000) and inter-object similarity and recognition (Tokudome & Wang 2012). However, this ERP may be detected over most regions of the scalp, where typically a phase shift may be observed moving posteriorly from the frontal regions. A transient P2 (or P200) develops predominantly through the central and anterior sites, occurring 150 - 275 ms after stimulus presentation. It is believed to be associated with processes relating to visual search, attention, and working memory retrieval (Freunberger et al. 2007). A P2 wave may also be located in the posterior temporo-occipital regions, although little is known of it due to the difficulty in identifying its features through summation with the N1, N2, and P3 waves.

### **The N2 and P3 Components**

The N2 (or N200) potential is a cognitive ERP component which peaks maximally over the anterior scalp sites. It is most often associated with the *orienting response*, which occurs as a result of unexpected stimuli (termed *deviants*) within a series of sufficiently high frequency. The evoked response reflects reflex-like attention to the deviant (Empson 1986, p.46). If the deviants are related to the task, an N2 component is elicited, most easily observed over the posterior sites, and is again bilateral. By transferring visual objects from a temporal series to a spatial array, an N2 variant may be evoked upon detection of a deviant. The N2pc (or N2 posterior contralateral) is associated with selective attention mechanisms and is a measure of attentional-direction, occurring contralateral to the attended stimuli, with a peak latency of 200 - 300 ms (Luck 1995). In contrast, an N2 component may be observed over the parietal region. At this location, it is usually indicative of encoding and maintenance processes during visual working memory tasks (Vogel & Machizawa 2004).

Possibly the most recognized cognitive ERP component is the P3 (or P300), occurring between 300 - 500 ms post-stimulus, this waveform consists of two distinct subcomponents, the P3a and P3b. The P3 waveform is related to a large variety of neurological processes and may be elicited using a visual 'oddball paradigm'. This task employs perceptually novel *distractor* stimuli randomly inserted within a sequence. When a novelty is detected, a P3a potential is evoked within a range of 250 - 280 ms, maximally observed in the centro-frontal regions of the scalp. Increasing the similarity between distractor and target stimuli has the effect of increasing peak amplitude and therefore giving a reliable measure of task difficulty (Hagen et al. 2006). During passive stimulus processing, the P3a component remains visible, though much decreased in amplitude (Jeon & Polich 2001). On the other hand, the P3b potential may only be evoked during active processing, upon detection of an improbable task-relevant trigger. The P3b component is observed over the parietal region with a peak latency of between 250 - 500 ms. The P3b component may also be evoked to examine the effects of task difficulty and attentive load with the introduction of a secondary task (dual task paradigm). In this way, it is possible to gain a measure of processing capacity and executive mechanisms driven by attention and the maintenance of visual load in memory (Kok 2001).

### **The Late Positive Complex**

The late positive complex (LPC) is a long-lasting waveform of a few hundred milliseconds, typically peaking between 400 - 800 ms over the parietal region. Similar positive deflections have been reported in the literature such as the P3, P3b, and P600 components. The LCP is elicited during explicit memory function, particularly as part of the old/new effect, and often includes potential components similar to the N400 waveform. The N400 ERP component peaks between 200 - 600 ms at a maximal amplitude over the centro-parietal regions. The N400 usually occurs in response to meaningful stimuli across a range of modalities including semantic, auditory, visual, emotion, and recognition (Kutas & Federmeier 2011).

As well as the aforementioned visual and cognitive ERP components, there are of course a plethora of potential waveforms which may arise from cortical function associated with sensory, motor, and not previously mentioned cognitive and visual function. Although the devil is in the details, it is important to attempt to discern between each component whilst not necessarily assuming that a potential occurrence substantiates function.

## 1.4 Current Aims

This current work involves the determination of neural predicates involved in visual perception and recognition. More specifically, it is hoped to find evidence of interaction between the ITC and PFC during the upload and download of visual information. Potential distributions will be measured using 64-channel EEG recordings whilst a participant is engaged in a working memory task. A quantitative and topographical analysis of the electric field across the scalp should reveal changes in peak latency, polarity and amplitude generated as a consequence of external visual stimuli. As a task-relevant stimulus is encoded, maintained, and recalled from memory, an ERP analysis should reveal changes in activity across the scalp, indicating the neurophysiological substrates involved in such processes.

# Chapter 2

## Review of Literature

As described previously, visual working memory requires the maintenance and processing of information over a brief period of time. During this *retention period*, neural systems allow a vivid internal representation to be held for comparison to external stimuli. This process requires sustained neural activity in specific regions of the brain, which are associated with upload and download mechanisms. Evidence suggests that four main regions of the brain are associated with these mechanisms (Ungerleider et al. 1998). The posterior parietal cortex (PPC) is highly active in processes where the location of an item is relevant; the object-selective inferior temporal cortex (ITC) shows greater activity in the identification of objects; the pre-frontal cortex (PFC) shows delay-period activity sensitive to both location and identification; and the occipital lobe, particularly the primary visual cortex (PVC), shows activity associated with the perception and processing of visual stimuli (Figure 13).

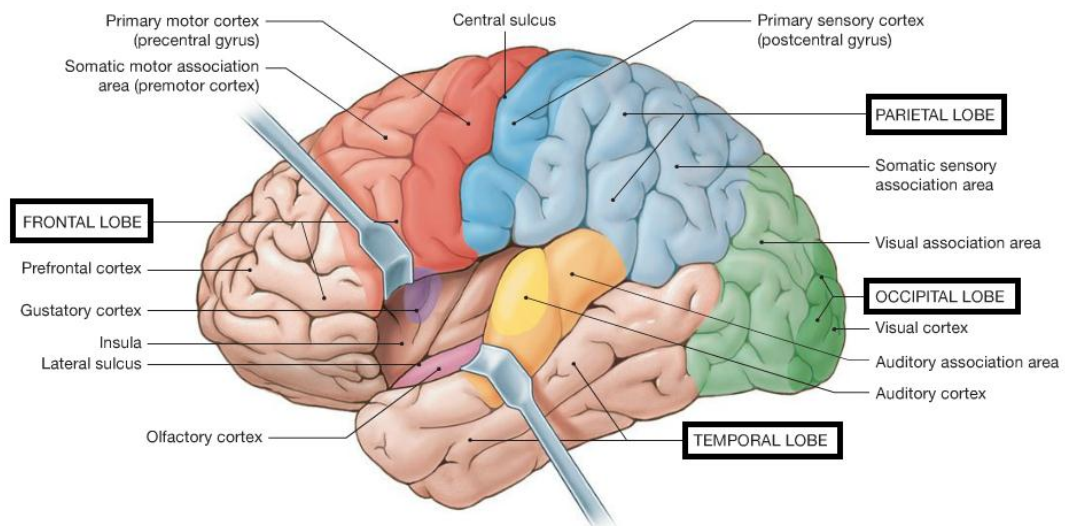


**Figure 13: Schematic representation of the human brain showing regions of importance and the major anatomical landmarks of the left cerebral hemisphere (adapted from Martini et al. 2011, p.473).**

It is worth noting that the specific functionality of these regions is difficult to determine and may in fact be responsible for multiple processes. This chapter will present a



review of current literature detailing research involved in the study of the processes involved in visual working memory and the identification of their neural correlates.

## 2.1 Delay Activity in Non-Human Primates

Much of our knowledge regarding cortical activity during visual working memory comes from single unit neurophysiological and neuroimaging studies conducted with nonhuman primates. Typically, subjects are trained to engage in a visual memory task, whereby a stimulus is presented and stored in working memory over a brief period of time, until a matching stimulus is received. The firing rates of individual neurons are recorded throughout each epoch and consistent increases in activity are observed during the retention period; this increase in activity is known as *delay activity*.

In 1982, Fuster and Jervey conducted a series of single-unit recordings in the ITC of a non-human primate performing delayed match-to-sample tasks (Fuster & P. Jervey 1982). It was observed that a large number of units displayed activity in reaction to specific coloured stimuli, denoting cell-selectivity. Moreover, delay activity was recorded and hypothesised to be a result of the temporary retention of the sample stimulus. Their work continued and in 1985 investigations were carried out into the functional interactions between the ITC and PFC regions (Fuster et al. 1985). This work consisted of a series of deactivation studies, whereby monkeys were trained to perform match-to-sample tasks whilst areas of their PFC lobes were artificially cooled. Reversible changes occurred, effectively reducing the selective colour-dependence of inferior temporal neurones. Additionally, observations were made of neuronal units responding to various processes within a trial. From these results, it was proposed that discrete processes could not be associated with specific localities, but rather multiple functions may be assigned to individual neurones. Furthermore, the reduction in neuron-selectivity implied regional interactions between the ITC and PFC, important for visual discrimination in working memory.

Several other single-unit studies have shown similar results, persistent stimulus-selective activity in the ITC, thought to be critical in the maintenance of visual object information over short delays (E. Miller et al. 1993). Furthermore, results showed an increase in neuronal firing when a match was found to a sample stimuli held in memory; this increase in activity is known as *match enhancement*. This phenomenon is observed only when a visual representation is actively maintained, whereas neuron-

selectivity is a completely passive mechanism which acts in parallel (E. Miller & Desimone 1994).

In 1994, Rolls & Tovee conducted single unit studies investigating the effect of visual masking on the processing speed of individual neurones within the ITC of macaques (Rolls & Tovee 1994). During this experiment, a face stimulus was presented for 16 ms, after which followed a delay period of variable interval, ending with a masking non-face stimulus. As with previous studies, delay activity was observed whilst the image was retained in memory. During unmasked trials, the delay activity in face-selective neurones continued for a period exceeding the length of time the face was originally presented (Figure 14a), indicating the presence of a short-term working memory store. However, during trials whereby a masking image (a non-effective stimulus for the cell) interrupted the period of delay, duration of activity varied directly with the inter-stimulus interval. Specifically, decreasing this interval to 20 ms resulted in a neuronal response of 20 - 30 ms (Figure 14b). Comparing these results with human trials, it was found that a delay period of 20 ms resulted in a 50% accuracy in facial identification, whereas a 40 ms gap produced correct results in 97% of trials (Rolls & Tovee 1994). This suggests that 20 ms is sufficient time for the PVC to process visual information sufficiently for object recognition.

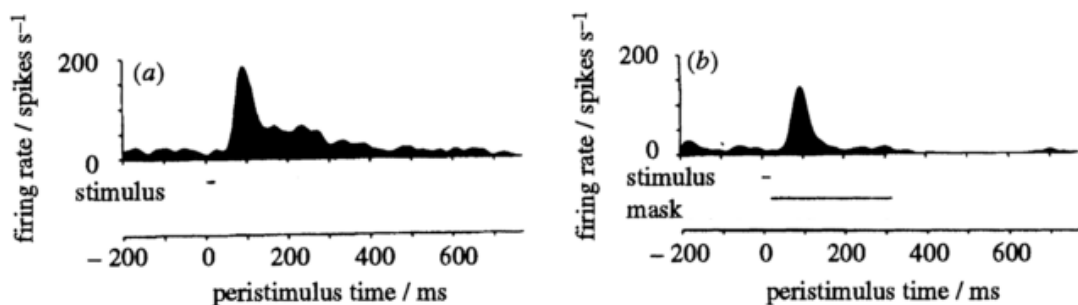


Figure 14: Peri-stimulus rastergrams showing neuronal activity in response to face stimulus. a) Unmasked trial - stimulus observed from 0 - 16 ms, causing activation at approximately 75 ms, which then continues for 200 - 300 ms. b) Masked trial - stimulus observed from 0 - 16 ms, causing activation, which is inhibited by a masking image from 20 - 320 ms (Rolls & Tovee 1994).

Work by Miller et al. in the neural mechanisms of the macaque showed that both the ITC and PFC play an important part in visual working memory (E. Miller et al. 1996). Using a delayed match-to-sample task, monkeys were trained to hold a sample stimulus in memory, through subsequent stimuli, and intermediate delays. The task was to find a match for the sample image presented earlier in the sequence. Whilst sample-selective delay activity was recorded in both the ITC and PFC, activity was disrupted in the ITC as

each new stimulus was presented, whereas in the PFC activity was maintained throughout the test. It was also found that as the trial progressed, activity in the PFC continued to increase. This suggested some level of anticipation of the matching stimuli, a characteristic known as a *prospective memory*; usually associated with the formation of intent to complete a task after a period of delay.

Previous studies by Sakai and Miyashita to assess retrieval mechanisms from long term memory identified neuronal correlates in the anterior temporal lobe (Sakai & Miyashita 1991). Monkeys were trained to complete a paired-association task whilst intracranial EEG was recorded from single unit cells (Figure 15). They observed an increase in activity in two types of cell within the anterior temporal cortex. The first they called a “*pair-recall neuron*”, it produced a selective response to specific images and their paired-associate, with lowered or null activity in response to others. The second was associated with a strong response to a cue-optimal picture (Figure 15b) with an increase in delay activity evoked by its paired-associate (Figure 15c). From these results they concluded that through associative learning individual neurones become selective to specific images. Furthermore, the observed increase in delay activity was considered to be due to some anticipatory response within the ITC, perhaps associated with the pair-recall neurones.

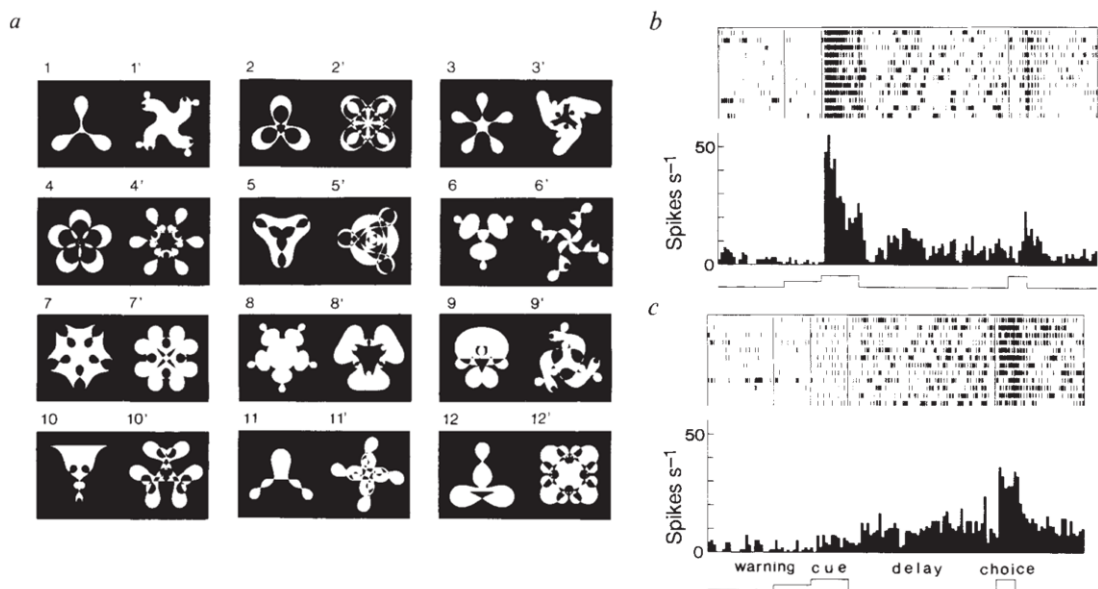


Figure 15: Sakai and Miyashita’s paired association task. Monkeys are trained to retrieve the other member of the pair associated with a cue. a) 12 sets of paired-associate fractal stimuli. b) Trials for cue 12 – note the strength of response to the cue. c) Trials for cue 12’ - note the increase in delay period activity greater than the cue (Sakai & Miyashita 1991).

Although single-unit recordings conducted on non-human primates may provide highly detailed information regarding the activity of the brain on a neurophysiological level, it is important to note that the neuroanatomical structures of these animals differ considerably from their human counterparts. For this reason a range of neuroimaging studies have been considered. Studies in humans using fMRI have shown similar results to those of single-unit studies in terms of delay activity and locality. The high spatial resolution inherent in fMRI may be used to measure local hemodynamic changes as an index of change in neural activity across the entire surface of the brain simultaneously. From this, it is possible to determine which neural systems become active during a specific cognitive function such as visual working memory.

An interesting study by Courtney et al. discusses the role of the pre-frontal cortex in working memory, focusing primarily on visual object-identity (Courtney et al. 1998). In this work, previous fMRI data was compared with single-unit monkey studies in an attempt to determine the neuroanatomical locality of various processes within the cortex. As in monkey studies, delay activity was maintained within the human PFC during visual working memory tasks. Specifically, results showed that object and spatial representations evoked sustained activity within the ventral and dorsal regions of the PFC, respectively. It has also been shown that, as in primates, delay activity originating from the PFC is typically greater than that observed in the ITC, and not subject to disruption upon presentation of new stimuli (Ungerleider et al. 1998). This suggests that the PFC may aid in maintaining an internal representation via feedback projection to posterior visual areas. This is where the monkey-human similarities end. Further domain specificity, unique to humans, detailed the inclusion of analytical representations in the left-hemisphere, with right-hemispheric maintenance of image-based representations (Courtney et al. 1998).

Thus far, evidence has been presented suggesting that visual maintenance is sustained by the activation of the PFC, ITC, PPC, and PVC. Interactions between these regions is required to support visual working memory, linking perception with higher cognitive functions involved in the maintenance and manipulation of internal representations. Immediately after an image is perceived, signals from the eye are transmitted through the optic nerve to the occipital lobe forming a retinotopic map. Within 20 – 30 ms of visual exposure, the PVC is able to process and identify the image. Studies have shown neurones to be highly selective in terms of the type of visual stimuli they respond to. If a response is evoked, a peak in activity may be observed in the temporal lobe which is

sustained long after removal of the stimulus whilst the object is held in working memory. Upon presentation of a masking image which does not provoke a response within the cell-unit, activity is disrupted. Alternatively, exposure to visual stimuli which does evoke a response replaces the previous image in the internal representation. If an image is presented in a sequential matching task, delay activity is observed within the PFC, which continues to rise in association with prospective memory and intent to match. Exposure to subsequent images should not disrupt delay activity within the PFC, whereas activity within the ITC should update intermittently as each new image replaces the previous one. The relative amplitude of activity within the PFC is thought to aid in the maintenance of internal representations within the extrastriate regions of the PVC. When an image is identified as a match, delay activity within the ITC should increase. But how is an object recognised? In order to better understand these mechanisms, thought must be given to the contextual influences surrounding perception and object identification.

## 2.2 Contextual Influence and Object Recognition

Conventional understanding dictates that visual perception is obtained in a bottom-up cascade, whereby sensory information propagates through a series of processing regions that become increasingly more complex. In 2004 however, Bar proposed a contesting model detailing a two-way mechanism engaging the PFC in the contextual facilitation of object recognition (Bar 2004).

It was suggested that information received at the visual cortex is rapidly projected to the PFC and parahippocampal (PHC; within the medial temporal cortex) regions as a blurry, low-frequency representation. The PHC identifies the contextual frame of the object, whilst the PFC identifies probable interpretations of the object itself, highlighted by attentional and foveal vision. Contextual associations and distinct object representations then intersect at the ITC resulting in a logical depiction of singular identity, which is progressively enhanced by high frequency detail projected from the visual cortex (Figure 16).

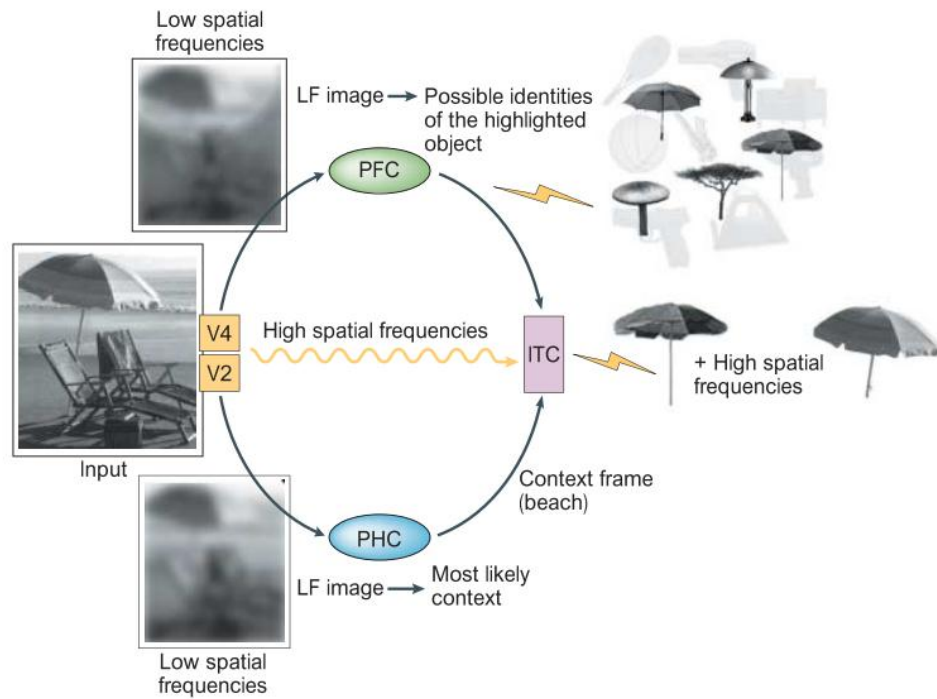


Figure 16: Flow diagram showing the processes involved in the recognition of objects by the ITC (Bar 2004); PFC- pre-frontal cortex, PHC- parahippocampal (within the medial temporal cortex), ITC- inferior temporal cortex, V2 & V4- regions of the visual cortex, LF- low frequency, 'lightning symbol'- activation of representations.

This model agrees with previous electrophysiological studies comparing the ITC and PFC of monkeys during a category matching task (Freedman et al. 2003). It was found that the ITC was involved in an online analysis of shapes, whereas the PFC was implicated in stimulus categorization, memory encoding, and match/non-match status. The ITC response was more rapid than that of the PFC, peaking as the image was observed, whereas delay activity present in the PFC was maintained after the stimulus was removed. Furthermore, visual category effects were most evident within stimulus-selective PFC regions. A minority of neuronal-units exhibited these features in the ITC, but were not maintained across the delay period. Reintroducing a relevant category item caused PFC activity to peak, whereas neuronal-firing within the ITC region, having already returned to baseline, regained its previous activity. This activity is consistent with top-down feedback illustrated in Figure 16.

Recent studies combining magnetoencephalography (MEG) with fMRI techniques allowed this model to be examined (Bar et al. 2006). By means of a visual recognition test, it was found that the PFC, specifically the left orbitofrontal complex, developed peak activity 50 ms in advance of the ITC recognition-related areas. Again substantiating the PFC facilitation of object-recognition paradigm proposed by Bar (Bar

2004). Providing further evidence to support this model, a study by Harrison and Tong presented fMRI data in an attempt to identify the mechanisms involved in image-feature retention within the PVC (Harrison & Tong 2009). Using visual classification methods, although minimal activity was sustained within these regions, it was possible to predict the orientation of a grating with a high degree of success. These results provide further evidence for the role of the PVC in early image categorisation and recognition.

Based on these findings and building, in part, on Baddeley's tripartate model (Baddeley et al. 2011), it is possible to envisage an architectural representation of the various processes involved in working memory with their corresponding substrates (Figure 17; Zimmer 2008).

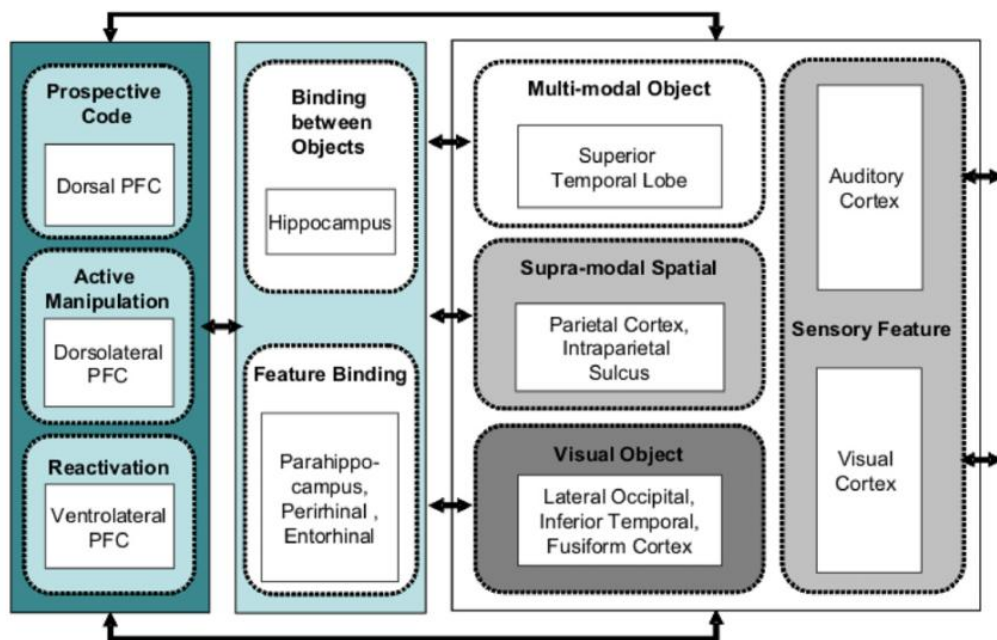


Figure 17: Diagrammatic representation of the major components of visual working memory and corresponding neuroanatomy (Zimmer 2008).

At this point, having given a detailed account of visual working memory ranging from object perception to recall mechanisms, it is considered appropriate to introduce the ground on which this current research is based.

## 2.3 Wallis' Paradigm

This study is based on Wallis' proposed model of transformation invariant recognition (Wallis 1998). During this work, he simulated neural architecture capable of testing the activation of neurones within the ITC in response to transformation invariant objects. The rationale behind this experiment was to reproduce previous results obtained by Miyashita, recording single unit activity in macaque monkeys (Miyashita 1988).

Miyashita's monkeys were required to attend to the brief presentation of a randomly generated fractal image (Figure 18a), maintain an internal representation of this image across a period of delay, and determine whether a subsequent image was a match. This experiment was performed using two image subsets of previously learned (via a repetitive *over-training* session) and unlearned stimuli. They observed that neurones within the ITC maintained activity during the delay period whilst the stimulus was retained in working memory. It was also found that for a number of neurones, response activity was increased within subsets of learned images, rather than those which were unlearned. He discovered that individual cells were able to respond to specific temporally-related stimuli and postulated neuronal selectivity was dependent on temporal relation rather than spatial similarity.

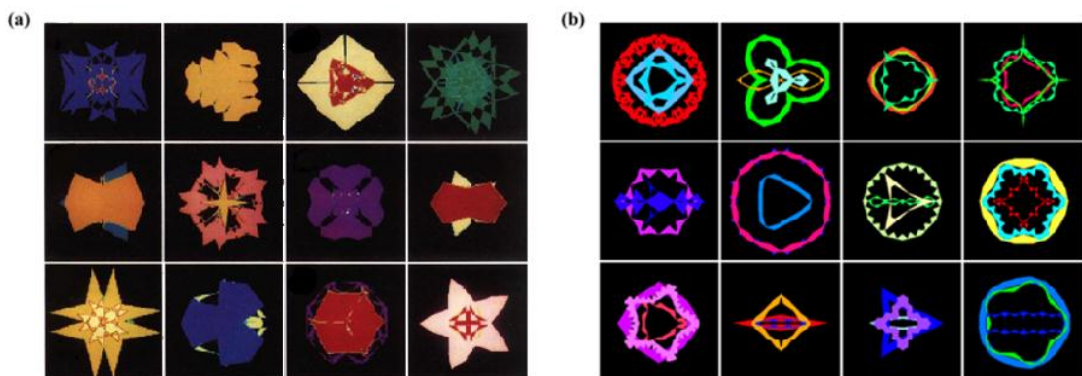


**Figure 18: Examples of randomly generated fractal images. a) Original stimuli used in Miyashita's experiments (Miyashita 1988). b) Randomly generated fractal images used in Wallis' paradigm, produced using methods described by Miyashita (Wallis 1998).**

The Hebbian learning rule suggests that repetitive and synchronous neuronal firing between cells increases their synaptic strength as cortical learning takes place. Wallis argued in favour of a revised model, suggesting that object recognition may have occurred via the trace rule, where a time-averaged value of neuronal activation replaces singular repetitive post-synaptic firing. This premise may be explained by understanding how the mind is able to identify an object which is continually changing



location, orientation, and size, relative to the observer. Evidence shows that the mind is able to store numerous representations of an object undergoing perceptual-transformation within a discrete temporal sequence (Wallis & Bühlhoff 1999). However, in Miyashita's results, the connective memory should have been disrupted by a temporal discontinuity caused by the period of delay. It may be postulated that a local temporal-overlap caused by the presentation of a secondary stimulus within the period of neuronal activity caused by the maintenance of explicit visual memory, triggers the strengthening of synaptic connections and associative neuronal selectivity.

Wallis attempted to replicate these results in order to ascertain the various processes evident within the underlying neurophysiology of the ITC during object recognition and learning. He created a neural network with which to simulate learning using fractals comparable to those created by Miyashita (Figure 18b). The network was exposed to an image which evoked a response from the neurones. After removal of the stimulus, activity was maintained, mimicking that of ITC described in previous literature. After a period of delay, the network was exposed to a second image; match or non-match. The sequence was repeated 97 times using a pre-learned set and another 97 times using a novel set.

Results matched those of Miyashita, again suggesting a temporal correlation between neuron-selectivity. Figure 19a shows the response of selective cell units to serial proximity during over-training. It can be seen that fractals within five image-steps from the stimulus exhibit a high correlation, indicating the presence of a strong temporal influence in neuron-selective associative learning (Figure 19a). Figure 19b shows the results of a second simulation undergoing training via the Hebbian rule of learning. Minimal correlation is shown within the serial position of images being learned, indicating the critical role of the trace rule underlying delay activation in individual neurones.

Using this proposed model and the methods described in Chapter 3, it is hoped to identify evidence of neuronal activation associated with the active transmission of information from the ITC to the PFC, accompanied by a passive, continuous flow in the opposing direction. The present study will assess ERP waveforms in order to differentiate these regions of activity.

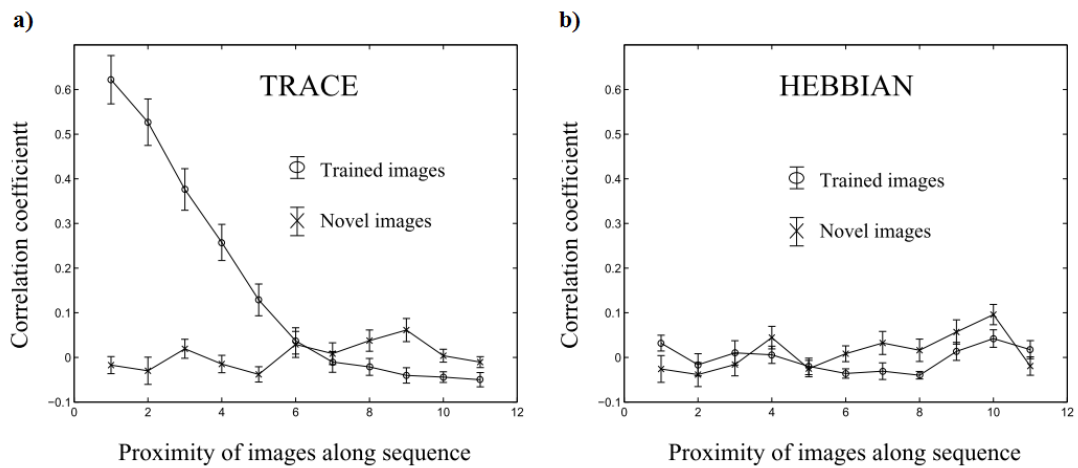


Figure 19: Results of Wallis' simulated trials. a) Average auto-correlation function showing response of cells to trained and novel image sets, indicative of the trace rule. b) Average auto-correlation function showing response of cells to trained and novel image sets, using Hebbian learning.

## 2.4 Event-related Potentials

An alternative method of evaluating delay activity during the retention period is by conducting electrophysiological measurements. McCollough et al. (McCollough et al. 2007) conducted a study whereby images were presented to a subject on a bilateral display. By recording ERPs, they observed large negative potentials at approximately 200 ms contralateral to the position of the memory items, with a delay directly proportional to the number of items to be held in memory, which became asymptotic as memory capacity was reached; 3-4 items. These results, analogous to those obtained during single unit and fMRI studies, indicated that contralateral delay activity over the posterior parietal and occipital regions may act as neural predicates of working memory maintenance related to load-capacity.

A recent study by Gjini et al. obtained 64-channel EEG recordings from subjects engaged in a 1-back visuospatial working memory task (Gjini & Maeno 2007). They obtained results comparable with other studies, verifying the involvement of the parietal cortices in spatial processing. The left superior parietal area, however, was associated with the anterior temporal and pre-frontal regions, indicating involvement in memory encoding mechanisms, predominantly activated at approximately 400 ms. The matching process appeared to correlate with activity exhibited in the left inferior parietal module.

As mentioned previously (Section 2.1), prospective memory entails the formation of intention to complete a task after a period of delay (West et al. 2001). It is hypothesised that certain parallels may be drawn between prospective memory and this task paradigm. In this instance, intention refers to the detection of a prospective memory trigger, event 120, and the realization of original intent would refer to the match itself, event 40. According to West et al. the occurrence of a relevant cue and corresponding intention formation evokes a strong phasic negative deflection, N300, peaking 300 - 400 ms post-stimulus, over the occipital-parietal region (West et al. 2001). In subsequent studies it was found that the N300 may also be observed over the fronto-polar region with a slightly delayed peak latency (West & Ross-Munroe 2002). During trials in which intention was realized negative-amplitude increased, compared to trials in which intention was not realized. The retrieval of memory associated with the initial intention was found to associate with a much broader LPC distributed over the parietal area which was not found to be affected by realization of intention. Finally, associated with the LPC was a negative slow-wave peak over the right frontal cortex, thought to be supportive of a system related to the disengagement of activity relevant to the cue.

This current study will attempt to determine a functional correlation between the ITC and PFC within a visual working memory paradigm. An EEG ERP study will be applied to human participants using Wallis' paradigm to find evidence of links between the cortical areas discussed in this review.

# Chapter 3

## Methodology

Having described appropriate background information and presented work from current literature relevant to working memory, the following chapter will detail the experimental methodology intended for use.

### 3.1 Experimental Paradigm

The purpose of this study was to establish electrophysiological evidence of neural interactions between the temporal lobe and pre-frontal cortex. Periods of heightened or lowered activity during the retention period within these regions should indicate functional connectivity during corresponding upload and download mechanisms involved in visual working memory. Task relevant responses will be examined directly using ERPs, reflecting the level of synchronous activity for a population of neurones. By examining these waveforms, it is hoped to gain some measure of the underlying activity associated with these processes. If evidence is found, a correlative investigation may reveal whether activity is driven by either the temporal lobe or the pre-frontal cortex, and if these mechanisms are unidirectional or bidirectional.

For this study, a sequential matching task was designed to be specific enough to suitably differentiate between mnemonic activity related to the trial itself and executive processes or other more general processes which may occur during the retention period; such as the expectation of memory items, arousal, attention, distraction, or the anticipation of making a response. To allow these non-mnemonic activities would ambiguate electrophysiological temporo-frontal activations occurring during the retention period, such as delay activity, concerned specifically with the storage and processing of visual stimuli. It is imperative that the experimental procedure creates precisely controlled conditions in which to collect useful data.

### 3.2 Participants

Seventeen healthy volunteers of similar age were recruited for this study. Four participants were excluded due to impedance issues and technical problems with the

equipment. Two sets of EEG data were disqualified from analysis due to excessive noise caused by movement and blink artefacts (Table 2). A further two were deemed unusable due to poor task performance (Table 3). The remaining nine subjects (4 male and 5 female) had a mean age of 27 (SD = 5.16) with normal or corrected-to-normal vision. All subjects reported no history of neurological problems or relevant visual disturbances such as colour blindness. Prior to experimentation, the procedure was explained thoroughly and written informed consent obtained.

### 3.3 Experimental Design

The task employed in this experiment was a novel modified sequential matching task. Each subject was required to attend to a series of visual stimuli presented on an 18" CRT monitor. Stimuli consisted of view-invariant fractal images, preventing recognition by familiarity or contextual cues from influencing memory and activating other parts of the brain (Figure 20). Images were displayed in a 16-colour palette against a black background to avoid ambiguity. As mentioned previously, it is also important to account for visuo-spatial working memory and so each image was displayed in the same position at the centre of the screen.

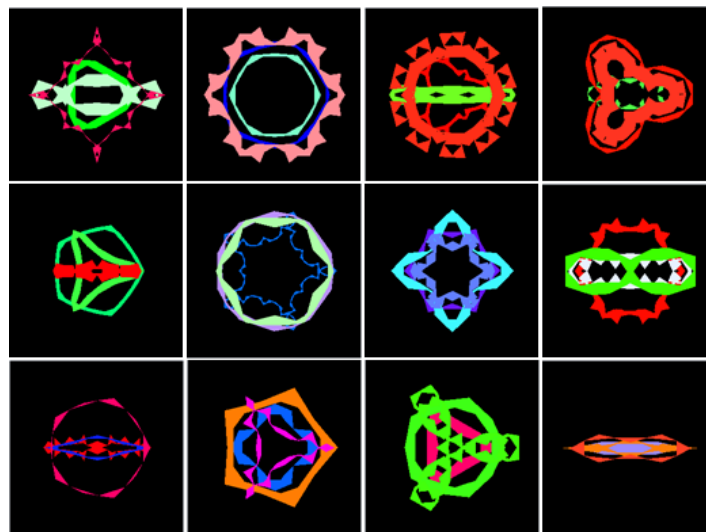


Figure 20: Examples of randomly generated fractal images used in the current paradigm, produced by Wallis (Wallis 1998).

Images were displayed for 750 ms, after which a fixation cross was displayed for a subsequent 750 ms. The fixation cross acted as an imperative stimulus, the colour of which signalled to the participant whether to 'store' or 'ignore' the preceding image, forcing the subject to maintain attention throughout the trial. Detection of a dark blue

cross (displayed only once during each trial) prompted the user to store the previous memory item and attempt to ‘match’ it with subsequent stimuli in the trial (Figure 21).

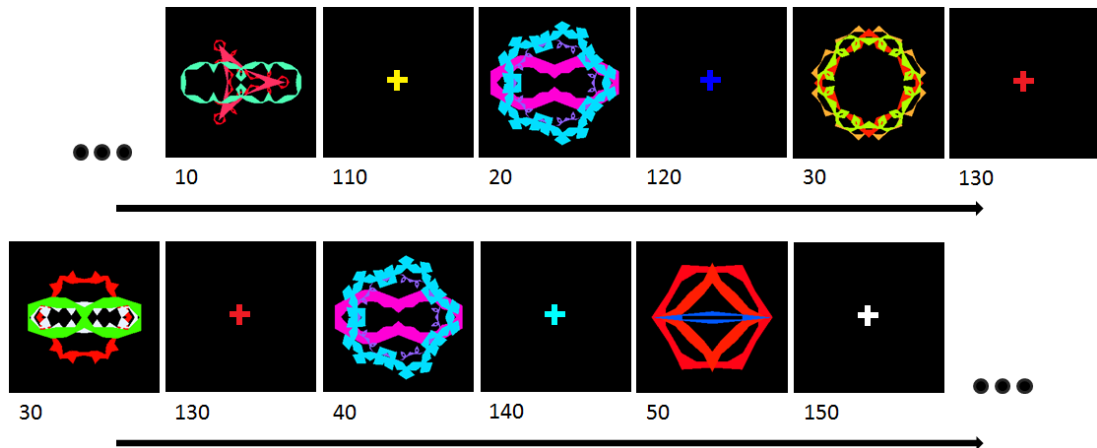


Figure 21: Example sequence of trial events consisting of randomly generated images followed by fixation crosses. Corresponding event labels are illustrated below each image / cross, indicating the sequence of events; where each event lasts 750 ms and the black arrow represents the passage of time.

Table 1 lists the various labels for every image and cross displayed during each trial. The stimulus image (to be matched) was programmed to appear randomly and with equal distribution within the first 2-6 images, with the matching image appearing between the last 8-15 images. This distribution ensured maximal attention from the subject and was designed to avoid effects due to load or serial position from biasing the data. The match appeared in only 50% of the trials, forcing subjects to give equal attention throughout the experiment.

All participants were asked to complete one study session comprising 100 single trials. Each trial began with a white fixation cross, giving the subject time to prepare for the initial image and drawing their attention to the centre of the screen. The remainder of each trial consisted of 15 images, plus 15 crosses, taking a total of 23.25 seconds including the initial white cross. A complete study session involved 100 repetitions of computer-generated random sequences, totalling 38.75 minutes excluding a period of variable pause following each trial. The period of pause gave the subject opportunity to indicate whether or not a matching image was seen; and to stretch, reposition themselves, or ask questions of the experimenter if required.

**Table 1: List of events (triggers) per trial; event labels and corresponding descriptions relative to the stimulus (blue fixation cross) and matching image.**

<b>Event label</b>	<b>Event description</b>
10	Image(s) preceding the stimulus
20	Stimulus image
30	Image(s) between the stimulus and the matching image
40	Matching image
50	Image(s) following the match
110	Cross(es) preceding the stimulus
120	Imperative stimulus (dark blue cross)
130	Cross(es) between the stimulus and the matching image
140	Cross accompanying the matching image
150	Cross(es) following the matching image
255	Indicated response from participant: "No"
254	Indicated response from participant: "Yes"

### 3.4 Experimental Setup

The task took place in a semi-darkened room, free of any distractions such as noise or movement, to avoid interference from deviant neurological activity. Participants were asked to sit in a comfortable chair and perform the memory task whilst their EEG was recorded. Two computers were set up for this experiment, one hosting NeuroScan hardware and software (Delorme & Makeig 2004), whilst another PC ran the MATLAB script that controlled the presentation of stimuli and generation of triggers to send to the Scan PC. The inclusion of triggers allowed data to be synchronised, time-locking each stimulus and response to the continuous EEG signal.

Recordings were made using the NeuroScan SynAmps<sup>2</sup> system and Acquire software (Compumedics). Also available for use were the medium and large sized NeuroScan Quick-Caps (55-59 cm and 60-65 cm respectively; manufactured by Compumedics), comprising Ag/AgCl recording electrodes pre-attached to an elasticated cap in a 64-channel montage (Figure 22). The QuickCap was fitted over the head of the participant after positioning electrode Cz at the central point on the scalp; located at the central intersection of the sagittal and coronal planes, midway between the pre-auricular points, the nasion and the inion (Sanei & Chambers, 2008, pg.7). Figure 23 shows the position of Cz in relation to these anatomical landmarks, according to the International 10/20 Electrode Placement System, as standardized by the American Electroencephalographic Society. 10/20 refers to the fact that electrodes are placed equidistantly at either 10% or 20% intervals in the transverse and median planes of the skull.

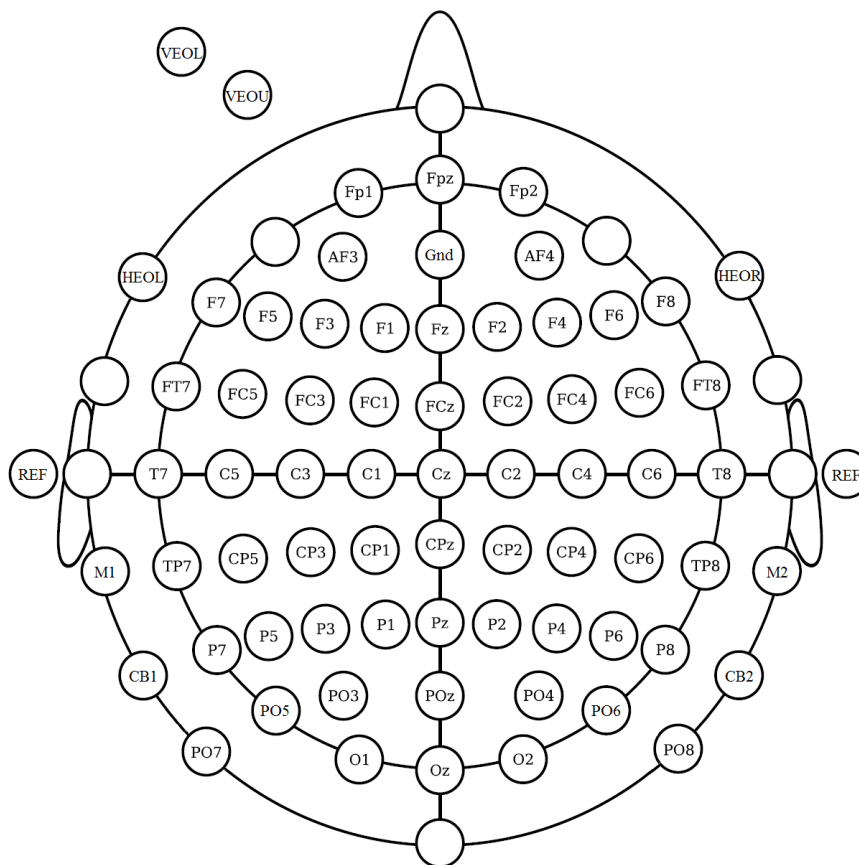


Figure 22: SynAmps<sup>2</sup> Quick-Cap 64-channel montage, in accordance with the International 10/20 System.

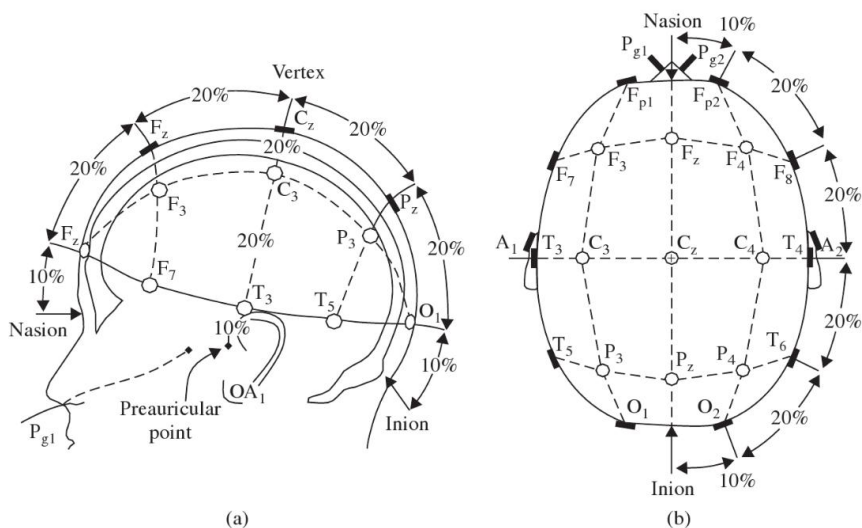


Figure 23: Location of electrode placement according to the International 10-20 System (Sanei & Chambers, 2008, pg.7).



In this particular setup, electrodes were pre-attached in a 64-channel standard 10/20 setup. In addition to the 60 primary recording electrodes, additional channels CB1 and CB2 were used to monitor head movement and jaw clenching at the back of the head. Reference electrodes were also placed on the ear lobes, with M1 and M2 attached over the bilateral mastoid processes, and a ground located between electrodes Fpz and Fz. EOG electrodes were placed superior and inferior to the left ocular orbit (VEOG), and on the outer canthi of each eye (HEOG) to monitor eye movement, blinks and associated artefacts. Prior to attaching these electrodes, the subject was prepped by abrading the skin surface using an abrasive gel (NuPrep ECG & EEG Abrasive and Prepping Gel); this cleaned the skin and removed dead skin cells, reducing the impedance of the scalp. Each reference and EOG electrode was then filled with a water soluble electrode gel (Electr-Gel, Brain Vision UK) and attached to the skin with double-sided adhesive o-rings (manufactured by EasyCap). All other recording electrodes were also filled with electrode gel after light scalp abrasion and hair follicle manipulation with a blunt needle tip (SRS needles). The purpose of the electrode gel was to match the impedance of the electrode with the impedance of the skin and to create a conductive path between the two. Care was taken to avoid injecting excessive quantities of gel into the electrode cavity as this increased the likelihood of spreading gel between adjacent positions on the scalp, integrating previously distinct EEG signals.

As shown in Figure 24, NeuroScan Acquire was used to monitor electrode impedance levels. After attaching the reference electrodes, preparing the ground, abrading the scalp, and filling each electrode with gel, the electrodes change from pink to blue/black (indicating decreased levels of impedance) according to a number of variable factors including skin type and expertise of the experimenter. It is preferable to get impedance levels as low as possible, however anything less than 10 k $\Omega$  is usually considered acceptable as long as all electrodes are of a similar impedance.

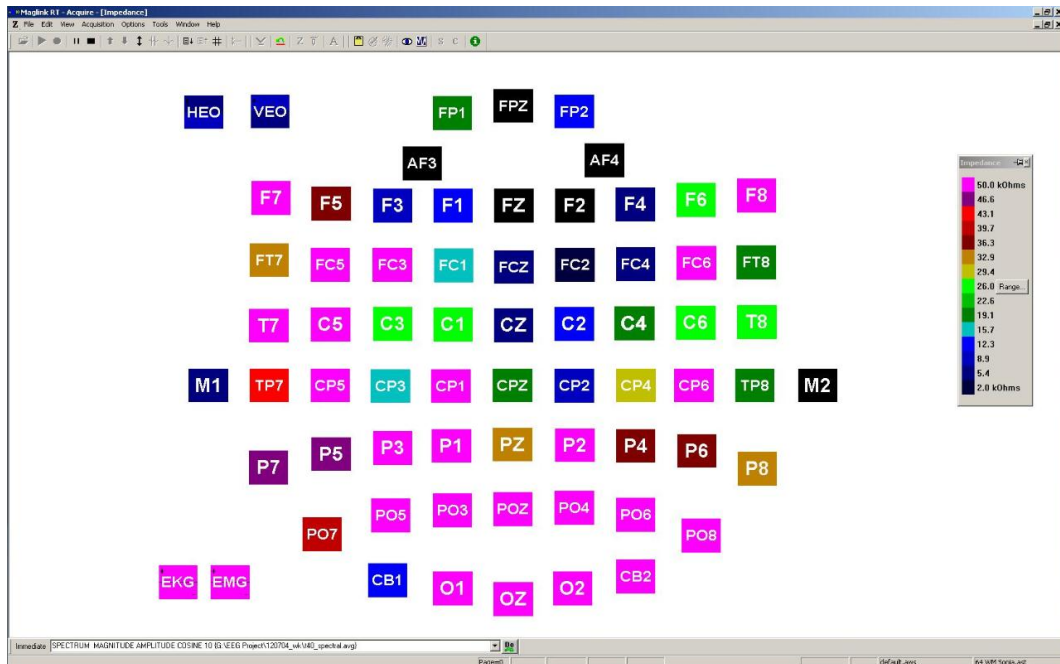


Figure 24: NeuroScan Acquire screen capture showing EEG montage with colour-coded legend corresponding to electrode impedance level.

Before beginning the experiment, participants were invited to observe their EEG data channels on the Scan PC. During this time, it was shown that any jaw clenching, blinking, or eye movement caused considerable artefact. Participants were asked to try to relax and behave as naturally as possible, rather than refraining from these actions. It was preferred that subjects attempt to direct their gaze towards the centre of the screen and hold any excessive movement until the period of variable pause at the end of each trial. The EEG recording equipment and the Scan PC were positioned behind the subject as this may have affected their performance and caused unnecessary distraction.

As mentioned previously, the rationale and methods of this study were explained to the participant prior to setup. At this point, the procedure was further clarified and participants were able to rehearse a 5-image test before beginning the study session proper (Figure 25). The primary reason for this was to give each subject opportunity to rehearse the procedure and ask any questions. Occasion was also given to ensure event triggers were being recorded correctly by the SynAmps<sup>2</sup> system.

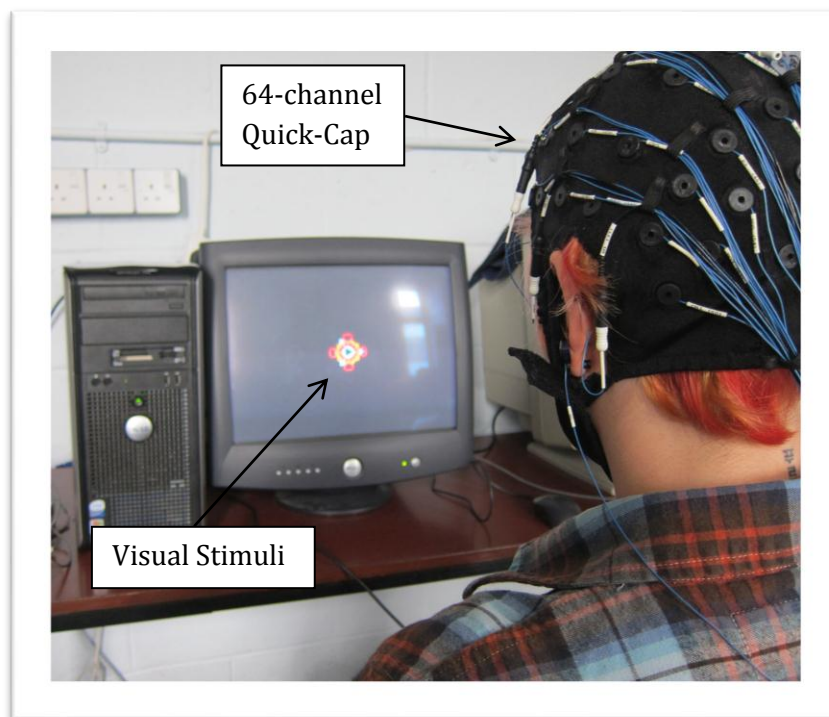


Figure 25: Subject 9 attending to visual stimuli during the working memory task.

### 3.5 Data Processing

Prior to analysis, pre-processing was required to convert the data into a manageable size and format. This was essential, not only due to computational limitations, but to aid in the detection of artefacts, and as a prerequisite for further analysis.

EEG data was recorded as a continuous waveform and amplified by the SynAmps<sup>2</sup> system, at a sampling rate of 2000 Hz, using NeuroScan Acquire software (Figure 26). Event data corresponding to each image, cross, and response was incorporated into the waveform as a visible 'trigger' received from the fractal image program. Twelve triggers were coded into the software, five triggers representing various categories of image, another five for their corresponding crosses, and two indicating a "yes" or "no" response from the participant (Section 3.3: Table 1).

A notch filter of 50 Hz was used to remove any interference which may have been caused by the mains and a DC filter was set to 500 Hz.

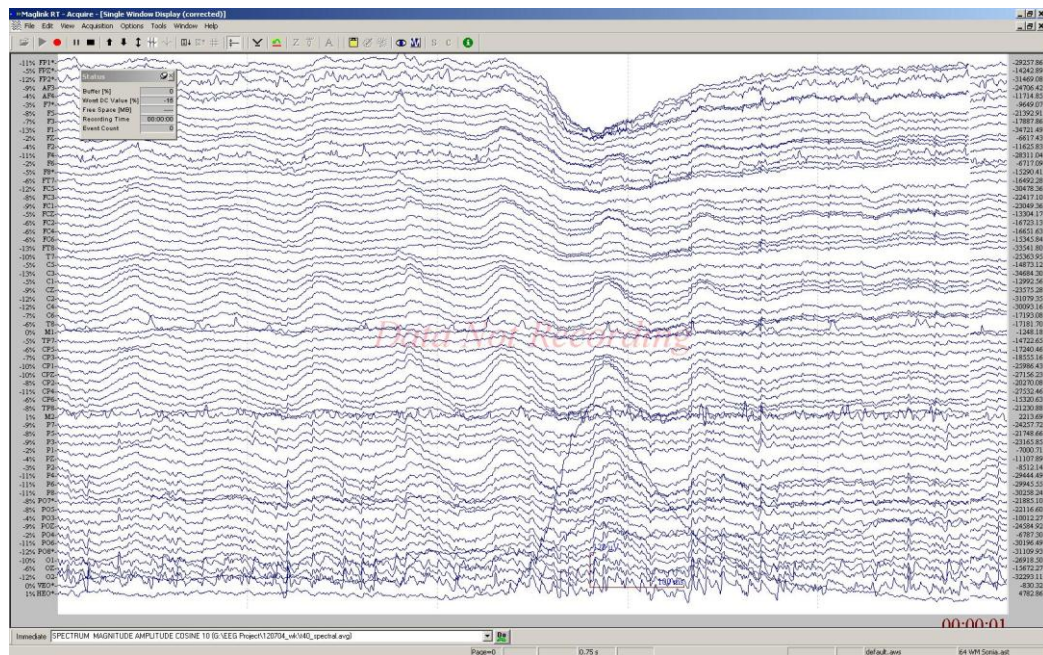


Figure 26: Screen capture of NeuroScan Acquire software showing continuous EEG waveform of a drowsy subject (large amplitude, slow waveform visible in the middle channels) creating a blink artefact; evidenced by a large peak in the vertical eye channel (at the bottom of the screen) and corresponding artefact in frontal channels (at the top of the screen).

### 3.5.1 NeuroScan

NeuroScan Edit was used to epoch the data by event type into a series of individual sweeps 0-750 ms (1501 data points) from each trigger point. After epoching the data from each subject according to event type, sweeps were baseline corrected and epochs containing artefacts such as eye blinking were rejected (Figure 26). For the majority of subjects this was done automatically using Neuroscan Edit software, by selecting electrode positions which may be affected by such artefacts: on the forehead, FP1, FPZ, and FP2; at the temples, F7 and F8; and at the back of the head, PO8 and PO7; plus the horizontal and vertical eye electrodes, HEO and VEO respectively. Automatic rejection of epochs at these positions was determined by filtering the data to exclude peaks greater than 50  $\mu\text{V}$  and less than -50  $\mu\text{V}$ . In cases where rejection criteria resulted in the majority of epochs being rejected, fewer electrodes were selected for artefact rejection, or alternative electrodes selected. In these cases, sweeps were also observed manually to discriminate unusable data.

To create event related potentials (ERPs), averages were calculated from each series of accepted single sweeps. Ten time-domain ERP averages (one for each image and cross event type) were computed for each subject, displaying the changes in voltage

amplitude over the entire epoch during each event at each electrode location. Finally, ten grand averages were computed over all nine subjects for each event type.

Figure 27a shows a measure of electrical activity recorded at electrode Fz. A visual inspection of the waveform revealed clear N1 and P2 ERP components. However, superimposed on this signal was an obvious regular artefact of unknown origin. For the artefact to appear in the averaged waveform, the signal generating it had to be time-locked to the experimental protocol. After some consideration, this signal was attributed to the refresh rate of the CRT monitor (75 Hz); the MATLAB script used to generate images used the refresh rate of the monitor to time events within each trial. It was also possible that higher frequency harmonics generated from equipment in neighbouring labs were picked up by electrodes, although these signals would not be time-locked to the task and would be cancelled out through the averaging process. Using NeuroScan Edit it was possible to remove this noise prior to averaging with a 70 Hz low pass FIR filter at 96 dB/oct (Figure 27b).

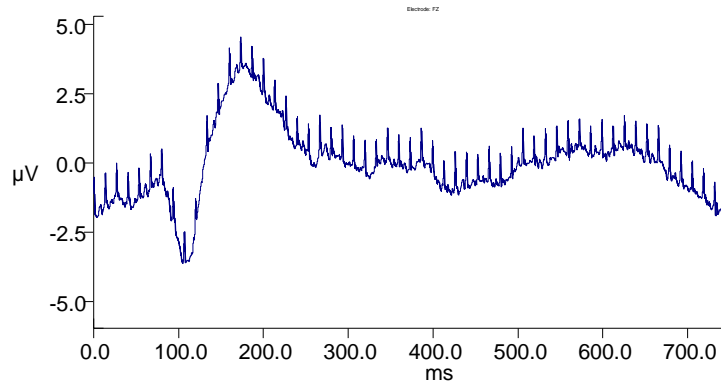
### 3.5.1 *EEGLab*

A secondary route of analysis involved using a MATLAB toolkit called EEGLab. This program was not compatible with NeuroScan's averaged \*.avg files and required epoched \*.eeg data to be imported and resaved with a \*.set extension before manipulation. Each waveform was imported at a resolution of 32 bits and associated with a specified electrode location map exported from NeuroScan. After which the EMG, EKG, CB1, and CB2 channels were removed to bring the montage down to the 64 channels used during recording. Again, each epoch was low pass filtered at 70 Hz to remove the time-locked CRT signal; for convenience a small MATLAB program was written to automate EEGLab's filter function (Appendix A).

After having correctly classified data according to event type, rejected artefacts based on specified criteria, and created individual subject averages and group level grand-averages in both NeuroScan Edit and the EEGLab toolbox, the EEG data was ready for analysis. Analysis was conducted over the time-domain, identifying regions of statistical importance using paired t-test data.

**a)** Subject: GA\_10.avg Recorded: 15:01:32 04-Jul-2012  
EEG file: GA\_10.avg Rate - 2000 Hz, HPF - 0 Hz, LPF - 500 Hz, Notch - 50 Hz

Neuroscan  
SCAN 4.5  
Printed: 12:47:05 23-Jul-2012



**b)** Subject: GA\_10.avg Recorded: 15:01:32 04-Jul-2012  
EEG file: GA\_10.avg Rate - 2000 Hz, HPF - 0 Hz, LPF - 500 Hz, Notch - 50 Hz

Neuroscan  
SCAN 4.5  
Printed: 12:48:13 23-Jul-2012

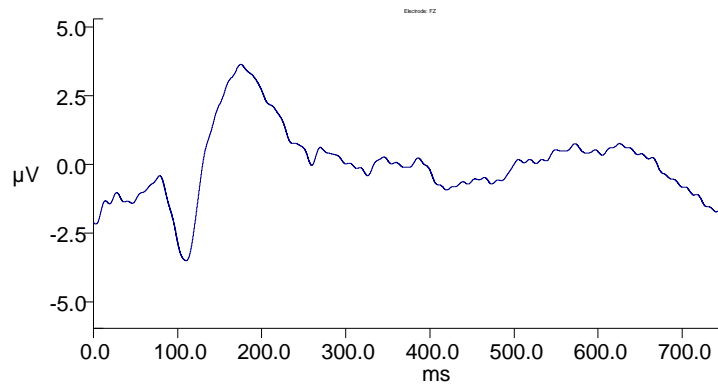


**Figure 27: NeuroScan Edit capture of grand averaged ERP data of event type '10'. (a) Raw data (b) 70 Hz low pass FIR filter, zero phase shifted, 96 dB/oct.**

# Chapter 4

## Results

The preceding chapters have laid the theoretical groundwork that forms the rationale behind the experimental procedures used in this current work. The following chapter will provide details of the results obtained.

### 4.1 Subject Selection

As stated in Chapter 3, NeuroScan Edit software was used to epoch continuous EEG recordings between 0 and 750 ms post-stimulus. Epochs were then baseline corrected and sweeps containing artefacts were removed. Table 2 shows the number of sweeps accepted during each event type, per subject.

**Table 2: Total number of accepted sweeps for each subject, relative to event type; subjects 3 and 9 (highlighted) were rejected due to the low number of accepted sweeps during event 40.**

Subject	Number of sweeps accepted per event type									
	10	20	30	40	50	110	120	130	140	150
1	262	90	576	45	257	229	81	570	38	197
2	190	70	555	36	231	177	69	535	36	237
3	105	53	115	15	71	76	17	186	10	84
4	207	92	455	43	202	176	73	476	29	215
5	53	32	208	21	142	52	28	233	23	140
6	76	44	383	27	178	61	42	386	27	180
7	192	66	458	36	192	180	61	469	34	186
8	144	58	340	31	142	121	48	338	20	138
9	91	32	102	12	75	47	9	93	9	56
10	199	80	582	37	236	183	78	579	43	250
11	126	40	321	27	147	107	43	337	20	152
12	109	43	261	22	93	140	50	248	21	113
13	232	83	576	43	235	200	65	535	39	216
<b>Mean</b>	153	60	379	30	169	135	51	383	27	166
<b>Standard Deviation</b>	63	21	166	10	61	59	22	153	10	57

In order to make use of this information, pertinent events within the trial were identified. In this case these were events 40 and 120, the matching image and imperative stimulus, respectively. Looking at the data presented in Table 2, it may be



observed that subjects 3 and 9 had particularly low sweep counts. It was therefore unquestionable that these subjects be removed from further analysis.

A second factor to consider was that of accuracy. Recalling that during a full sequence of trials, correct matches would only occur 50% of the time, it followed then that an averaged ERP from any subject could only ever contain a maximum of 50 epoched sweeps. Given that a mean of 30 sweeps survived the artefact rejection process (Table 2; event 40) it was important to make sure that these waveforms represent an accurate match-response. Allowing too many false matches to be averaged would produce erroneous modulations within the ERPs. From the results obtained in Table 3, it can be seen why subjects 8 (63% correct matches) and 12 (60% correct matches) were excluded from analysis.

**Table 3: Number of correct and incorrect matching and non-matching trials for each subject; subjects 8 and 12 (highlighted) were excluded due to their low accuracy during matching trials.**

Subject	Matching trials		Non-matching trials		Grand total
	Correct (incorrect)	Percentage correct	Correct (incorrect)	Percentage correct	
1	42 (10)	81%	47 (3)	94%	87%
2	46 (4)	92%	49 (1)	98%	95%
3	48 (1)	98%	48 (1)	98%	98%
4	42 (2)	95%	48 (2)	96%	96%
5	48 (2)	96%	49 (1)	98%	97%
6	46 (4)	92%	47 (3)	94%	93%
7	50 (0)	100%	47 (3)	94%	97%
8	31 (18)	63%	46 (4)	92%	78%
9	46 (4)	92%	49 (1)	98%	95%
10	47 (3)	94%	48 (2)	96%	95%
11	45 (5)	90%	43 (7)	86%	88%
12	30 (20)	60%	46 (4)	92%	76%
13	45 (5)	90%	48 (2)	96%	93%
<b>Mean</b>	44 (6)	88%	47 (3)	95%	91%
<b>Standard deviation</b>		< 1%		< 1%	

Having systematically pre-processed the data using conventional methods and rigorous criteria, the initial phase of analysis was ready to begin.



## 4.2 Electrode Selection

In order to locate regions of interest, Neuroscan Edit software was used to calculate paired t-scores between each electrode at each data point over the whole epoch, using the following formula:

$$\frac{(difference\ scores)}{(difference\ score\ variance/sq\ root\ of\ (n - 1))}$$

where  $n = 9$  is the number of participants in the study.

Paired t-scores were calculated by comparing each image event to type 10 (and each cross event to type 110). Given that event 10 occurs at the start of the task, prior to any task-relevant processes, any disparity between subsequent events (Table 4) would likely reflect functional activity relating to visual working memory. Using significant t-test data and assuming a null hypothesis where the voltages between two event types are the same (i.e. there is no significant difference in the voltage at time,  $t$ , between event 10 and each comparative event), regions of significant interest were located.

**Table 4: Listing of event types and associated behaviour.**

<b>Event</b>	<b>Event related behaviour</b>
10	Attention is paid to each image prior to receiving the cue to retain and match
20	Attention is paid to each image prior to receiving the cue to retain and match
30	Image (event 20) is held internally whilst subsequent images are compared
40	A match is found and the image (event 20) is released from working memory
50	Subsequent images are passively observed until the trial ends
110	Attention is paid to each cross (awaiting imperative stimulus)
120	Imperative stimulus is recognised (signal to retain the previous image)
130	Cross is ignored
140	Cross is ignored
150	Cross is ignored

Given that EEG recordings were made using a 64-channel montage and adding to that the fact that each trial contained 10 distinctive events to be compared, it was impossible to make any kind of visual interpretation of these results; 512 t-tests were to be analysed and compared for significance. For this reason, it was imperative that a method be determined in order to obtain an unbiased and meaningful representation of significant changes in activity across the scalp. The goal now was to identify which electrodes were exhibiting the greatest response to the task and establish whether these could be compared across events. To do this, data was exported to Microsoft Excel and manipulated in the following manner.

First,  $T_{\text{significant}}$  was calculated from a T-test table, where the significance level,  $\alpha = 0.01$ , and the number of degrees of freedom,  $r$ , for two sample means was found using the equation:

$$r = n - 1$$

where  $n = 9$  is the number of participants in the study. From this,  $T_{\text{significant}}$  for a significance level of 0.01 was found to be equal to 3.355 (or -3.355). Significant differences were calculated at each electrode (60 recorded channels; excluding CB1, CB2, M1, and M2) for each data point (1501 samples per 750 ms epoch); positive and negative differences represented regions where event 10 was significantly greater or lesser in amplitude than the compared distributions (20, 30, 40, and 50, respectively).

T-tests were calculated from grand-averaged ERP waveforms such as those previously illustrated in Section 3.5.1 (Figure 27). Each waveform gives a measure of voltage modulation with time. As mentioned in Section 1.3.2, specific ERP component may be identified, reflecting certain task-related events. The introduction of new events or alteration of those currently occurring, such as increasing load, causes distinct variations in the peak amplitude and latency of each component. In the context of this experiment, the largest observable change in activity was predicted to occur during event 40; the observation of a matching image (Table 4). Considering that regions of difference (modulations in peak amplitude over time) were likely to have a substantial duration rather than occurring sporadically at individual time points, it was safe to assume that summing significant t-values at each electrode over an entire epoch would give an accurate representation of deviations in ERP modulation relevant to each event.

Table 5 lists an ordered ranking of the summation of significant t-values accompanied by their respective electrode labels, comparing each image event to type 10 (e.g. 10>20 represents regions where the amplitude of event 10 is significantly larger than event 20, and 20>10 vice versa). The first thing to note from this preliminary analysis is the significant differences expressed across event 40. In this regard, these findings match what was expected, in that the largest observable change in activity presented across event 40 (in comparison to event 10). It is clear that the identification of a matching image caused explicit changes in neuronal activity triggered by recall and recognition mechanisms within the brain.

Table 5: Ordered listing of t-test results with the largest number of significantly different data points for each image event.

Rank	T-test values comparing each event type							
	10>20	10>30	10>40	10>50	20>10	30>10	40>10	50>10
1	Po5 23.0	Ft7 204.2	C3 1364.5	Cp6 339.3	Tp7 -58.4	Fc3 -133.9	P2 -1165.0	Po8 -117.1
2	F2 16.5	F7 92.6	Cp5 1015.5	Po3 206.6	T7 -31.9	Fc1 -85.7	Cp4 -1034.1	Pz -108.4
3	P3 14.0	Fc5 66.1	Cp3 1010.3	Cpz 182.9	O2 -29.8	C5 -70.5	Cp2 -1022.8	Pcz -76.6
4	Fz 12.5	F5 54.5	C5 957.0	P1 176.9	Cp5 -26.0	C3 -63.4	Po4 -997.7	Cpz -70.9
5	O1 9.3	T7 32.0	P3 845.8	C6 163.0	Fp2 -25.0	Fc5 -61.5	P4 -989.6	Cp2 -49.0
6	Fcz 5.5	Ft8 14.4	P5 804.5	Cp1 160.2	Ft8 -23.7	Fcz -55.2	Cp1 -984.7	P2 -48.7
7	T7 5.0	C6 7.2	C1 801.3	P3 159.7	Fc1 -22.5	Cp5 -39.4	Cp3 -971.7	C4 -46.3
8	Ft7 3.7	F3 7.0	Cp1 727.1	Pz 150.5	C5 -19.9	F1 -39.1	Pz -957.1	P4 -41.2
9	Fc1 2.8	Fp1 5.4	Fc3 708.5	Cp4 144.4	C1 -18.4	Ft7 -38.1	P1 -948.5	C6 -40.3
10	Po7 2.5	C4 5.3	Fc1 664.8	Cp2 139.7	Fc2 -18.3	C1 -35.4	C3 -943.8	Cp4 -40.2

Comparing the maximum t-scores (reflecting the largest change in activity) across each event gives an absolute mean of 425.7 with a standard deviation of 495.2 (Table 6). Bearing in mind that any difference in amplitude (an increase or decrease with respect to event 10) reflects an observable change in underlying neuronal activity, the mean and standard deviation were calculated from absolute values. Determining the number of standard deviations from the mean gives a measure of relative maximal activity for each event. It is clear from Table 6 that '10>40' (regions of significant difference where the grand averaged type 10 ERP is significantly greater in amplitude than type 40) and '40>10' exhibit the largest significant differences, with the maximum number of significant data points for '10>40' and '40>10' lying 1.90 and 1.49 standard deviations above the overall mean, respectively. From these results it can be concluded that simply selecting a range of electrodes most commonly presented within Table 5 is not the way forward.

**Table 6: Comparison of electrodes exhibiting the greatest significant difference with respect to event 10, including the number of standard deviations from the mean.**

<b>Comparison</b>	<b>Electrode label</b>	<b>Maximum t-score per event</b>	<b># of Standard Deviations</b>
<b>10&gt;20</b>	Po5	23.0	0.81
<b>10&gt;30</b>	Ft7	204.2	0.45
<b>10&gt;40</b>	C3	1364.5	1.90
<b>10&gt;50</b>	Cp6	339.3	0.17
<b>20&gt;10</b>	Tp7	-58.4	0.74
<b>30&gt;10</b>	Fc3	-133.9	0.59
<b>40&gt;10</b>	P2	-1165.0	1.49
<b>50&gt;10</b>	Po8	-117.1	0.62
<b>Absolute Mean</b>	-	425.7	-
<b>Absolute SD</b>	-	495.2	-

A quantitative analysis of this phenomenon can be seen in Table 7, listing the number of electrodes across the scalp exhibiting a significant difference greater than the absolute mean value. Again, this highlights the dominance of event 40 as a significant event.

**Table 7: Total number of electrodes for each event comparison presenting an absolute t-score greater than the absolute mean value.**

<b>Event</b>	<b>10&gt;20</b>	<b>10&gt;30</b>	<b>10&gt;40</b>	<b>10&gt;50</b>	<b>20&gt;10</b>	<b>30&gt;10</b>	<b>40&gt;10</b>	<b>50&gt;10</b>
<b># of electrodes (Abs. t-score &gt; Abs. mean)</b>	0	0	22	0	0	0	23	0

It is obvious that a top ten ranking of electrodes is not enough to accurately depict regions of the brain responding to events. In an effort to find a reasonable distribution of electrodes containing data significant enough for comparison, the montage was split into regions (Table 8). From which one electrode was selected for each event comparison, exhibiting the greatest difference in activity (Table 9). Regions were chosen based on two criteria. Firstly, grand averaged ERP maps were evaluated, comparing waveforms for relative similarity. Secondly, attempts were made to account for the pre-defined conventions stated in the 10-20 system. Ultimately, nine regions were selected to represent a definitive distribution of neurological activity (Table 8).

Table 8: Electrode categorization with associated anatomical locations and relevant nomenclature.

Label	Region	Electrodes
<b>AF / FP</b>	Anterio-frontal / Fronto-polar	Fp1, Fpz, Fp2, Af3, and Af4
<b>F</b>	Frontal	F7, F5, F3, F1, Fz, F2, F4, F6, and F8
<b>FC</b>	Fronto-central	Fc5, Fc3, Fc1, Fcz, Fc2, Fc4, and Fc6
<b>C</b>	Central	C5, C3, C1, Cz, C2, C4, and C6
<b>CP</b>	Centro-parietal	Cp5, Cp3, Cp1, Cpz, Cp2, Cp4, and Cp6
<b>P</b>	Parietal	P7, P5, P3, P1, Pz, P2, P4, P6, and P8
<b>PO</b>	Parieto-occipital	Po7, Po5, Po3, Poz, Po4, Po6, and Po8
<b>O</b>	Occipital	O1, Oz, and O2
<b>FT / T / TP</b>	Fronto-temporal / Fronto-central / Temporal / Temporo-parietal	Ft7, Ft8, T7, T8, Tp7, and Tp8

Table 9 compares the most significant electrodes from each of these regions, along with the absolute standard deviation (SD) of each t-test value, relative to each event type. Other than the prevalence of activity at electrode O2 within occipital region, it is difficult to select electrodes with sufficient significance across all events.

Table 9: Listing of the most significant electrodes per region, per image event.

Region	Comparative t-test values							
	10-20		10-30		10-40		10-50	
	Label	t-score (# SDs)	Label	t-score (# SDs)	Label	t-score (# SDs)	Label	t-score (# SDs)
<b>AF / FP</b>	Fp2	-25.0 (0.1)	Fp1	5.4 (1.0)	Fp1	-38.6 (1.4)	Af4	-5.1 (1.2)
<b>F</b>	F2	16.5 (0.8)	F7	92.6 (0.1)	F3	99.0 (1.3)	F6	-7.0 (1.2)
<b>FC</b>	Fc1	-22.5 (0.3)	Fc3	-133.9 (0.6)	Fc3	708.5 (0.1)	Fc6	64.2 (0.6)
<b>C</b>	C5	-19.9 (0.5)	C5	-70.5 (0.2)	C3	1364.5 (1.5)	C6	163.0 (0.4)
<b>CP</b>	Cp5	-26.0 (0.0)	Cp5	-39.4 (0.6)	Cp4	-1034.1 (0.8)	Cp6	339.3 (2.1)
<b>P</b>	P3	14.0 (1.0)	P1	-4.6 (1.0)	P2	-1165.0 (1.1)	P1	176.9 (0.5)
<b>PO</b>	Po5	23.0 (0.3)	Po5	-0.7 (1.0)	Po4	-997.7 (0.7)	Po3	206.6 (0.8)
<b>O</b>	O2	-29.8 (0.3)	O2	239.5 (1.8)	O2	-298.6 (0.8)	O1	56.6 (0.7)
<b>FT / T / TP</b>	Tp7	-58.4 (2.6)	Ft7	204.2 (1.4)	T7	382.9 (0.6)	T8	123.2 (0.0)
<b>Absolute Mean</b>	-	26.1	-	87.6	-	676.5	-	126.9
<b>Absolute SD</b>	-	12.3	-	83.4	-	461.1	-	101.8

In an attempt to improve these results and determine the most significant electrode within each region, t-test significance was summed across all events for each electrode within the montage (Table 10).

Table 10: Most significant electrodes, per region (calculated by summing differential activity over all image events).

Region	Electrode label	Summed significance
AF / FP	Fp1	44.4
F	F3	162.6
FC	Fc3	902.3
C	C3	2430.3
CP	Cp3	2146.8
P	P3	1879.3
PO	Po4	1536.2
O	O2	591.0
FT / T / TP	Tp7	565.9

Plotting these locations on a scalp map, there is an obvious linearity in the position of electrodes exhibiting strong changes in activity (Figure 28). However, from previous examination it is fair to assume that these results are strongly biased towards event 40 and so, further manipulation was required.

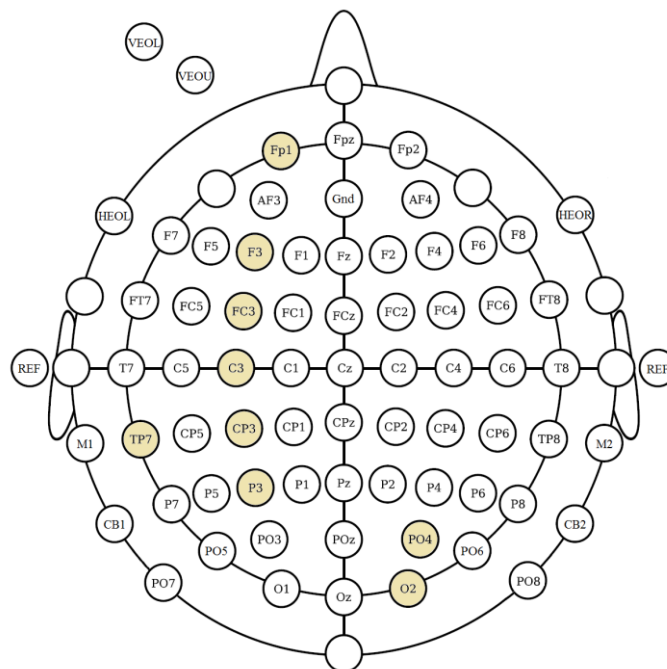


Figure 28: 64-channel montage displaying electrodes exhibiting the most significant differential activity in response to events per region (calculated by summing differential activity over all image events).

To remove any possible bias each value was normalised across each region as a percentage value and summed over all events (Table 11). A maximum 'percentage' of 800 could be obtained if significant activity is repeatedly recorded from a single electrode (and no others; relative to its defined region) for each event comparison.

**Table 11: The most significant electrodes per region (calculated as the relative proportion of activity per region, summed over all image events).**

Region	Electrode label	Significance
<b>AF / FP</b>	Fp1	197.8%
<b>F</b>	F7	146.3%
<b>FC</b>	Fc5	178.9%
<b>C</b>	C6	121.1%
<b>CP</b>	Cp5	143.4%
<b>P</b>	P2	184.3%
<b>PO</b>	PO5	208.7%
<b>O</b>	O2	282.8%
<b>FT / T / TP</b>	T7	176.1%

Figure 29 shows the final distribution of electrodes which were determined to be an unbiased but meaningful representation of activity across all events.

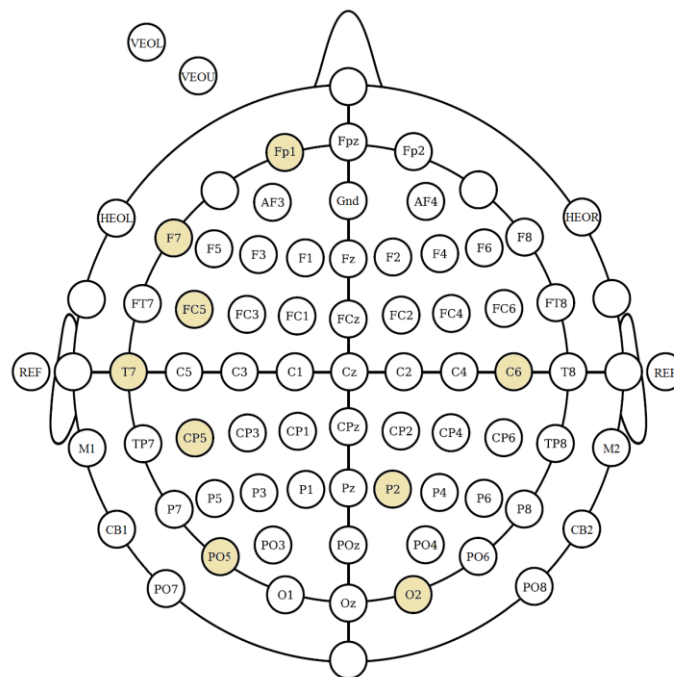


**Figure 29: 64-channel montage displaying electrodes exhibiting the most significant differential activity in response to events, per region (calculated as the relative proportion of activity per region, summed over all events).**

Using the same procedure for the crosses (Appendix B shows an ordered ranking of the summation of significant t-values), Table 12 lists the most significant electrodes per region, per event. These results are comparable in size to those obtained during the 10-20, 10-30, and 10-50 comparisons and again, considerably smaller than those obtained in 10-40.

**Table 12: Listing of the most significant electrodes per region, per cross event.**

Region	Comparative t-test values							
	110-120		110-130		110-140		110-150	
	Label	t-score (# SDs)	Label	t-score (# SDs)	Label	t-score (# SDs)	Label	t-score (# SDs)
<b>AF / FP</b>	Fpz	45.5 (0.9)	Fp2	54.6 (0.4)	Af4	61.7 (0.9)	Fpz	80.4 (1.4)
<b>F</b>	F3	-29.2 (0.2)	F8	-141.2 (2.2)	F6	-48.5 (1.0)	F4	158.5 (0.2)
<b>FC</b>	Fc6	-33.0 (0.0)	Fc5	-48.9 (0.2)	Fc6	-215.3 (0.5)	Fc6	204.8 (1.2)
<b>C</b>	C3	-28.1 (0.3)	C6	-3.7 (0.8)	C6	296.8 (1.3)	C6	112.1 (0.8)
<b>CP</b>	Cp2	52.3 (1.4)	Cp5	-2.0 (0.8)	Cp6	-370.9 (2.0)	Cpz	-195.9 (1.0)
<b>P</b>	P2	42.6 (0.7)	P8	0.2 (0.8)	P8	127.1 (0.3)	Pz	-195.7 (1.0)
<b>PO</b>	Po5	19.9 (0.9)	Po7	-7.9 (0.7)	Po6	-107.0 (0.4)	Po4	-150.7 (0.1)
<b>O</b>	O1	-1.5 (2.1)	Oz	-5.79 (0.7)	O2	-32.7 (1.1)	O2	-68.0 (1.7)
<b>FT / T / TP</b>	Tp7	-38.9 (0.5)	Ft8	82.4 (1.0)	T8	-143.4 (0.1)	T8	168.4 (0.4)
<b>Absolute Mean</b>	-	32.4	-	38.5	-	155.9	-	148.3
<b>Absolute Standard Deviation</b>	-	14.4	-	45.8	-	109.8	-	47.9

Calculating normalized significance for individual electrodes across each region and summing over all events, Table 13 lists the most significant electrodes.



**Table 13: The most significant electrodes per region (calculated as the relative proportion of activity per region, summed over all cross events).**

Region	Significance	Electrode label
<b>AF / FP</b>	Af3	236.3%
<b>F</b>	F6	237.8%
<b>FC</b>	Fc6	324.1%
<b>C</b>	C6	296.8%
<b>CP</b>	Cp6	191.7%
<b>P</b>	P8	241.4%
<b>PO</b>	Po7	212.5%
<b>O</b>	O2	354.6%
<b>T</b>	Ft8	250.3%

Plotting these locations on a scalp map, a pleasing linearity is attained across the right hemisphere (Figure 30).

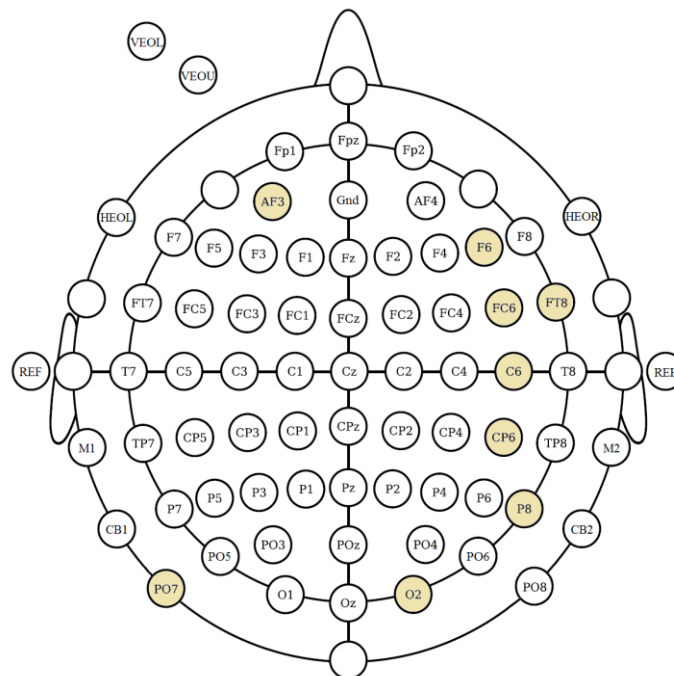


**Figure 30: 64-channel montage displaying electrodes exhibiting the most significant differential activity in response to events per region (calculated as the relative proportion of activity per region, summed over all cross events).**

Having selected a robust distribution of electrodes representative of each anatomical region across the scalp, the next section presents a comparative ERP analysis indicative of neuronal activity associated with task-related events in visual working memory.

### 4.3 Grand Averaged ERPs

EEGLab has the option of creating 'study' datasets from multiple subjects and event types. This function allows the user to make comparisons between data and visualize results. It is first necessary to 'precompute channel measures', for which the default parameters were used. Figures 31 to 34 compare grand averaged ERP plots of event 10 to events 20, 30, 40, and 50, where the grey bars indicate regions of statistical interest. Differential activity was calculated using a paired t-test with a critical significance level of  $\alpha = 0.01$ . Such strict criteria allowed comparisons to be made which emphasized only the most significant differences between events.

#### **Image Event ERPs**

Figure 31 compares grand averaged ERP plots obtained during events 10 and 20. At this point, EEG data recorded during observation of the image to be 'stored' and those that were 'ignored' are being compared. However, since the trigger event '120' has not yet arrived, it was expected that minimal differences in neuronal activation would be observed between the two datasets. This hypothesis was confirmed with little disparity noted between the waveforms (Figure 31). It can be seen however, that an increase in positivity seems to occur between 400 - 450 ms post-stimulus, over sites Fc5, C6, Cp5, and T7.

Comparing events 10 and 30 (Figure 32) produced similar results. At this stage the imperative stimulus has been recognized, the stimulus image is stored in memory (event 20) and participants are actively engaged in finding a match. As predicted, the main components of the ERP show considerable similarity. The greatest response to stimuli was recorded over the parieto-occipital region (Po5), peaking at approximately 4  $\mu$ V. Other noteworthy features include: an increase in negativity between 400 - 500 ms over F7, and rather interestingly, the recurrence of significant activity over Fc5, Cp5, and T7 between 400 - 500 ms.

Events 10 and 40 are assessed in Figure 33, illustrating the greatest comparative disparity. These results demonstrate an increase in neuronal activity associated with match recognition. Attention is drawn to the development of an LPC peaking maximally over the parietal region between 600 - 700 ms, indicating recognition. Additional regions of interest include the development of a large N3 peak, over the parietal and occipital regions (Cp5, P2, Po5, O2). Over Cp5 and P2, this was preceded by a possible N1 and N2 deflection. Although numerous additional features may be noted, for the

purpose of this project, it was required only to observe evidence of upload and download mechanisms between the ITC and PFC. Examining these two regions, Fp1 produced a large increase in positivity with a peak latency of 300 - 400 ms, whilst T7 exhibited transient activity seeming to originate from Cp5.

Figure 34 compares ERP waveforms representative of events 10 and 50. Images presented at this point are no longer actively attended to as a match has already been made. Regions of interest are primarily located over the central and parietal regions. Contrary to events 20 and 30, the increase in positivity recorded at approximately 450 ms is observed as a negative deflection (C6, Cp5, and T7). A second feature to note occurs at P2, a dramatic increase in positivity between 200 - 300 ms.

### **Cross Event ERPs**

Comparing the cross events, a dramatic contrast may be observed. These waveforms do not possess the same distinct modulations as the image ERPs. Figure 35 compares event 110 with the trigger, 120 (signalling the participant to store the previous image and find a match). Although these waveforms are considerably more difficult to read, regions of interest were observed over numerous locations. The easiest to identify was the emergence of an N1 component over electrodes C6, Cp6, P8, Po7, and O2. T-test significance also suggested a significant increase in negativity over P8 (approximately 300 ms post-stimulus), Cp6, and C6 (approximately 200 ms post-stimulus).

Events 110 and 130 are compared in Figure 36. Although expected to present similar characteristics, two regions of interest were identified. Firstly, increased late negativity was observed over Af3, F6, Fc6, C6, and Ft8. Again, these features were difficult to identify, partially due to the initial positivity at 0 ms. However, in comparison to event 110, an increased positive deflection over the centro-frontal regions was observed, 200 - 300 ms after stimulus onset.

Comparing event 110 to events 140 and 150 produced similar results. Although disparities were not expected, numerous regions were highlighted in statistical analysis, predominantly late negativity and increases in the amplitude of early ERP components.

As described previously, electrodes C6, Cp5, and T7 present significant differences between 400 - 500 ms (Figure 31). Regions of interest, denoted by the grey band, indicate a noticeably smaller region of significant difference over electrode Fc5. However, a visual inspection reveals that the relative differences in amplitude remain consistent across each channel, suggesting a large variability between participants.

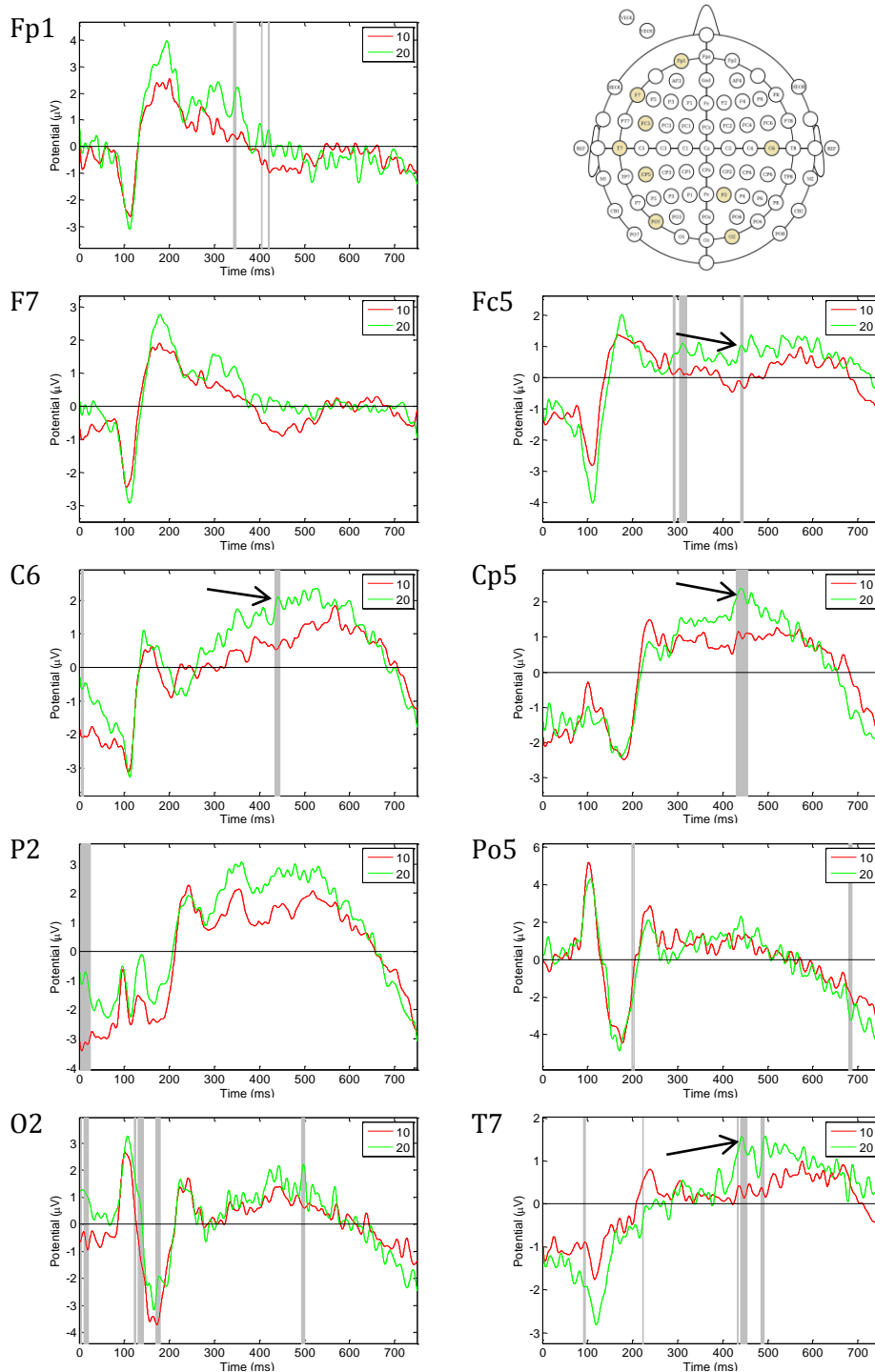


Figure 31: Grand averaged ERP comparison of event 10 (red) against event 20 (green).

Figure 32 compares events 10 and 30. The most significant difference highlighted during this comparison was recorded at channel Cp5. Increases in positivity are observed between 300 - 400 ms, indicating the summation of an additional component. It may also be noted that this feature is missing from C6 (and substantially reduced over Fc5 and T7), caused by an effective decrease in amplitude between 400 - 700 ms.

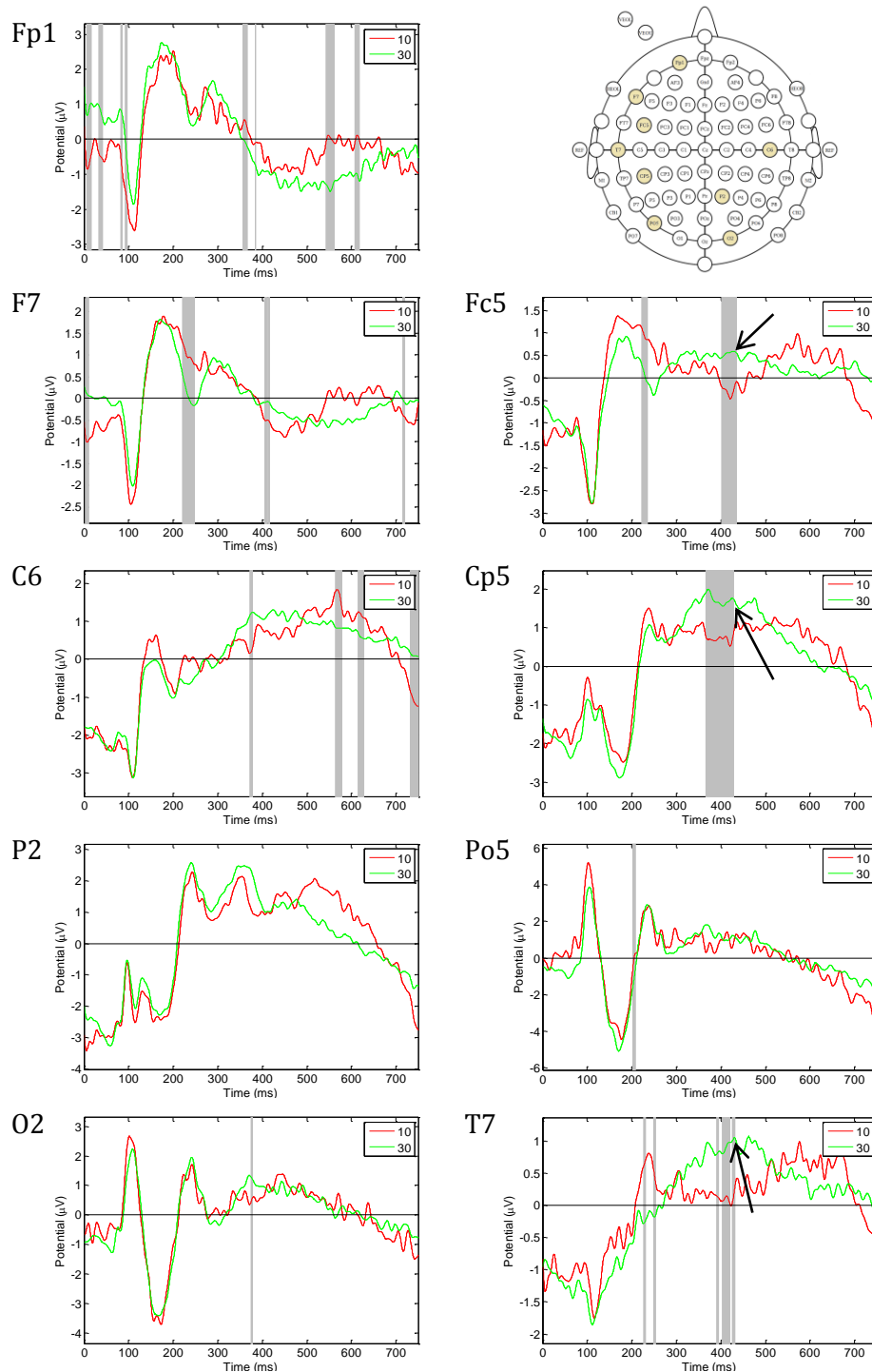


Figure 32: Grand averaged ERP comparison of event 10 (red) against event 30 (green).

The first thing to note from Figure 33 is the signal to noise ratio. As illustrated in Section 4.1, grand averaged ERPs for event 40 were obtained from a mean of 30 individual sweeps, per subject. Event 10 ERPs on the other hand, were constructed from a mean of 153 sweeps (Section 4.1: Table 2). These differences are significant and are most noticeable in channels Fp1 and T7, perhaps due to the EEG cap fitting looser at the extremities of its form.

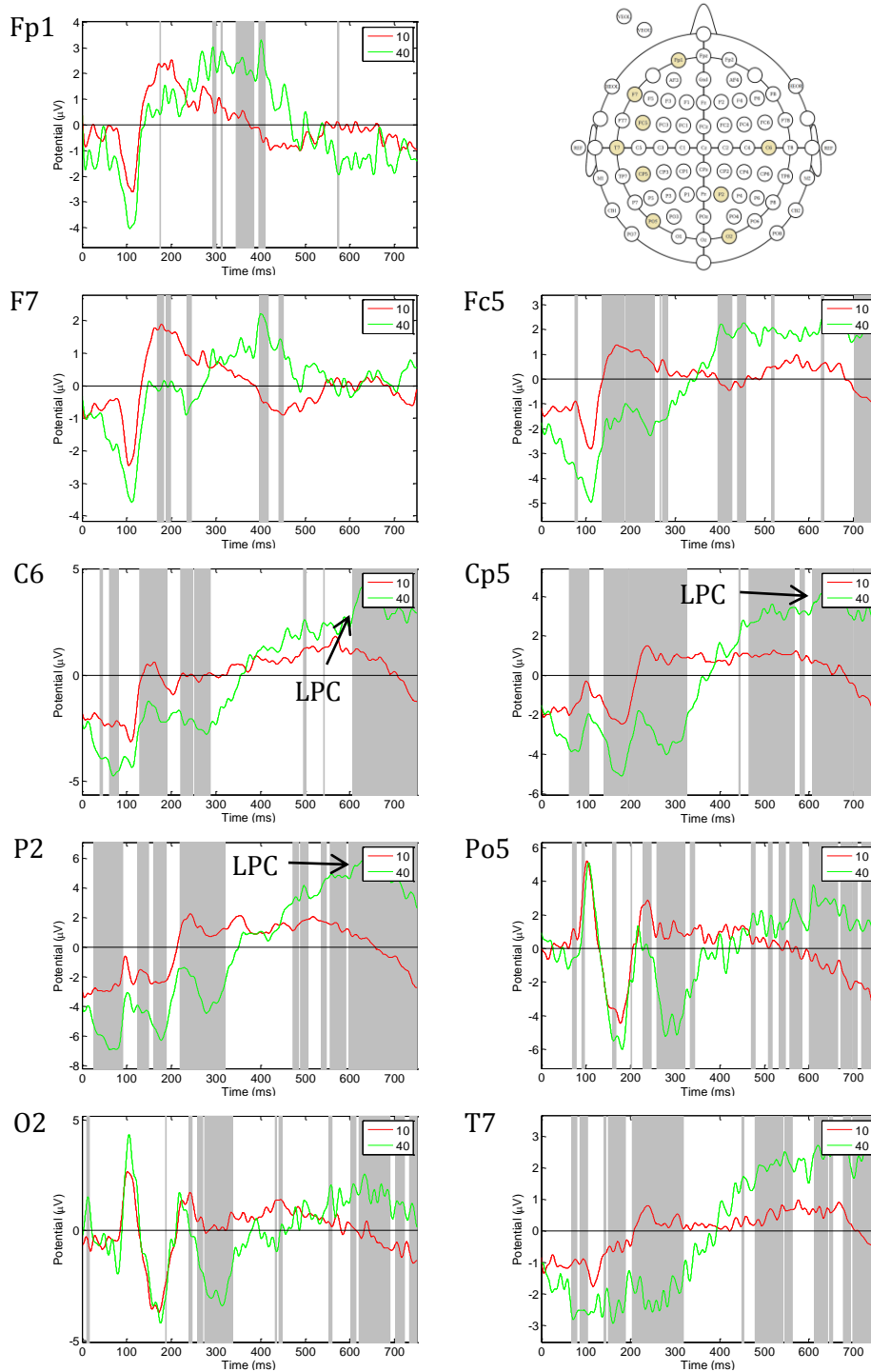


Figure 33: Grand averaged ERP comparison of event 10 (red) against event 40 (green).

Figure 34 illustrates regions of significant difference between ERP from events 10 and 50. It is important to be aware of features such as those highlighted in channel C6 at 75 and 90 ms. Although t-test results have indicated regions of interest, a visual comparison of the relative modulations in amplitude show little difference. The statistical test does not take into account the voltage difference at 0 ms, which may have resulted from neuronal activity associated with the previous event.

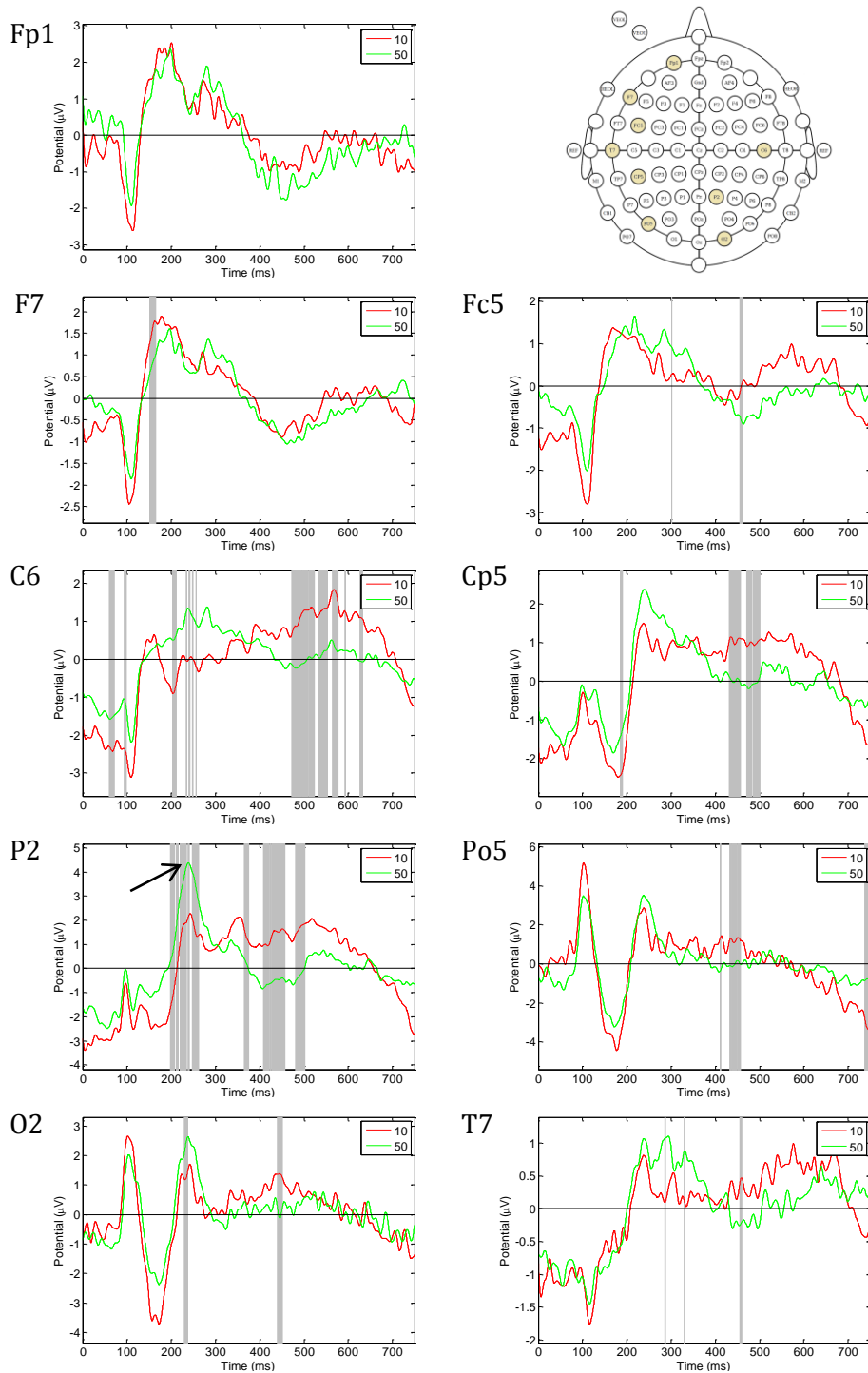


Figure 34: Grand averaged ERP comparison of event 10 (red) against event 50 (green).

A comparison of ERPs recorded during events 110 and 120 are displayed in Figure 35. Although N1 components were indicated as being significant and observed over the central and posterior regions of the scalp, a P1 peak may also be identified at electrodes Af3 and F6, indicating a change in PFC activity upon detection of the trigger. Possibly, these were not picked up as being statistically significant due to the large amount of variation present within the waveforms and relatively small signal strength.

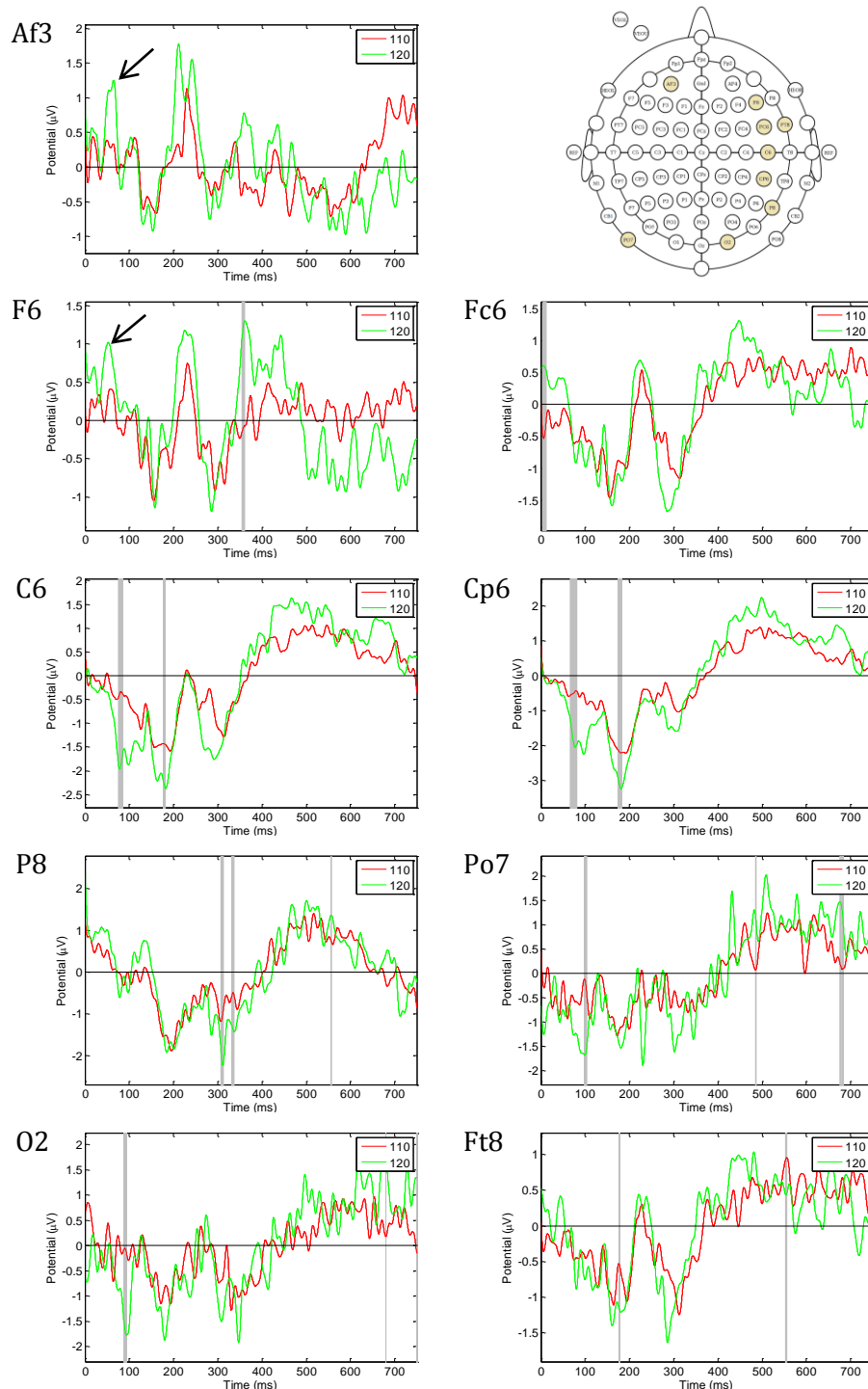


Figure 35: Grand averaged ERP comparison of event 110 (red) against event 120 (green).



Figure 36 illustrates a comparative study between events 120 and 130. Distinct to this comparison, regions of significance are highlighted at 200 ms and 260 ms post stimulus. This activity is observed primarily over the fronto-central regions, Af3, F6, Fc6, C6, and Cp6. Given that this response is not detected during other events and that event 30 denotes a cross which is ignored, it is assumed that these modulations have occurred as a result of inter-subject variability during tasks of low cognitive demand.

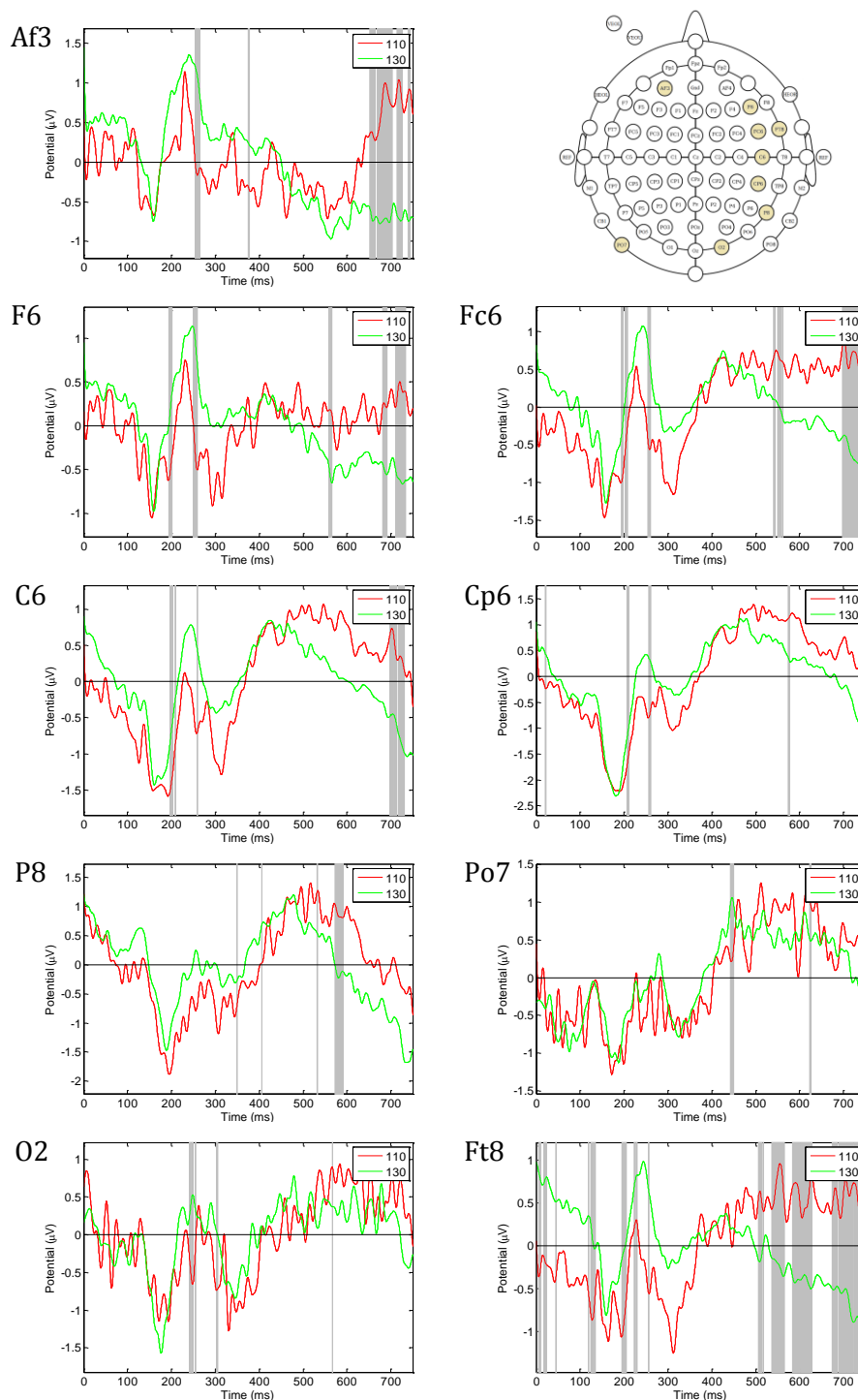


Figure 36: Grand averaged ERP comparison of event 110 (red) against event 130 (green).

A comparison of events 110 and 140 is shown in Figure 37, showing a considerably greater quantity of statistically relevant regions than previous cross-events. Curiously, event 140 corresponds to another ignored cross, this time following the matching image. Since a match has already been found and the cross itself contains no significant information with which to attend to, any regions of significance must be a result of late activity associated with the previous event, the matching image (event 40).

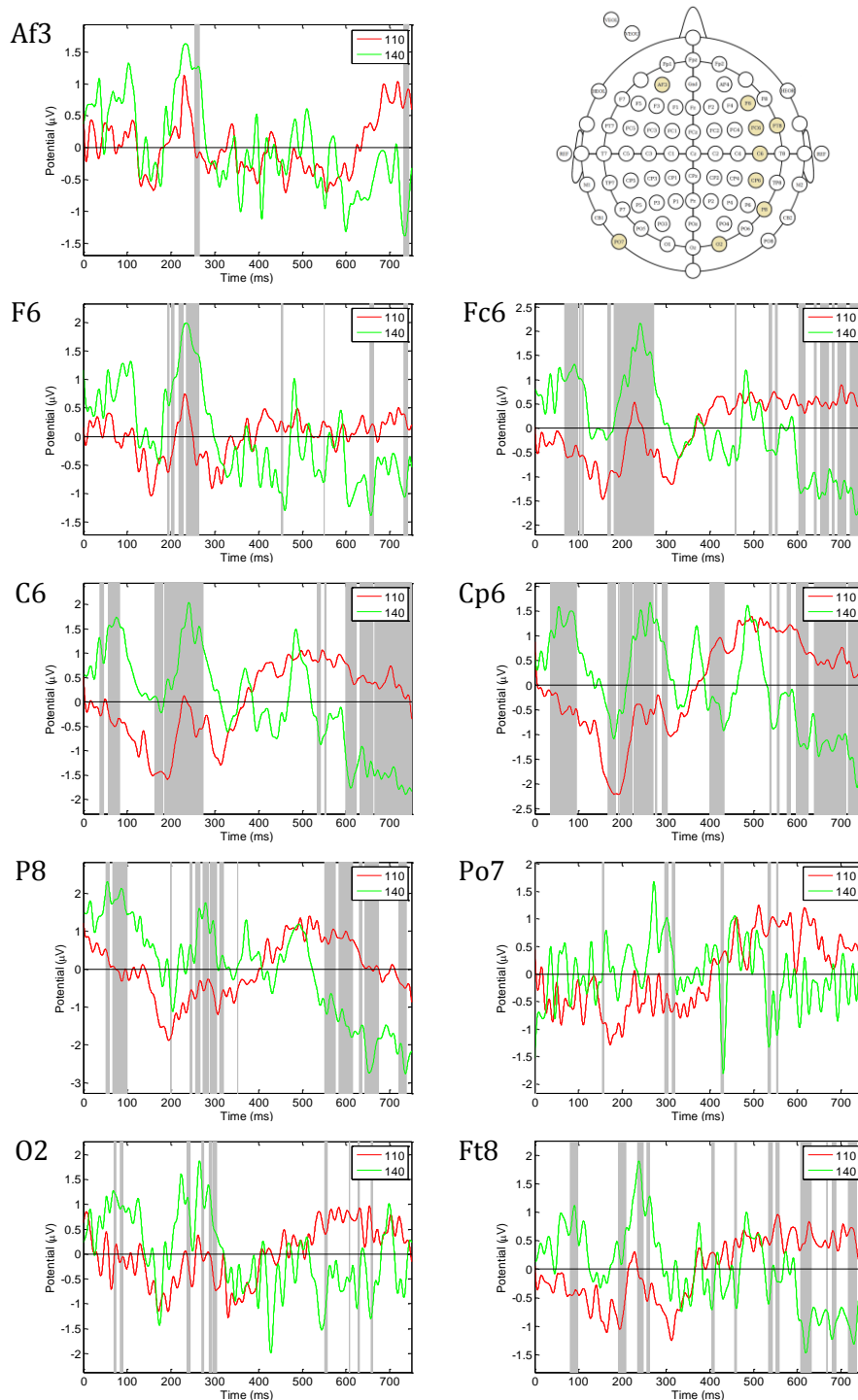


Figure 37: Grand averaged ERP comparison of event 110 (red) against event 140 (green).

The comparison between events 110 and 150 shows similar results, with regions of significance evident at comparable latencies (Figure 38). The information encoded in the cross contains very little information and at this point is essentially ignored. Regions of significance are therefore attributed to residual effects from the previous event.

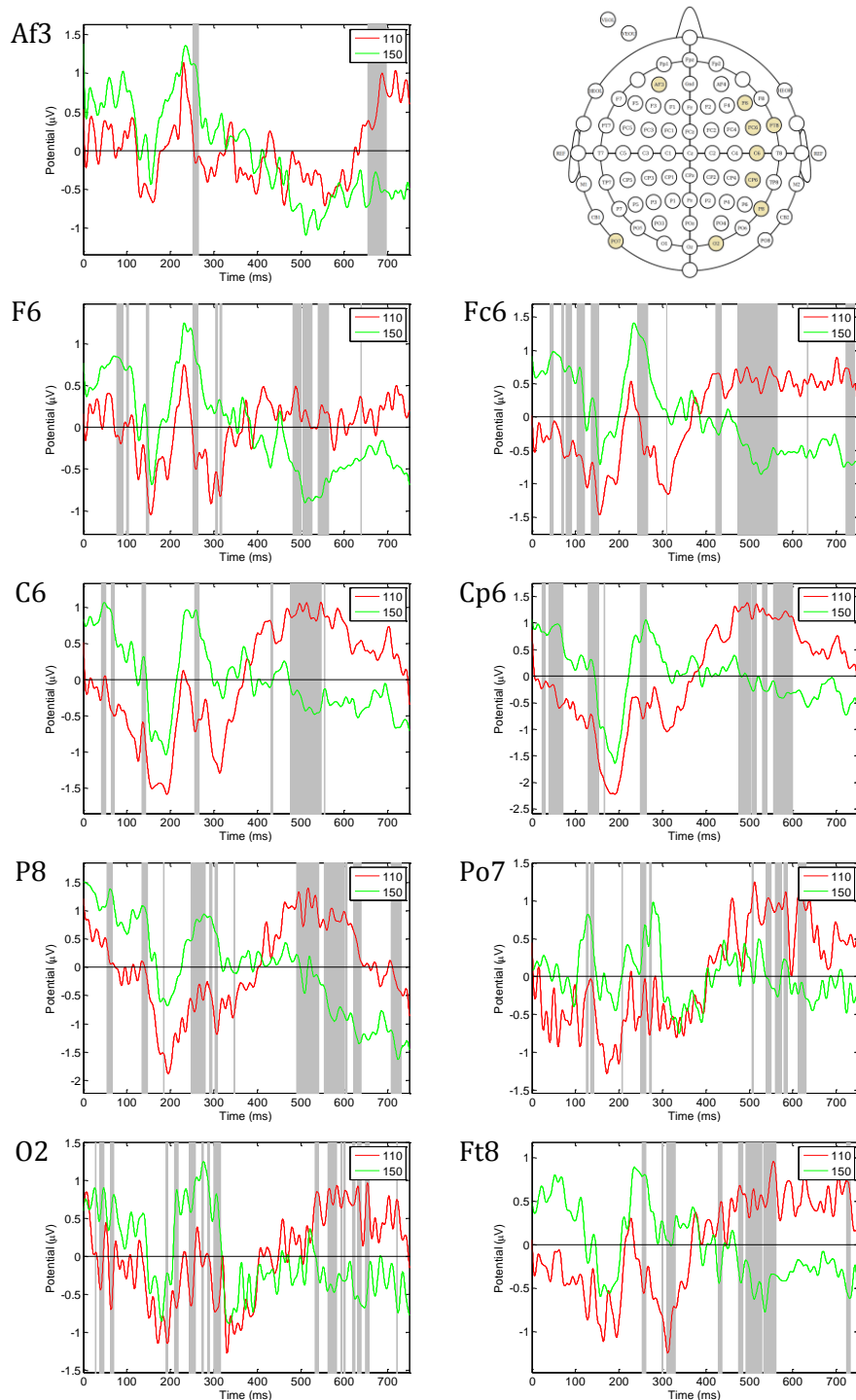


Figure 38 Grand averaged ERP comparison of event 110 (red) against event 150 (green).

As originally expected, significantly higher activity was observed between image events 10 and 40, compared to other events. This agrees well with the prior assumption that greater degrees of neuronal response occur as a consequence of task-related processes. Furthermore, an indication of functional correlation occurs between 400 - 500 ms over electrode sites Fc5, Cp5, and T7, indicating some level of interaction between these regions during the working memory task.

The development of an LPC over the central and posterior regions (reflected anteriorly) is observed as a match is detected during event 40. This late component is seen to peak maximally over the parietal lobe, indicating some level of spatial processing and recognition. The P1 component, a well-known visually evoked peak, is observed over the extrastriate regions. A substantial increase in amplitude is observed, indicating image-related processing related to match recognition. Also indicative of event-related function during the match is the emergence of new negative components, most clearly visible over the parietal and occipital regions.

All of this evidence points towards an agreement with this project's hypothesis. That is, visual stimuli are briefly maintained within the ITC (aided by the medial temporal cortex) as images are presented on screen. When a trigger to hold an image in memory is received, changes in activity are observed over the PFC, indicating an upload mechanism from the temporal lobe. This activity is sustained whilst subsequent images are compared for a match. After a match is found, activity within the PFC and ITC (and parietal and occipital lobes) is observed to increase significantly. Notably, an increase in positivity between 300 - 400 ms post-stimulus at Fp1 (PFC) and the emergence of a LPC with a peak-latency of approximately 600 ms at T7 (ITC). Following a match, activity across all regions decreases substantially and waveforms become less defined as the participant passively observes the remaining images, whilst awaiting the end of the trial.

# Chapter 5

## Discussion

The aim of this project was to determine the neuroanatomical substrates of visual working memory, and in particular to find evidence of interaction between the ITC and PFC. Subjects were asked to attend to a series of view-invariant fractal images whilst their EEG was recorded. Upon detection of an imperative stimulus (event 120), they were required to match the previous image (event 20) with subsequent stimuli.

Continuous EEG data was prepared as grand averaged ERP waveforms and statistically analysed using a paired t-test (calculated using NeuroScan Edit). Quantitative differential evaluations were performed between electrodes to obtain an unbiased and meaningful distribution across the scalp. One electrode was selected from each region and grand average ERPs plotted; each image and cross event were compared against the image event 10 and cross event 110, respectively. Regions of significant difference were highlighted, using paired t-scores (calculated using EEGLab), to aid examination of the waveforms.

A cursory analysis, listing t-test results for each electrode, in numerically descending order, allowed locations to be compared across each image event (Section 4.2: Table 5). As was expected, in line with the present hypothesis, considerable differences were observed across event 40, in comparison to event 10, indicating a comparative change in neuronal activation when a matching image was observed. The fact that this activity most often occurred over the central and parietal regions is interesting, and may reflect additional task related processing which will be discussed later.

### 5.1 T-score Analysis

The hypothesis presented in this project predicted that the greatest disparity would occur over the ITC and PFC. However, in order to avoid biasing the results and ignoring activity in other regions that could also be relevant and of interest, a classification algorithm was developed.

Table 14 lists the most significant electrodes (exhibiting the greatest voltage disparity) per region, for each image event. Absolute mean values were calculated for each comparison (10-20, 10-30, 10-40, and 10-50), as was standard deviation. As mentioned in Section 4.2, absolute values were used, since only the relative difference in amplitude was of interest, reflecting a change in neuronal activity relevant to each event. The number of standard deviations accompanying each t-score was calculated relative to the mean of each comparative event. Recalling that the null hypothesis in these distributions assumes each event type to be equal to event 10, it is possible to obtain a quantitative description of the relative neuronal activity of each region (with respect to event 10). Given that event 10 represents images prior to any task-relevant stimuli, this is considered a reasonable comparison. What follows is an examination of the data obtained during the image event analysis (Table 14) and how it pertains to visual working memory and the paradigm of this study.

**Table 14: Extracted from Section 4.2 (Table 9): Listing of the most significant electrodes per region, per image event.**

Region	Comparative t-test values							
	10-20		10-30		10-40		10-50	
	Label	t-score (# SDs)	Label	t-score (# SDs)	Label	t-score (# SDs)	Label	t-score (# SDs)
<b>AF / FP</b>	Fp2	-25.0 (0.1)	Fp1	5.4 (1.0)	Fp1	-38.6 (1.4)	Af4	-5.1 (1.2)
<b>F</b>	F2	16.5 (0.8)	F7	92.6 (0.1)	F3	99.0 (1.3)	F6	-7.0 (1.2)
<b>FC</b>	Fc1	-22.5 (0.3)	Fc3	-133.9 (0.6)	Fc3	708.5 (0.1)	Fc6	64.2 (0.6)
<b>C</b>	C5	-19.9 (0.5)	C5	-70.5 (0.2)	C3	1364.5 (1.5)	C6	163.0 (0.4)
<b>CP</b>	Cp5	-26.0 (0.0)	Cp5	-39.4 (0.6)	Cp4	-1034.1 (0.8)	Cp6	339.3 (2.1)
<b>P</b>	P3	14.0 (1.0)	P1	-4.6 (1.0)	P2	-1165.0 (1.1)	P1	176.9 (0.5)
<b>PO</b>	Po5	23.0 (0.3)	Po5	-0.7 (1.0)	Po4	-997.7 (0.7)	Po3	206.6 (0.8)
<b>O</b>	O2	-29.8 (0.3)	O2	239.5 (1.8)	O2	-298.6 (0.8)	O1	56.6 (0.7)
<b>FT / T / TP</b>	Tp7	-58.4 (2.6)	Ft7	204.2 (1.4)	T7	382.9 (0.6)	T8	123.2 (0.0)
<b>Absolute Mean</b>	-	26.1	-	87.6	-	676.5	-	126.9
<b>Absolute SD</b>	-	12.3	-	83.4	-	461.1	-	101.8

### **Image Event Analysis**

As mentioned previously, event 20 corresponds to the image to be remembered prior to receiving the trigger to do so (event 120). The 10-20 comparison should therefore contribute little significant difference in activity, which is reflected in the absolute mean value of 26.1, compared with other conditions (Table 14). The response detected over the temporal lobe (Tp7), may be due to an increase in expectation as each image was attended to and replaced previous representations in visual working memory. The response indicated over the parietal lobe (P3) may be explained by the maintenance of visual representation. Whilst minimal change was detected over the occipital region (O2), this was to be expected and agrees with results reported in literature (Harrison & Tong 2009). As no task-relevant cognition is required, negligible activity was recorded over the PFC (Fp2).

Event 30 denotes the internal representation of a visual stimulus (event 20) prior to finding a match (event 40; only occurring in 50% of the trials). At this point, the PFC is involved in maintaining an internal representation free from interference (Fp1). As subsequent images are presented, a large increase in activity was observed over the occipital lobe (O2). This response may be explained by an increase in visual attention to features whilst comparisons are made on the retinotopic map. The temporal lobe exhibited similarly high levels of activity (Ft7), as subsequent images were briefly held for comparison as a match was sought.

Event 40 corresponded to finding a match and was associated with a surge of activity within the frontal regions of the brain (Fp1 and F3), reflecting image recall and recognition processes, including sensitivity to object shape and colour (Sereno & Amador 2006). Relative activity over the temporal lobe began to fall (T7) since temporary storage was no longer required, with detection of a match occurring early in the epoch.

Finally, after a match was found (event 50) minimal attention was given to subsequent images as participants awaited the end of the trial. The relatively high levels of activity observed anteriorly (Af4 and F6) may be explained by the retention of a yes or no response and intent to perform the motor task (pressing a keyboard button to indicate having seen a match). Levels of activity were still observed over the PVC as images were passively viewed. However, the response over the temporal lobe was negligible,

as the internal representation of an image was no longer actively maintained and any function associated with visual working memory was not required.

### Cross Event Analysis

A similar analysis may be performed by comparing each cross event type (Appendix B shows an ordered listing of the most significant t-test results for each cross event comparison). As before, standard deviations and mean values were calculated with respect to each event comparison. The number of standard deviations accompanying each t-score was calculated relative to its group mean and standard deviation value. Cross-type comparisons describe significant differences in neuronal output, relative to event condition 110.

**Table 15: Extract from Section 4.2 (Table 12): Listing of the most significant electrodes per region, per cross event.**

Region	Comparative t-test values							
	110-120		110-130		110-140		110-150	
	Label	t-score (# SDs)	Label	t-score (# SDs)	Label	t-score (# SDs)	Label	t-score (# SDs)
<b>AF / FP</b>	Fpz	45.5 (0.9)	Fp2	54.6 (0.4)	Af4	61.7 (0.9)	Fpz	80.4 (1.4)
<b>F</b>	F3	-29.2 (0.2)	F8	-141.2 (2.2)	F6	-48.5 (1.0)	F4	158.5 (0.2)
<b>FC</b>	Fc6	-33.0 (0.0)	Fc5	-48.9 (0.2)	Fc6	-215.3 (0.5)	Fc6	204.8 (1.2)
<b>C</b>	C3	-28.1 (0.3)	C6	-3.7 (0.8)	C6	296.8 (1.3)	C6	112.1 (0.8)
<b>CP</b>	Cp2	52.3 (1.4)	Cp5	-2.0 (0.8)	Cp6	-370.9 (2.0)	Cpz	-195.9 (1.0)
<b>P</b>	P2	42.6 (0.7)	P8	0.2 (0.8)	P8	127.1 (0.3)	Pz	-195.7 (1.0)
<b>PO</b>	Po5	19.9 (0.9)	Po7	-7.9 (0.7)	Po6	-107.0 (0.4)	Po4	-150.7 (0.1)
<b>O</b>	O1	-1.5 (2.1)	Oz	-5.79 (0.7)	O2	-32.7 (1.1)	O2	-68.0 (1.7)
<b>FT / T / TP</b>	Tp7	-38.9 (0.5)	Ft8	82.4 (1.0)	T8	-143.4 (0.1)	T8	168.4 (0.4)
<b>Absolute Mean</b>	-	32.4	-	38.5	-	155.9	-	148.3
<b>Absolute SD</b>	-	14.4	-	45.8	-	109.8	-	47.9

It was expected that only the trigger event, 120, would exhibit differences from the null hypothesis. Looking at Table 15, a peak in differential activity is seen over the occipital lobe (O1), presumably indicating the detection of the imperative stimulus (event 120).



It may also be said that the levels of activity obtained at the PFC are due to the formation of intent to match the previous image and subsequent upload from the ITC.

Multiple regions of interest are also found during events 130, 140, and 150. Recalling the grand averaged ERP waveforms, Figures 35 to 38, it is clear from the relatively small amplitudes (with respect to image ERPs) and 'noisy' peaks that very little task-relevant function occurred during cross presentation. This is to be expected, since a very small amount of information is being processed. Although ERPs are comparable and almost certainly contain specific time-locked components, the considerable disparity between amplitudes at  $t = 0$  should be noted. This variability can be explained by late ERP components such as the LPC (beginning prior to the presentation of the cross) influencing the waveform. It should therefore be concluded that a functional analysis of cross ERP components will most likely be contaminated by previous processes.

At this point, having identified regions of interest associated with variations in neural activity during each task-related event, it may be useful to examine these components in greater detail. The following section conducts an ERP analysis relating to the previously identified components.

## 5.2 ERP Analysis

In Section 4.3, an initial analysis of the relative differences between ERP waveforms revealed some interesting features which will now be discussed. This project attempted to find evidence of interaction between the PFC and ITC during a visual working memory task. ERPs represent a measure of underlying neuronal activity associated with various processes such as memory encoding and maintenance. As mentioned in Section 4.3, an indication of functional correlation was observed at electrodes Fc5, Cp5, and T7.

Figure 39 compares ERPs recorded over the PFC (electrode Fc5), across all events. Significant activity was observed from 400 to 450 ms post-stimulus, similar to results reported in the literature (Gjini & Maeno 2007). Initially, during event 10, activity is minimal, reflecting an absence of cognitive function as images are observed but not processed (Figure 39). A small change in activity is detected during event 20 (Figure 39a). This may be due to reaching attentional capacity during maximum load conditions. The image to be matched (event 20), occurs randomly between positions

2 and 6 in the trial sequence. Given that the presentation of the event is distributed equally over all trials, it can be said that event 20 presents on average at position 4. This means that an average of three type 10 images will be observed during each trial. It may be suggested that although these images are not stored permanently, the dynamic distribution of attentional resources proposed by Gorgoraptis et al. (Gorgoraptis et al. 2011) may still apply. The speed at which the images are presented may cause an overlap in attentional resources, contributing to an increase in cognitive load as attention is refocused through consecutive images. It may also be suggested that this attentional capacity should approximate 4 items (Luck & E. Vogel 1997), matching the peak in activity indicated by the difference in recorded voltage between events 10 and 20 (Figure 39a).

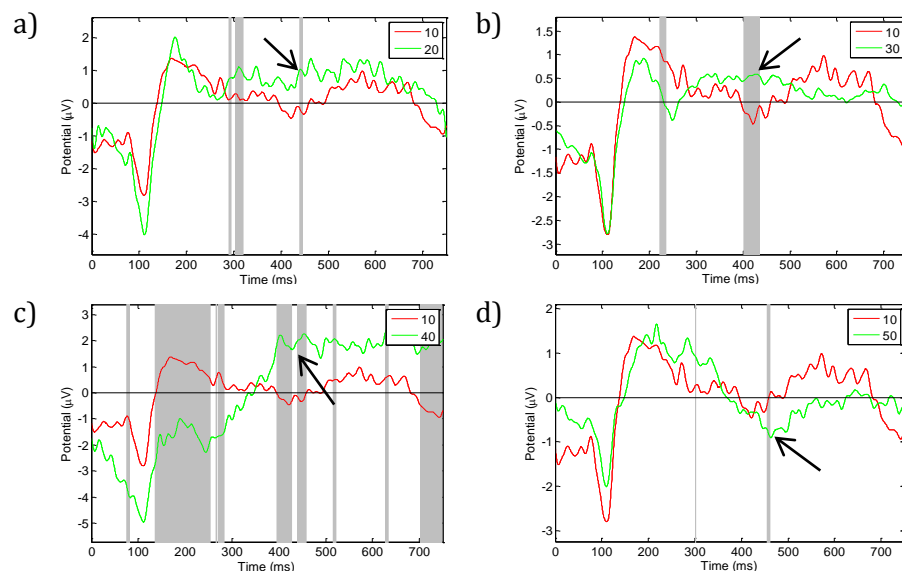


**Figure 39: Comparative analysis of the PFC, electrode Fc5. a) Events 10 and 20. b) Events 10 and 30. c) Events 10 and 40. d) Events 10 and 50; with grey bars indicating regions of interest as calculated from paired t-test results.**

After the cue to ‘store’ the image is received (event 120), a representation is held within the PFC (event 30; Figure 39b). The slight decrease in positivity suggests that this process is relatively stable, requiring less cognitive activity to maintain. As a match is found, a substantial increase is observed; indicating higher-order cognitive functions such as recognition and image recall (Figure 39c). Finally, a substantial decrease in positivity is detected at event 50 as images are passively observed, whilst participants await the end of the task.

As mentioned previously, similar changes in activity occur over the centro-parietal and temporal regions (electrodes Cp5 and T7). This indicates some level of functional

interaction between these areas, reflecting a flow of information associated with memory encoding mechanisms and the recognition of a matching image. Examining regions of statistical significance over the central and parietal regions are beyond the boundaries of this project. However, some interesting observations may be found. Figure 40 shows the relative activity of each event, over the centro-parietal regions, at each stage of the working memory task. An initial examination was made of the statistical differences occurring around 400 ms post-stimulus. This figure illustrates regions of increased positivity across events 20 and 30 (Figure 40a&b), reflecting the internal maintenance of memory. A relative absence of statistical difference was observed during event 40 during the same time period (Figure 40c). The reason for this could be the development of a LPC after 400 ms, indicating memory retrieval (West & Ross-Munroe 2002). Finally, at event 50, an increase in negativity was recorded (Figure 40), reflecting the task-realization after having found a match (West et al. 2001; Kutas & Federmeier 2011).

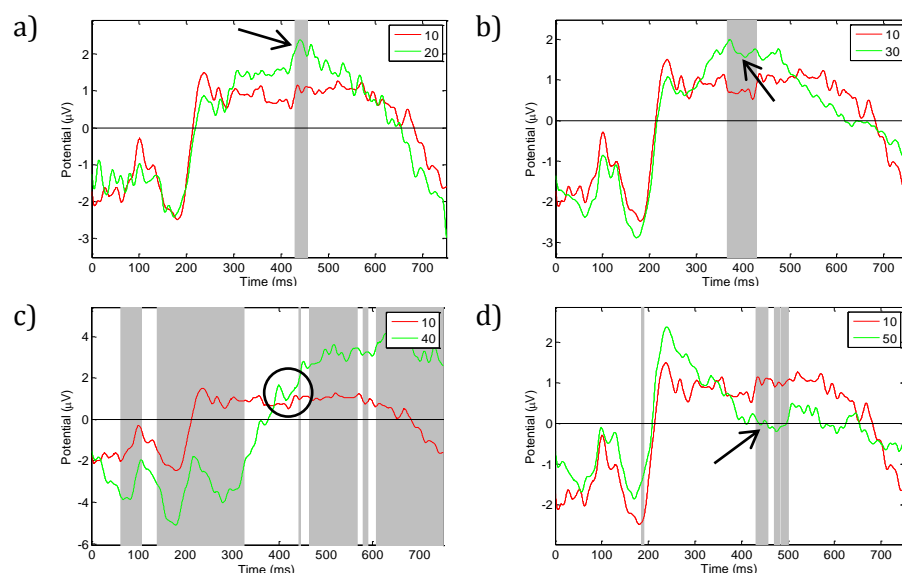


**Figure 40: Comparative analysis of the centro-parietal region, electrode Cp5. a) Events 10 and 20. b) Events 10 and 30. c) Events 10 and 40. d) Events 10 and 50; with grey bars indicating regions of interest as calculated from paired t-test results.**

A comparison of events illustrating statistical significance over the temporal lobe is shown in Figure 41. Again, activity was noted around 400 ms after stimulus onset. Prior to making a match, increased positivity was observed, indicative of stimulus selective activity and the anticipation of a match (Sakai & Miyashita 1991). This effect is no longer seen through events 40 and 50 as a match was no longer expected. During event 40, a substantial region of negativity was observed between 80 and 320 ms. This may be explained by specific task-related processes associated with a matching image.

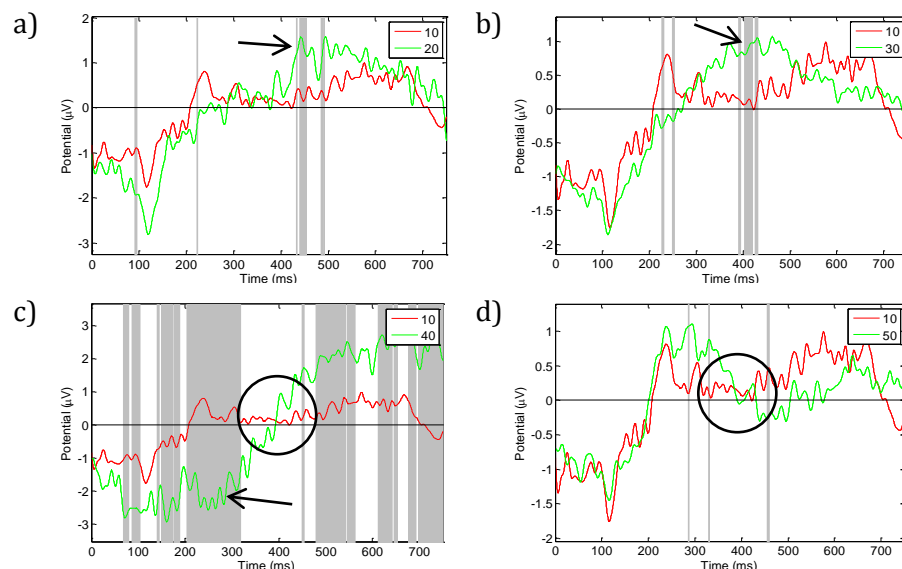


**Figure 41: Comparative analysis of the temporal lobe, electrode T7. a) Events 10 and 20. b) Events 10 and 30. c) Events 10 and 40. d) Events 10 and 50; with grey bars indicating regions of interest as calculated from paired t-test results.**

These results are strong indicators of functional interaction between the ITC, PFC, and parietal regions, once again indicating that the original hypothesis was correct. Further evidence will now be presented by means of an ERP analysis; transient components time-locked to the presentation of stimuli and therefore associated with processes related to visual working memory.

### The C1 and P1 Components

The P1 component, which usually occurs over the PVC regions, is associated with visual processes related to colour perception, spatial orientation, and contour detection. Figure 42 compares the extrastriate electrode, O2, across each event. An initial comparison showed a slight increase in P1 positivity during event 20, reflecting a gradual increase in visual attention with expectation of a cue to ‘store’ post-stimulus (Figure 42a). Although this increase was not highlighted in the t-test scores (regions highlighted in grey), this may be due to the relatively strict alpha value,  $\alpha = 0.01$ , or inter-subject variability. After the image was stored in working memory, the P1 amplitude decreased to levels almost identical to those observed during event 10 (Figure 42b). This may be explained if an assumption is made, suggesting that intent to store an image requires a higher level of activity to permit complex feature retention, whereas subsequent comparisons elicit a smaller response. An increase in activity was detected through event 40, as visual features were perceived within a matching image (Figure 42c). Finally, as subsequent images are passively observed and there was less

need to attend to specific object-features, peak amplitude was once again reduced (Figure 42d).

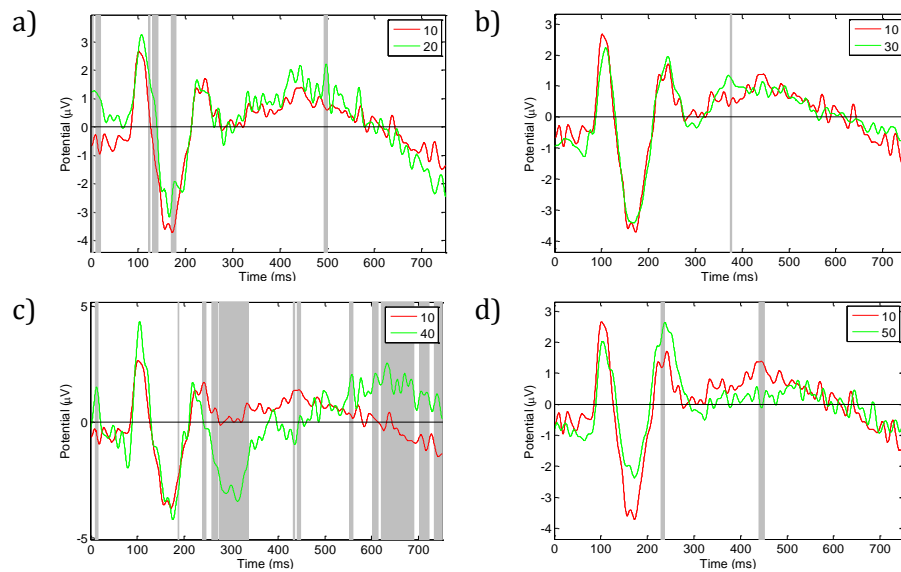


**Figure 42: Comparative study of ERP components C1 and P1 during image perception recorded from electrode O2. a) Events 10 and 20. b) Events 10 and 30. c) Events 10 and 40. d) Events 10 and 50; with grey bars indicating regions of interest as calculated from paired t-test results.**

Component C1 is also present in the extrastriate regions, typically occurring between 80 - 100 ms post-stimulus. As described previously, the C1 component is dependent on the locality of the visual image in the field of vision (Section 1.3.2). Objects presented in the lower field of vision exhibit a positive deflection, whilst those in the higher field of vision respond with a negative deflection. During EEG recording, the display monitor was located slightly below the midline, in the lower field of vision. For this reason, the C1 component should be occluded within the P1 waveform. The relative contribution to P1 is dependent on the height of each participant. Although it may be argued that a C1 component is visible, particularly during events 30, 40, and 50, these components are not visible during event 10, and are not highlighted as being statistically significant.

### **The N2 and P3 Components**

The N2 component is typically observed peaking in the posterior regions, associated with the detection of an unexpected stimulus accompanying an attentional reflex. Looking back at Figure 40, the N2 amplitude remained fairly consistent during events 10, 20, 30, and 50. However, as a match was recognised (event 40), a rapid increase in negativity was observed, developing over the centro-parietal regions. Figure 43 shows clear evidence of a task related difference in activity reflecting recognition of a match-to-sample stimulus.

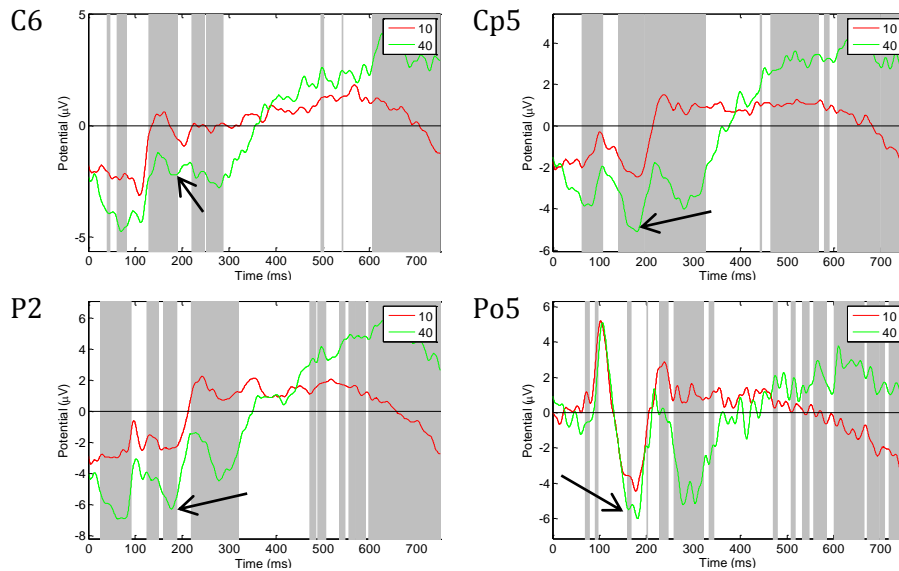


**Figure 43: Comparative study of ERP component N2 during image perception, with grey bars indicating regions of interest as calculated from paired t-test results.**

Similarly, the N2pc component, observed contralateral to a spatially-variant stimulus, is associated with selective attention mechanisms. Due to time restrictions, this feature could not be studied. Therefore, a point of further study would be to examine ERPs for hemispheric differences during presentation of a centrally-fixated stimulus.

The P3a component is generally associated with mechanisms involving the detection of a novel stimulus between 250 and 280 ms post-stimulus (Hagen et al. 2006). It is possible that early presentations of fractal images elicit such a response (Figure 44a). The P3a component was also detectable during passive observation (Figure 44d).

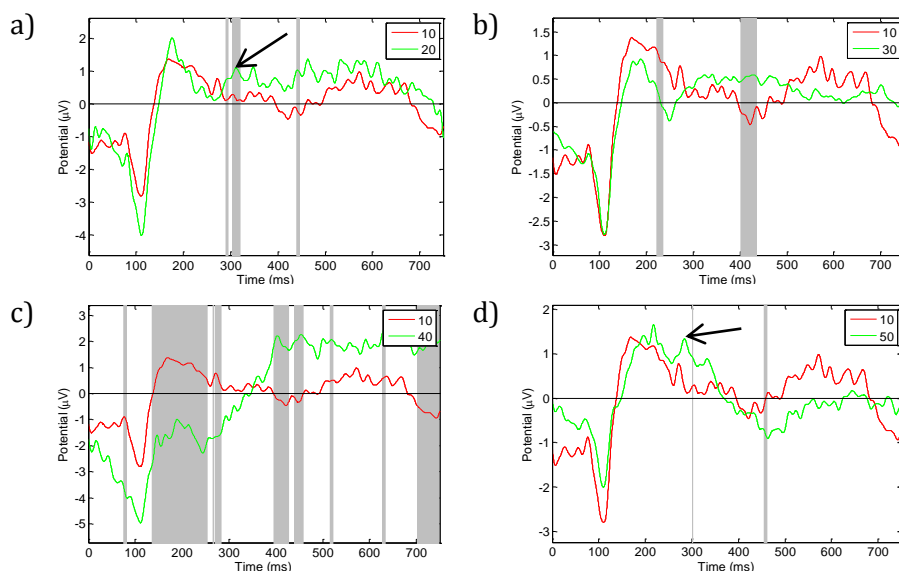


**Figure 44: Comparative study of ERP component P3a during image perception recorded from electrode Fc5. a) Events 10 and 20. b) Events 10 and 30. c) Events 10 and 40. d) Events 10 and 50; with grey bars indicating regions of interest as calculated from paired t-test results.**

Although the analysis of these components was not essentially part of the main paradigm, the initial hypothesis has been further validated. The detection of these ERP components reflect underlying neuronal activity which confirm the incidence of task-related processes such as those related to visual processing, detection, and recognition.

### 5.3 Additional Results

In addition to results obtained during the main thread of the experiment, analysis of results and subsequent review of literature produced additional observations which are described in the following section.

#### Classification Algorithm

As mentioned earlier, regions of differential activity were observed between events 10 and 40, reflecting underlying neuronal activity as a matching image is observed. These observations were made from a numerically descending listing of t-scores, comparing electrode locations across each image event (Table 16).

Table 16: Extracted from Section 4.2 (Table 5): The t-test results listing electrodes with the largest number of significantly different data points for each image event.

Rank	T-test values comparing each event type							
	10>20	10>30	10>40	10>50	20>10	30>10	40>10	50>10
1	Po5 23.0	Ft7 204.2	C3 1364.5	Cp6 339.3	Tp7 -58.4	Fc3 -133.9	P2 -1165.0	Po8 -117.1
2	F2 16.5	F7 92.6	Cp5 1015.5	Po3 206.6	T7 -31.9	Fc1 -85.7	Cp4 -1034.1	Pz -108.4
3	P3 14.0	Fc5 66.1	Cp3 1010.3	Cpz 182.9	O2 -29.8	C5 -70.5	Cp2 -1022.8	Pcz -76.6
4	Fz 12.5	F5 54.5	C5 957.0	P1 176.9	Cp5 -26.0	C3 -63.4	Po4 -997.7	Cpz -70.9
5	O1 9.3	T7 32.0	P3 845.8	C6 163.0	Fp2 -25.0	Fc5 -61.5	P4 -989.6	Cp2 -49.0
6	Fcz 5.5	Ft8 14.4	P5 804.5	Cp1 160.2	Ft8 -23.7	Fcz -55.2	Cp1 -984.7	P2 -48.7
7	T7 5.0	C6 7.2	C1 801.3	P3 159.7	Fc1 -22.5	Cp5 -39.4	Cp3 -971.7	C4 -46.3
8	Ft7 3.7	F3 7.0	Cp1 727.1	Pz 150.5	C5 -19.9	F1 -39.1	Pz -957.1	P4 -41.2
9	Fc1 2.8	Fp1 5.4	Fc3 708.5	Cp4 144.4	C1 -18.4	Ft7 -38.1	P1 -948.5	C6 -40.3
10	Po7 2.5	C4 5.3	Fc1 664.8	Cp2 139.7	Fc2 -18.3	C1 -35.4	C3 -943.8	Cp4 -40.2

The greatest overall activity was distributed over the parietal and central cortices. Having already accounted for the N2 component (Figure 43) and LPC (Figure 33) in the previous sections, further detail may be observed which is as yet unaccounted for. Figure 45 indicates the presence of a distinct negative modulation, which may perhaps indicate the presence of neuronal activity associated with recall or matching mechanisms. An alternative hypothesis, given that the central region is home to a vast array of motor neurones, is that the participant may be forming intent to perform motor function; deciding upon which button to press. During 10-50 comparisons, this behaviour continues, with increased activity observed over the parieto-occipital regions, perhaps indicating the spatial component of the aforementioned intent to perform movement.

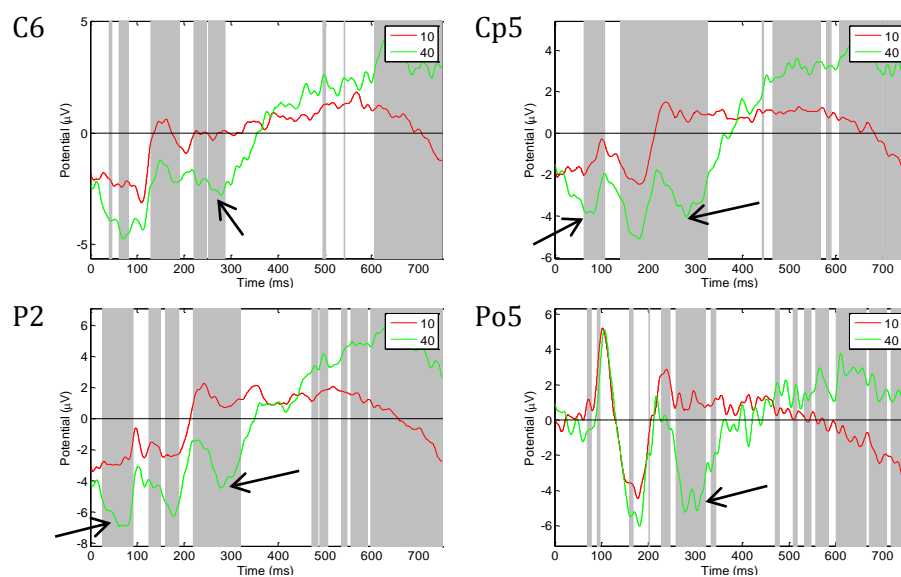


**Figure 45: Comparison of 10-40 ERP waveforms over the central and parietal regions, with grey bars indicating regions of interest as calculated from paired t-test results.**

Interestingly, it was found that the highest distribution of ITC and PFC activity relative to each event was recorded during the 10-30 comparison (Section 4.2: Table 5). During this event, visual stimulus is held in working memory whilst the participant looks for a match in subsequent images. Therefore, the change in activity observed during this event may be explained by the continuous and repetitive upload of images into working memory as a match is sought.

Once again, even at a basic level of processing, the original hypothesis is proven with a substantial change in activity observed over the PFC and ITC whilst an image was retained in memory, and a large neuronal response detected upon finding a match.



## Conscious Perception

In 2011, Railo et al. proposed a model consisting of three distinct correlates of consciousness (Railo et al. 2011), an early P1 component followed by a differential negative offset termed *visual awareness negativity* (VAN) typically observed prior to a wave of late positivity (LP). Comparing ERPs obtained during exposure to unperceived and perceived stimuli showed decreased positivity in P1 at approximately 100 ms post-stimulus over the extrastriate regions of the primary visual cortex. This was assumed to reflect the preconscious sensory processing of visual features. Between 200 and 250 ms after stimulus presentation, VAN was observed over the occipito-temporal regions. It was proposed that this component could be associated with conscious visual perception, independent of non-spatial attention. The final LP component was observed to peak between 300 and 400 ms predominantly over the parietal and central regions and was thought to be caused by higher order cognitive functions related to the manipulation and processing of consciously perceived stimuli. Figure 46 shows an ideal waveform illustrating the components of conscious perception as proposed by Railo et al.

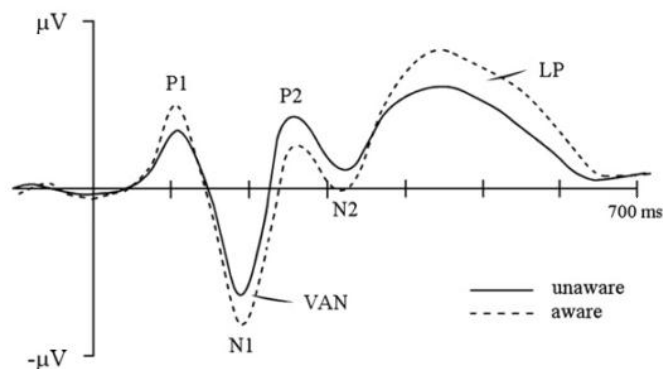
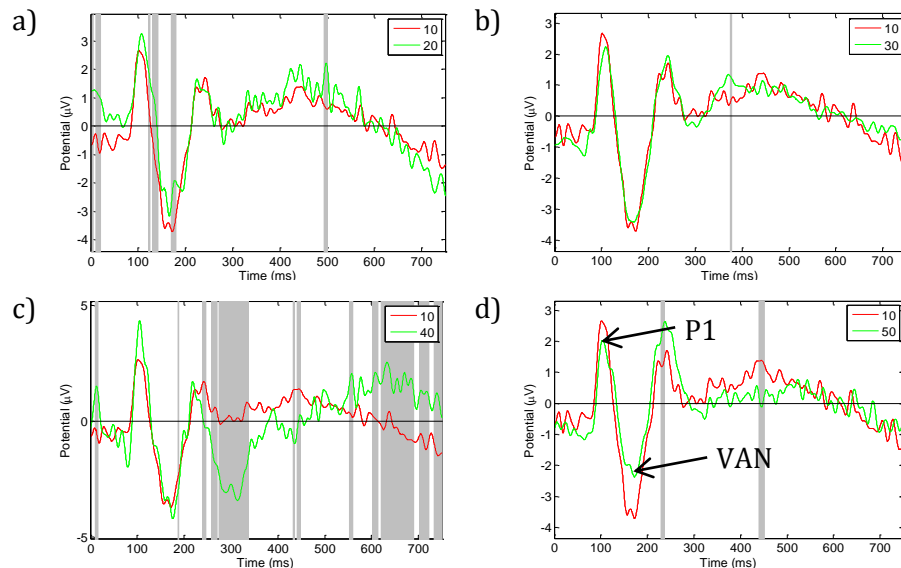


Figure 46: An idealized ERP waveform illustrating the three proposed correlates of consciousness, P1, VAN, and LP. VAN- visual awareness negativity, LP- late positivity (Adapted from Railo et al. 2011).

Examining the results obtained during this current study, it is easy to observe the P1 and VAN components (Figure 47d) over the primary visual cortex (electrode O2). The VAN component is explicitly observed at a peak latency of 180 ms, which is equivalent to the idealized waveform in Figure 46.



**Figure 47: Grand averaged ERPs reflecting activity over the primary visual cortex, electrode O2. a) Events 10 and 20. b) Events 10 and 30. c) Events 10 and 40. d) Events 10 and 50; with grey bars indicating regions of interest as calculated from paired t-test results.**

It can be assumed that participants, having already made a match during event 40, did not make a concerted effort to attend to subsequent stimuli (events 10 and 50 correspond to aware and unaware visual perception, respectively). Thus, reducing the amount of preconscious processing required within the extrastriate regions. Minimal attention required during passive observation caused a reduction in activity over the occipito-temporal region. It should be noted that electrode O2 was assumed to provide an adequate representation of these regions.

Figure 48 shows a comparison of grand averaged ERPs over the centro-parietal region, electrode Cp5. Observing again, event 50 (the ‘unaware’ condition), the late positive deflection clearly shows increased negativity (compared to an increase in positivity during the ‘aware’ conditions, events 20 and 30), matching results obtained by Railo et al., indicating a reduction in conscious processing. Given that images at this point in the trial were given considerably less attention, it is sensible to assume that less visual processing was required. However, contrary to what was reported by Railo et al., the LP component observed during event 50 is here shown peaking between 500 and 600 ms. The reasons for the delay are potentially a task-specific difference due to the fact that events 20 and 30 match the results of Railo et al., peaking between 400 and 500 ms, whilst event 40 (Figure 48c) continues to increase positively over the whole epoch. What is potentially more interesting is the relative amplitude of event 10, compared to the positive deflection present in events 20 and 30, and decreased positivity of event 50. Recalling the LPC described in Section 1.3.2, it may be suggested that the LP

component may be linked to processes other than VAN, such as explicit memory functions linked to the 'old/new' effect.

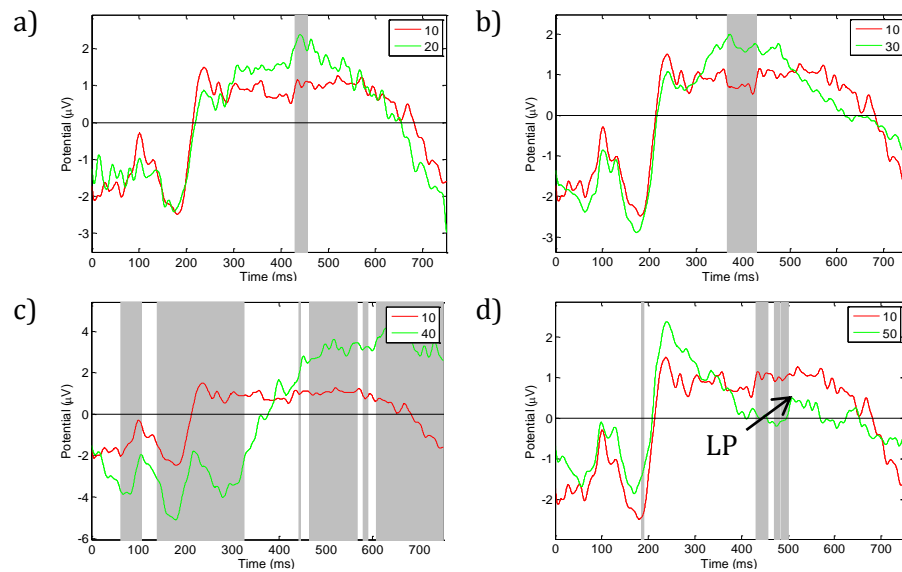


Figure 48: Grand averaged ERPs reflecting activity over the centro-parietal region, electrode Cp5. a) Events 10 and 20. b) Events 10 and 30. c) Events 10 and 40. d) Events 10 and 50; with grey bars indicating regions of interest as calculated from paired t-test results.

## 5.4 Limitations of Study

The results obtained from this study matched well with the original hypothesis. However, there is always room for improvement. For this reason, the following section will describe the limitations present within the current paradigm, whilst indicating suggested improvements.

### EEG Recording

Although clear results were obtained from this study, a more detailed analysis may be achieved if recorded signal strength is improved. This may be done in a number of ways, the simplest of which being to increase the number participants, or development of EEG technique. During the course of this project, through training and practice, clear improvements were made in the technical abilities presented during experimental preparation.

Performing the experiment in an electrically isolated location would reduce high frequency noise received from other equipment. Whilst increasing the distance between the participant and the image display would reduce and potentially remove the noise generated by the CRT monitor refresh rate. Eliminating these sources of man-made noise would allow the entire EEG frequency spectrum to be retained, preserving

lower harmonic frequencies, and resulting in a more complete frequency summation within potential waveforms.

### **Software Limitations**

Care was taken during the course of this work to maintain consistency between the analytical methods used in NeuroScan Edit and EEGLab. However, it is of course preferable to achieve some level of continuity and conduct all pre-processing and analysis of EEG data within EEGLab. This would allow access to the full range of functionality within the software (Delorme & Makeig 2004), allowing a powerful analysis to be accomplished.

### **Mnemonic Devices**

It has been shown that the results obtained during this work clearly agree with the experimental hypothesis regarding working memory, however, the appearance of a late positive component may indicate some degree of longer term memory encoding. Although the task was designed to minimize the use of mnemonic devices, a variety of primitive methods were exploited by each subject. One particular technique involved the internal repetition of a verbal label, figurative or in the abstract to describe the image. Studies have shown that words are easier to retain than images (Doty & Savakis 1997), therefore assigning a semantic label to an unfamiliar stimuli would be considerably advantageous. Participants reported using a variety of descriptive phrasing including, "big red triangle" or "Mick Jagger's lips". Figurative labels generally consisted of 3 to 5 words describing some component of the image, its colour, shape, or size. Abstract labels typically described the object as a whole and most often evoked highly vivid imagery such as "Christian doily", "evil Mexican god" (Figure 49), "the flying plectrum", and "Star Fox ship". Less imaginative participants employed lower level descriptions with numerous references made to images with imagined teeth, star ships, and flowers. Due to the speed with which the sequence of images progressed, subjects were not able to consistently maintain this level of linguistic creativity, meaning that quite often amalgamations between the two styles arose. It is suggested that highly vivid imagery may encourage certain associations and registrations in semantic memory. Hence, there is a difficulty ensuring that subjects are maintaining a visual representation and not a label. Furthermore, the registration of semantic labels and deconstruction of complex images into single features such as colour and shape reduces the likelihood of interference since these features are encoded in different parts of the brain (Allen et al. 2006). This hypothesis is reinforced by the increase in

activity over the occipital lobe during the 10-30 comparison, observed in Section 5.1 (Table 14).

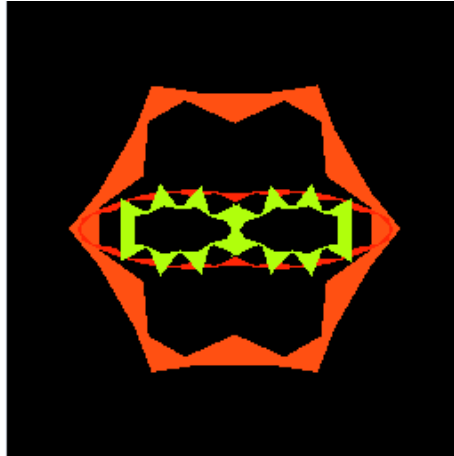


Figure 49: Randomly generated fractal image number 109, the 'evil Mexican god'.

It is suggested, though unlikely, that there may also be some emotional connection to the images. It is known that responses to emotional stimuli differ greatly between the sexes. Work conducted by Lithari et al. observed that females were likely to exhibit a greater reaction to emotive imagery than males, particularly if it was unpleasant (Lithari et al. 2010). The consequences of this are most likely negligible since individual responses to arousing stimuli would most certainly average out in an ERP. However, differences between brain anatomy, chemistry, and function may still have considerable impact on recorded EEG. An interesting review published by Cahill illustrates a range of cognitive and behavioural distinctions between the sexes, including working memory and vision (Cahill 2006). This current study analysed grand averaged data from 4 male and 5 female participants. It may be assumed then, that these ERP components essentially represent a generalized human response, rather than a true account of brain activity. Whilst being rather inconsequential for the purposes of this study, it may be interesting to investigate this further in an effort to detail specific activity relevant to each gender.

## 5.5 Further Study

The recording of EEG data allows a wealth of information to be obtained regarding cognitive functioning. Although the aims of this project were accomplished and evidence was found to intrinsically link the ITC and PFC with the upload and download of information in visual working memory, recorded EEG will not simply be discarded.

Future work and analysis may be carried out in order to obtain valuable insight into the complex mechanisms and interactions between these, and other regions of the brain.

### **Data Processing and Analysis**

Due to the time constraints placed on this project it was not possible to conduct a fully comprehensive analysis. However, it is hoped that additional future work will be carried out. Further analysis of the time-domain correlates of visual working memory, to confirm t-tests are genuine differences and not false positives could be explored with an ANOVA comparing across all permutations, followed by post hoc comparisons to explore where differences occur.

In this work, EEG data was analysed solely in the time-domain by producing event related averages. It would be interesting to conduct a time-frequency analysis in order to identify particular frequency bands. Event-related spectral perturbation (ERSP) measures changes in power, at each frequency, over time. These measures can be associated with the ERP to determine whether individual components are caused by specific power differences in specific frequency bands. Comparing across scalp locations under various experimental conditions allows the identification of varying levels of activity in particular regions. To determine functionality, a topographical analysis of frequency distribution would enable the localization of neuronal activity.

As evidenced by this project, a visual working memory task involves a multitude of neuronal activations, including: visual perception and processing, identification of task-relevant stimuli, formulation of intent to perform a task, internal visual representation and encoding of memory, manipulation and retrieval of memory, cognitive processing involved in the determination of a match, and motor function intent and execution. Using information gained from a coherence analysis, features such as phase may be used to assess how alike two signals are for a specific event at a specific point in time. Performing clustering or ICA decomposition should identify regions of synchronicity and substantiate interaction, or functional connectivity, between cortices. Furthermore, the relative contribution of each frequency to the overall waveform may be determined by decomposing individual epochs into frequency components. From this, the directional flow of information may be identified, reflecting driving mechanisms, whether unidirectional or bidirectional, within the brain.

One such study by Sarnthein et al. measured EEG coherence between the PFC and posterior electrodes of subjects performing a delayed response task (Sarnthein et al. 1998). In accordance with Baddeley's working memory model (Baddeley et al. 2011), they accounted for both visual and verbal working memory by requiring the retention of abstract images or strings of characters. Phase-locked coherence was observed in the theta range (4-7 Hz) during retention intervals, which subsided during image presentation. Their results revealed a synchronicity between the PFC and posterior regions, implying an interaction between the frontal memory store and the posterior sensory association area.

### **Adjustment of Experimental Paradigm**

The working memory task utilized in this project achieved good results and most subjects were able to perform well. This is not to say however, that there is no room for improvement. Although subsequent analyses may be carried out using the data obtained in this project, it is suggested that further study is necessary using an alternate paradigm.

Delayed match-to-sample tasks ensure that late ERP components do not contaminate subsequent correlates of task-related processes, ensuring that only activity relevant to the task is analysed whilst allowing the observation of late neuronal activity. Bilateral presentation of visual stimuli at fixed spatial coordinates would allow hemispheric comparison of the N2pc component and contralateral delay activity (CDA), both of which are important neural correlates associated with visual working memory. Also, ERP components indicative of the old/new effect may be observed, reflecting the strength of recognition to a previously observed image.

Kessler and Kiefer conducted ERP studies in order to observe the functional involvement of the PFC during a visual working memory task (Kessler & Kiefer 2005). Their paradigm, a modified match-to-sample task (Figure 50), required participants to retain a shape in working memory (task difficulty was varied by increasing load) throughout a period of retention which may or may not include interference (complex shape). After a short recovery interval, participants were presented with the original shape and required to determine whether it had changed in size.

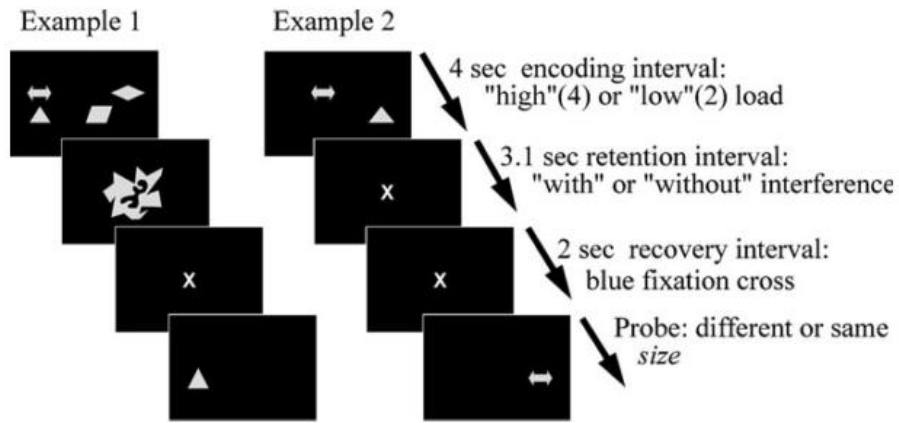


Figure 50: Experimental paradigm of Kessler and Kiefer's visual working memory task (Kessler & Kiefer 2005).

Their results (Figure 51) produced clear ERP waveforms, where baseline was calculated 200 ms prior to the onset of the stimulus. This type of paradigm ensured a distinct separation between transient ERP components, eliminating contamination from subsequent task-related activity.

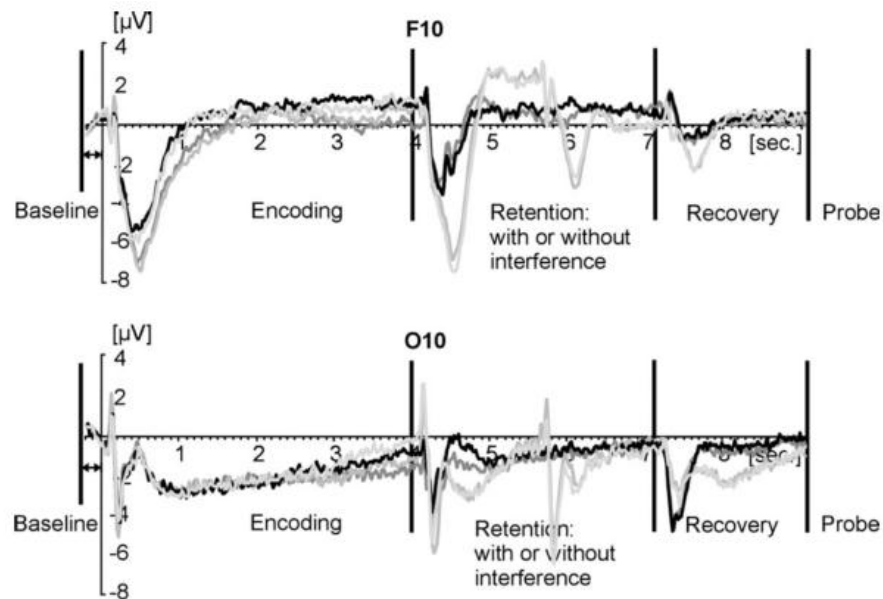


Figure 51: Time course of activation under electrodes F10 and O10 across trials, showing ERP modulation associated with various cognitive processing (Kessler & Kiefer 2005).

In a limited manner, this thesis began by introducing visual working memory. It is suggested that future studies delve deeper into the psychological aspects of this area in an attempt to better understand and correlate specific human behaviours with their neuroanatomical and electrophysiological predicates.



For the purposes of this thesis, Baddeley's working memory model was identified as a widely accepted theory, and therefore no further contentions were made. However, within the realms of psychological theory, multiple models exist and debate remains heated. One thought-provoking example is a "*core knowledge architecture of visual working memory*" by Justin Wood (Wood 2011). In this model he describes working memory as an innate core-knowledge system consisting of three subsidiary systems: spatiotemporal, object property/type, and view-dependant snapshots. An intriguing point of inquiry may be to build on this work, using the investigative methodology developed here to find evidence of the neural substrates involved in the support of this third subsidiary system.

### **Localisation of Function within Specific Domains**

Results obtained from this study, although accurate, suggest only a basic representation of the underlying neuroanatomical functionality during visual working memory (Ranganath & D'Esposito 2005). Work by Ranganath and D'Esposito suggested a complex network of interactions responsible for sustaining an internal representation of visual stimuli (Figure 52). Their proposed model defined functional connectivity between the ITC and medial temporal lobe (consisting of the medial temporal cortices and the hippocampus), aided by feedback mechanisms from the PFC. Citing that the medial temporal lobe, due to its considerable plasticity, may be responsible for the maintenance of novel, complex objects. This model suggests that the representation of visual stimuli in the ITC requires the activation of associated neurones within the medial temporal lobe, whilst top-down maintenance of visual working memory originates from regions of the PFC.

There is much debate regarding the identification of functional substrates within the PFC itself (Ranganath & D'Esposito 2005). As mentioned earlier, there is evidence to suggest the ventral and dorsal PFC areas are responsible for maintaining information pertaining to object and spatial features. Likewise, ventral and dorsal regions have been identified as being associated with the maintenance and monitoring/manipulation of information, respectively. The model suggested by Ranganath and D'Esposito is essentially an amalgamation of these theories (Figure 52). It may be suggested that the multi-functionality of the PFC may extend even further. Further domain specificity has detailed the inclusion of analytical representations in the left-hemisphere, with right-hemispheric maintenance of image-based representations (Courtney et al. 1998).

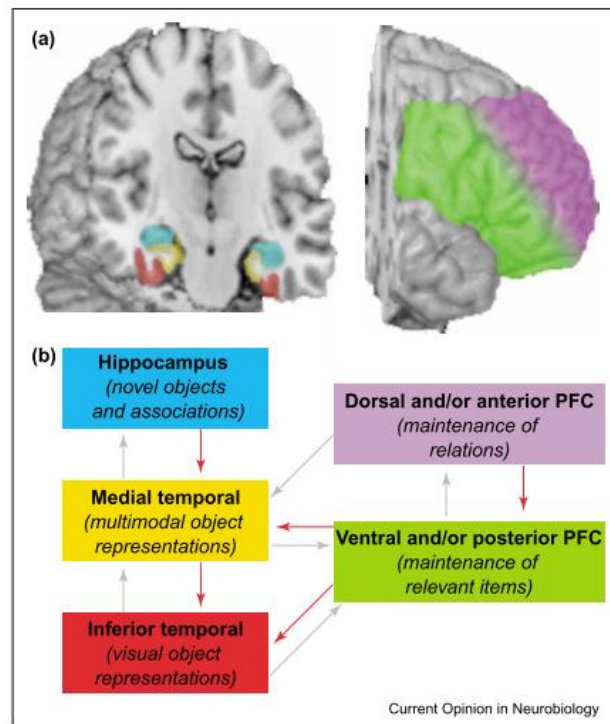


Figure 52: Regions of the brain implicated in the functionality of visual working memory. a) Neural substrates of visual working memory. b) Processes involved in the maintenance of internal visual representations and associated regional interaction. (Ranganath & D'Esposito 2005).

To obtain a truly comprehensive and detailed understanding of the interactions between the PFC and ITC, it is likely that the current methodology should be expanded on. The inclusion of imaging techniques such as fMRI would increase the accuracy in which the functionality of specific substrates may be determined. Alternatively, an increase from 64 to 128 channel EEG systems would enable continuous EEG recordings to be made at a much higher spatial resolution, whilst maintaining temporal detail. Combining these techniques would also allow a better indication of functional locality of activity within specific regions of the brain. MEG, similar to EEG, is able to detect tangential components of magnetic fields generated by neuronal units. Unlike EEG signals, MEG is not attenuated through the skull and intervening tissues, resulting in a higher temporal and spatial resolution. Last but not least, pioneering work conducted within the field of optogenetics (an innovative technique involving precise temporal control over the activation and deactivation of specifically targeted neuronal units), may someday soon, hold the key to unlocking this puzzle forever (Dolzani et al. 2012).

## 5.6 Final Note

It is important to remember that neural anatomy is an intricate and often convoluted system. Nevertheless, over the past few decades the inner workings of the brain have become much easier to access. Observations made and conclusions drawn from a plethora of physiological, medical imaging, and electroencephalographic studies have allowed a greater understanding of the functionality and locality of distinct processes within the brain. Meanwhile, advances have also been made in behavioural psychology, allowing a greater understanding of the sociological and cognitive aspects of this function. There are indeed exciting times ahead, which must be offset by the inevitable misconstructions along the way. For each idealised theory there is an opposing view and for each working model there are a multitude of enhancements. For all that is learned, there is a danger that assumptions be reflected in the choice of literature reviewed and the formation of any hypotheses. In this study, steps were taken to ensure unbiased results by conducting a critical review of the working paradigm and developing a robust analytical technique. Even so, the results obtained from this project indicate remarkable similarities with current literature. It is for this reason that the following declaration must be made. That is, to the best of this author's knowledge, all sources referred to within this document are accurate and verifiable, and that the results obtained are a true reflection of neurological activity.

# Chapter 6

## Conclusion

In conclusion, this study considered evidence of interaction between the inferior temporal lobe and pre-frontal cortex during a visual working memory task. The primary focus of this experiment was to determine whether the brain's ability to encode and maintain an internal representation of a visual stimulus for comparison to subsequent visual stimuli was linked to specific neural correlates. Visual working memory requires the activation of visual association areas of the inferior temporal lobe and pre-frontal cortex during task-related processes. The temporal lobe stores transient information about a visual image that is overwritten by subsequent images. The pre-frontal cortex is utilized in working memory and provides contextual information about a visual scene which can be accessed before an image is fully processed. It was hoped to identify the distinct mechanisms involved in these processes by conducting an electrophysiological analysis.

EEG data was recorded using a 64-channel montage whilst a participant was engaged in a modified sequential matching task. A classification algorithm was developed to select an unbiased, but meaningful, distribution of electrodes across the scalp. A statistical analysis found transient activity within the temporal lobe evident of the temporary storage of information, whilst each image was briefly maintained for comparison. Temporo-frontal interactions were observed during image recall and match recognition processes. An ERP analysis revealed functionally, temporally, and spatially distinct modulations associated with task-related activity and their neural correlates.

An understanding of cognitive and perceptual processes as they relate to neuroanatomical substrates allow clinical observations to be made regarding working memory functioning. This has implications in the assessment and understanding of various psychological and neurological conditions, including degenerative diseases where working memory is affected. In summary, the current protocol was successful in identifying differential activity during key task-related events. This activity is plausible evidence of memory based processes in a number of key areas, including the inferior temporal lobe and pre-frontal cortex.

# References

- Allen, R., Baddeley, A. & Hitch, G., 2006. Is the binding of visual features in working memory resource-demanding? *Journal of experimental psychology. General*, 135(2), pp.298–313.
- Alvarez, G. & Cavanagh, P., 2004. The capacity of visual short-term memory is set both by visual information load and by number of objects. *Psychological science*, 15(2), pp.106–11.
- Atkinson, R. & Shiffrin, R., 1968. Human memory: A proposed system and its control processes. In *The psychology of learning and motivation: Advances in research and theory*. New York: Academic Press, pp. 89–195.
- Atkinson, R. & Shiffrin, R., 1971. The control processes of short-term memory. *Scientific American*, 225(2), pp.83–90.
- Atwood, G., 1971. An experimental study of visual imagination and memory. *Cognitive Psychology*, 2(3), pp.290–299.
- Awh, E, Barton, B. & Vogel, E., 2007. Visual working memory represents a fixed number of items regardless of complexity. *Psychological science*, 18(7), pp.622–8.
- Baddeley, A., 2000. The episodic buffer: a new component of working memory? *Trends in cognitive sciences*, 4(11), pp.417–423.
- Baddeley, A., 1983. Working memory. *Philosophical Transactions of The Royal Society of London. Series B, Biological Sciences*, 302(1110), pp.311–324.
- Baddeley, A., 1986. *Working memory.*, New York: Oxford University Press.
- Baddeley, A., Allen, R. & Hitch, G., 2011. Binding in visual working memory: the role of the episodic buffer. *Neuropsychologia*, 49(6), pp.1393–400.
- Baddeley, A. & Hitch, G., 1974. Working memory. In *The psychology of learning and motivation, Vol VIII*. New York: Academic Press, pp. 47–90.
- Bar, M. et al., 2006. Top-down facilitation of visual recognition. *Proceedings of the National Academy of Sciences of the United States of America*, 103(2), pp.449–54.
- Bar, M., 2004. Visual objects in context. *Nature reviews. Neuroscience*, 5(8), pp.617–29.
- Becker, M., Pashler, H. & Anstis, S., 2000. The role of iconic memory in change-detection tasks. *Perception*, 29(1974), pp.273–286.
- Berger, H., 1929. Uber das Elektrenkephalogramm des Menschen. *European Archives of Psychiatry and Clinical Neuroscience*, 87(1), pp.527–570.

- Bressler, S. & Ding, M., 2002. Event-related potentials. In *The Handbook of Brain Theory and Neural Networks*. Cambridge: MIT Press, pp. 412–415.
- Broadbent, D., 1957. A mechanical model for human attention and immediate memory. *Psychological review*, 64(3), pp.205–215.
- Broadbent, D., 1958. *Perception and communication*, London: Pergamon Press, Inc.
- Brown, J., 1958. Some tests of the decay theory of immediate memory. *Quarterly Journal of Experimental Psychology*, 10(1), pp.12–21.
- Cahill, L., 2006. Why sex matters for neuroscience. *Nature reviews. Neuroscience*, 7(6), pp.477–84.
- Chapman, R. et al., 2011. Brain ERP components predict which individuals progress to Alzheimer’s disease and which do not. *Neurobiology of aging*, 32(10), pp.1742–55.
- Chun, M., 2011. Visual working memory as visual attention sustained internally over time. *Neuropsychologia*, 49(6), pp.1407–9.
- Cooper, R., Osselton, J. & Shaw, J., 1974. *EEG Technology*, Southampton: Butterworth & Co.
- Courtney, S. et al., 1998. The role of prefrontal cortex in working memory: examining the contents of consciousness. *Philosophical transactions of the Royal Society of London. Series B, Biological sciences*, 353(1377), pp.1819–28.
- Delorme, A. & Makeig, S., 2004. EEGLAB: an open source toolbox for analysis of single-trial EEG dynamics including independent component analysis. *Journal of neuroscience methods*, 134(1), pp.9–21.
- Dolzani, S., Nakamura, S. & Cooper, D., 2012. Brief Report neuroscience A novel apparatus / protocol designed for optogenetic manipulation and recording of individual neurons during a motivation and working memory task in the rodent. *Nature Precedings*.
- Doty, R. & Savakis, A., 1997. Commonality of processes underlying visual and verbal recognition memory. *Brain research. Cognitive brain research*, 5(4), pp.283–94.
- Empson, J., 1986. *Human Brain Waves*, New York: Stockton Press.
- Eng, H., Chen, D. & Jiang, Y., 2005. Visual working memory for simple and complex visual stimuli. *Psychonomic bulletin & review*, 12(6), pp.1127–33.
- Fisch, B., 1999. *Fisch and Spehlmann’s EEG Primer* Third rev., Amsterdam: Elsevier.
- Freedman, D. et al., 2003. A comparison of primate prefrontal and inferior temporal cortices during visual categorization. *The Journal of neuroscience: the official journal of the Society for Neuroscience*, 23(12), pp.5235–46.

- Freunberger, R. et al., 2007. Visual P2 component is related to theta phase-locking. *Neuroscience letters*, 426(3), pp.181–6.
- Fukuda, K., Awh, Edward & Vogel, E.K., 2010. Discrete capacity limits in visual working memory. *Current opinion in neurobiology*, 20(2), pp.177–82.
- Fuster, J., Bauer, R. & Jervey, J., 1985. Abstract: Functional integrations between inferotemporal and prefrontal cortex in a cognitive task. *Brain research*, 330(20), p.299.
- Fuster, J. & Jervey, P., 1982. Neuronal firing in the inferotemporal cortex of the monkey in a visual memory task. *The Journal of Neuroscience*, 2(3), pp.361–375.
- Gjini, K. & Maeno, T., 2007. A multichannel whole-head EEG study on visual working memory processing of spatiality in the human brain. *World Congress on Medical ...*, 14(16), pp.2752–2755.
- Gorgoraptis, N. et al., 2011. Dynamic updating of working memory resources for visual objects. *The Journal of neuroscience : the official journal of the Society for Neuroscience*, 31(23), pp.8502–11.
- Haas, L., 2003. Neurological stamp: Hans Berger (1873 - 1941), Richard Caton (1842 - 1926), and electroencephalography. *Journal of Neurology, Neurosurgery & Psychiatry*, 74(9), p.9.
- Haenschel, C. & Linden, D., 2011. Exploring intermediate phenotypes with EEG: working memory dysfunction in schizophrenia. *Behavioural brain research*, 216(2), pp.481–95.
- Hagen, G. et al., 2006. P3a from visual stimuli: task difficulty effects. *International Journal of Psychophysiology: Official journal of the International Organization of Psychophysiology*, 59(1), pp.8–14.
- Harrison, S. & Tong, F., 2009. Decoding reveals the contents of visual working memory in early visual areas. *Nature*, 458(7238), pp.632–5.
- James, W., 1891. *The Principles of Psychology*, London: Macmillan.
- Jaušovec, N. & Jaušovec, K., 2012. Working memory training: improving intelligence--changing brain activity. *Brain and cognition*, 79(2), pp.96–106.
- Jeon, Y. & Polich, J., 2001. P3a from a passive visual stimulus task. *Clinical neurophysiology : official journal of the International Federation of Clinical Neurophysiology*, 112(12), pp.2202–8.
- Jonas, J. et al., 1990. Histomorphometry of the human optic nerve. *Investigative ophthalmology & visual science*, 31(4), pp.736–44.

- Kessler, K. & Kiefer, M., 2005. Disturbing visual working memory: electrophysiological evidence for a role of the prefrontal cortex in recovery from interference. *Cerebral cortex (New York, N.Y. : 1991)*, 15(7), pp.1075–87.
- Kok, A., 2001. On the utility of P3 amplitude as a measure of processing capacity. *Psychophysiology*, 38(3), pp.557–77.
- Kutas, M. & Federmeier, K., 2011. Thirty years and counting: finding meaning in the N400 component of the event-related brain potential (ERP). *Annual review of psychology*, 62, pp.621–47.
- Lithari, C. et al., 2010. Are females more responsive to emotional stimuli? A neurophysiological study across arousal and valence dimensions. *Brain topography*, 23(1), pp.27–40.
- Luck, S., 2005. *An Introduction to The Event Related Potential Technique*, Cambridge: MIT Press.
- Luck, S., 1995. Multiple mechanisms of visual-spatial attention: recent evidence from human electrophysiology. *Behavioural Brain Research*, 71(1-2), pp.113–123.
- Luck, S. & Vogel, E., 1997. The capacity of visual working memory for features and conjunctions. *Nature*, 428, pp.748–750.
- Martini, F., Nath, J. & Bartholomew, E., 2011. *Fundamentals of Anatomy and Physiology* 9th ed., Pearson.
- Mccollough, A., Machizawa, M. & Vogel, E., 2007. Electrophysiological measures of maintaining representations in visual working memory. *Cortex*, 43(1), pp.77–94.
- Miller, E. & Desimone, R., 1994. Parallel neuronal mechanisms for short-term memory. *Science*, 263(5146), pp.520–522.
- Miller, E., Erickson, C. & Desimone, R., 1996. Neural mechanisms of visual working memory in prefrontal cortex of the macaque. *The Journal of neuroscience : the official journal of the Society for Neuroscience*, 16(16), pp.5154–67.
- Miller, E., Li, L. & Desimone, R., 1993. Activity of neurons in anterior inferior temporal cortex during a short-term memory task. *The Journal of neuroscience : the official journal of the Society for Neuroscience*, 13(4), pp.1460–78.
- Miller, G., 1956. The magical number seven, plus or minus two: some limits on our capacity for processing information. *Psychological review*, 101(2), pp.343–352.
- Miller, G., Galanter, E. & Pribram, K., 1960. *Plans and the structure of behaviour* H. H. and Company, ed., New York.
- Miyashita, Y., 1988. Neuronal correlate of visual associative long-term memory in the primate temporal cortex. *Nature*, 335(27), pp.817–820.



- Neuhaus, A. et al., 2011. Dissection of early bottom-up and top-down deficits during visual attention in schizophrenia. *Clinical neurophysiology : official journal of the International Federation of Clinical Neurophysiology*, 122(1), pp.90–8.
- Parra, M. et al., 2009. Selective impairment in visual short-term memory binding. *Cognitive neuropsychology*, 26(7), pp.583–605.
- Philips, W., 1974. On the distinction between sensory storage and short-term visual memory\*. *Perception & Psychophysics*, 16(2), pp.283–290.
- Pollux, P. et al., 2011. Event-related potential correlates of the interaction between attention and spatiotemporal context regularity in vision. *Neuroscience*, 190, pp.258–69.
- Prasad, S. & Galetta, S., 2011. *Anatomy and physiology of the afferent visual system*. 1st ed., Elsevier B.V.
- Railo, H., Koivisto, M. & Revonsuo, A., 2011. Tracking the processes behind conscious perception: a review of event-related potential correlates of visual consciousness. *Consciousness and cognition*, 20(3), pp.972–83.
- Ranganath, C. & D'Esposito, M., 2005. Directing the mind's eye: prefrontal, inferior and medial temporal mechanisms for visual working memory. *Current opinion in neurobiology*, 15(2), pp.175–82.
- Rauss, K., Schwartz, S. & Pourtois, G., 2011. Top-down effects on early visual processing in humans: a predictive coding framework. *Neuroscience and biobehavioral reviews*, 35(5), pp.1237–53.
- Rolls, E. & Tovee, M., 1994. Processing speed in the cerebral cortex and the neurophysiology of visual masking. *Proceedings of the Royal Society of London B*, 257(1348), pp.9–15.
- Sakai, K. & Miyashita, Y., 1991. Neural organization for the long-term memory of paired associates. *Nature*, 354(6349), pp.152–155.
- Sanei, S. & Chambers, J., 2008. *EEG Signal Processing*, Cardiff: John Wiley & Sons.
- Sarnthein, J. et al., 1998. Synchronization between prefrontal and posterior association cortex during human working memory. *Proceedings of the National Academy of Sciences of the United States of America*, 95(12), pp.7092–6.
- Sereno, A. & Amador, S., 2006. Attention and memory-related responses of neurons in the lateral intraparietal area during spatial and shape-delayed match-to-sample tasks. *Journal of neurophysiology*, 95(2), pp.1078–1098.
- Sligte, I., Scholte, H. & Lamme, V., 2008. Are there multiple visual short-term memory stores? *PloS One*, 3(2), p.e1699.

- Sturgeon, N., 2012. *Scotland's national dementia strategy: Two years on report (Government Report)*,
- Tokudome, W. & Wang, G., 2012. Similarity dependency of the change in ERP component N1 accompanying with the object recognition learning. *International journal of psychophysiology: Official Journal of the International Organization of Psychophysiology*, 83(1), pp.102–9.
- Treisman, A., 1996. The binding problem. *Current opinion in neurobiology*, 6(2), pp.171–8.
- Ungerleider, L., Courtney, S. & Haxby, J., 1998. A neural system for human visual working memory. *Proceedings of the National Academy of Sciences of the United States of America*, 95(3), pp.883–90.
- Vogel, E. & Luck, S., 2000. The visual N1 component as an index of a discrimination process. *Psychophysiology*, 37(2), pp.190–203.
- Vogel, E. & Machizawa, M., 2004. Neural activity predicts individual differences in visual working memory capacity. *Nature*, 428(6984), pp.748–51.
- Wallis, G., 1998. Spatio-temporal influences at the neural level of object recognition. *Network (Computation in Neural Systems)*, 9(2), pp.265–78.
- Wallis, G. & Bühlhoff, H., 1999. Learning to recognize objects. *Trends in cognitive sciences*, 3(1), pp.22–31.
- West, R., Herndon, R. & Crewdson, S., 2001. Neural activity associated with the realization of a delayed intention. *Brain research. Cognitive brain research*, 12(1), pp.1–9.
- West, R. & Ross-Munroe, K., 2002. Neural correlates of the formation and realization of delayed intentions. *Cognitive, affective & behavioral neuroscience*, 2(2), pp.162–73.
- Wood, J., 2011. A core knowledge architecture of visual working memory. *Journal of experimental psychology. Human perception and performance*, 37(2), pp.357–81.
- Zani, A. & Proverbio, A., 2003. *The Cognitive Electrophysiology of Mind and Brain*.
- Zimmer, H.D., 2008. Visual and spatial working memory: from boxes to networks. *Neuroscience and biobehavioral reviews*, 32(8), pp.1373–95.

# Appendix A

## MATLAB Script

```
set_files=dir('*.set');% collating all files with extention *.set
len=length(set_files);% the number of files within 'set_files'
newname=cell(1,len);% allocating space to save filtered epochs
for i=1:len
    disp(strcat('Processing   ',set_files(i).name))
    EEG =
    pop_loadset('filename',set_files(i).name,'filepath','I:\\EEG
    Project\\test\\');% loading each epoch
    EEG = eeg_checkset( EEG );
    EEG = pop_eegfilt( EEG, 0, 70, [], [0], 0, 0, 'fir1', 0);
    % 0 - 70 Hz band pass filter
    newname{i}=strcat(set_files(i).name(1:end-4),'_filter.set');%
    renaming file
    EEG.setname=newname{i};
    EEG = eeg_checkset( EEG );
    EEG = pop_saveset( EEG, 'filename',newname{i},'filepath','I:\\EEG
    Project\\test\\filter\\');% saving filtered data in new location
    EEG = eeg_checkset( EEG );
end
```

Figure 53: MATLAB script automating the filtering process within EEGLab.

# Appendix B

## Electrode Selection (Cross Analysis)

Table 17: Ordered listing of t-test results with the largest number of significantly different data points for each cross event.

Rank	T-test values comparing each event type							
	110> 120	110> 130	110> 140	110> 150	120> 110	130> 110	140> 110	150> 110
1	Cp2 52.3	Ft8 82.4	C6 296.8	Fc6 204.8	Tp7 -38.9	F8 -141.2	Cp6 -370.9	Cpz -195.9
2	Cp4 46.4	Fp2 54.6	Cp6 159.4	P8 195.5	Fc6 -33.0	Ft8 -58.7	C6 -273.5	Pz -195.7
3	Fpz 45.5	F4 29.7	Fc6 141.3	T8 168.4	F3 -29.2	Fc5 -48.9	Cp4 -245.5	Cp6 -186.2
4	P2 42.6	F6 14.0	P8 127.1	F4 158.5	Cp5 -28.8	Fc4 -27.8	Fc6 -215.3	Cp1 -172.3
5	P4 41.9	F2 13.7	T8 99.4	Tp8 156.7	C3 -28.1	T7 -20.1	Cpz -196.6	Cp2 -161.5
6	Pz 28.1	Fp1 11.6	C4 89.8	F6 137.8	F8 -25.6	Fc6 -16.8	Cp2 -194.9	Po4 -150.7
7	P8 27.0	F8 9.7	Fc4 78.1	Cp6 120.5	F7 -25.2	Ft7 -11.7	C2 -194.8	Po8 -138.1
8	Cp6 24.7	Af4 4.9	Tp8 76.6	C6 112.1	P2 -22.3	F6 -11.0	C1 -161.6	P1 -124.4
9	P1 23.5	Fc4 3.7	P6 68.8	P6 99.8	P7 -17.7	Tp7 -9.1	P6 -155.5	Cp5 -108.9
10	Cp5 23.3	Tp8 2.8	Af4 61.7	P5 99.0	Po4 -14.8	T8 -8.2	Fc4 -155.5	P8 -104.0

# Appendix C

## Participant Information Sheet

**University of Strathclyde**  
**Bioengineering Unit**  
**Neurophysiology Lab**



**University of**  
**Strathclyde**  
**Glasgow**

### **Title of the study**

*Interactions between the pre-frontal cortex and temporal lobe in visual working memory: An EEG study*

### **Introduction**

This experiment is conducted by Sonia Mitchell, an MSc student at University of Strathclyde, Bioengineering Unit, as part of her research experiment. Dr Campbell Reid, a Research Fellow also at the Bioengineering Unit will supervise all experiments.

Sonia Mitchell, MSc Student  
Neurophysiology Lab, Bioengineering Unit, University of Strathclyde  
Wolfson Centre, 106 Rottenrow, Glasgow G4 0NW, Scotland, UK  
Mobile: +44(0)7405736155 Fax: +44 141 552 6098,  
E-Mail: [sonia.mitchell@strath.ac.uk](mailto:sonia.mitchell@strath.ac.uk)

### **What is the purpose of this investigation?**

This experiment is designed to study the brain activity of normal healthy adults with no previous history of neurological impairments in response to visual stimuli.

You will be asked to sit on a chair and observe a series of images. The task involves comparing a target image with subsequent images and you will be asked at the end of each trial if you saw a matching image. During the experiment, you will be wearing a cap. Your brain activity will be recorded by the electrodes on the cap. A conductive gel fills the gap between the cap electrodes and your scalp. This is called Electroencephalography (EEG). After the experiment a towel and shampoo will be provided for washing your head.

### **Do you have to take part?**

Participation is completely voluntary. You are completely free to decide if you want to participate or not. There will be no consequences if you refuse to participate or if you withdraw from participation at any time before or during the experiment, for any reason.

### **What will you do in the project?**

You will sit for the experiment, as previously described. We will attach the electrode cap, as well as electrodes to record your eye movements. The conductive gel is injected through the top of the electrode. To help improve the signals we will lightly rub the scalp under the electrode using the blunt-nosed needle for injecting the gel, or a cotton-tipped swab. This may cause slight discomfort at the time, but is not painful and has no lasting effects. An alcohol swab will be used to clean the skin under the electrodes recording your eye movements. The gel itself is water soluble and easy to wash out. It is highly unlikely that you will have an allergic reaction to the gel or the swabs, and we will test your skin before continuing. If you have a reaction at this point, or at any point during the experiment we will remove the cap and electrodes and you can wash the gel off quickly and easily.

Recording the activity of your brain is easily affected by blinking, jaw clenching, swallowing, eye movements, or by moving your head. We do not expect you to be able to stop these actions during the course of the experiment, we just ask you to focus on the task and stay as relaxed as possible. There will be a short interval between trials as you indicate your response, feel free to blink and move during this time.

#### Task:

The task is a modified sequential matching task. You will sit facing a computer monitor in a darkened room. Each trial consists of a series of 15 images. The images are unique geometric shapes of different colours. Each image will be presented on screen for 750ms and after each image a fixation cross will be presented for 750ms. The colour of the fixation cross will change each time. Your task is to wait for a blue coloured fixation cross. The blue cross indicates that you should remember the image you saw *before* the cross appeared. Once you have an image to remember you then need to observe the subsequent images. At the end of the trial (after 15 images and 15 crosses) you will be asked if you saw a matching image. Use the keyboard provided to give your answer. There will be 100 trials in total, and the total time for preparing and performing the experiment will be around 1.5 hours. If you need to have a break at any point please inform the researcher. At the end of the experiment you will be asked how difficult you found the task and if you adopted any strategies for remembering the images.

Site: University of Strathclyde, Bioengineering Unit, Neurophysiology Lab.

Duration: Total time including the setup should not be more than 1.5 hours.

Compensation/Payments: None.

### **Why have you been invited to take part?**

For this experiment normal, young, healthy participants are recruited. Participants with no neural, psychiatric, or musculoskeletal impairment or disease are included. No specific skill is required for the experiment. Participants need to have normal sight, hearing, and upper limb function.

### **What are the potential risks to you in taking part?**

The recording equipment devices are of medical grade, electrically isolated and periodically inspected. Consequently no risk is predicted regarding the electrical or recording aspects. If you are allergic to EEG conductive gel or EMG abrasive gels and pads, please inform the experimenter.

**What happens to the information in the project?**

Your personal information will not be disclosed to individuals out of our research group without your permission, unless required by law. Your anonymous recording results will be used in reports and scientific publications without any identifiable information included. Your experiment results will be stored on the computers and servers of the University of Strathclyde and the researchers' personal computers.

**The University of Strathclyde is registered with the Information Commissioner's Office who implements the Data Protection Act 1998. All personal data on participants will be processed in accordance with the provisions of the Data Protection Act 1998.**

**Thank you for reading this information – please ask any questions if you are unsure about what is written here.**

**What happens next?**

If you are happy to take part, please sign the accompanying consent form for confirmation. You can ask to be informed if the results are published.

This investigation was granted ethical approval by the University of Strathclyde ethics committee, and by Bioengineering Unit Departmental Ethics Committee.

If you have any questions/concerns, during or after the investigation, or wish to contact an independent person to whom any questions may be directed or further information may be sought from, please contact:

Secretary to the University Ethics Committee  
University of Strathclyde  
McCance Building, 16 Richmond Street, Glasgow G1 1XQ, Scotland, UK.  
Telephone: +44 141 548 2752  
Email: [ethics@strath.ac.uk](mailto:ethics@strath.ac.uk)

Chief Investigator Details:

Bernard A. Conway, PhD, Professor and Head of Department,  
Bioengineering Unit, University of Strathclyde  
Wolfson Centre, 106 Rottenrow, Glasgow G4 0NW, Scotland, UK.  
Tel: +44 141 548 3316, Fax: +44 141 552 6098,  
E-Mail: [b.a.conway@strath.ac.uk](mailto:b.a.conway@strath.ac.uk)

Campbell Reid, PhD, Research Fellow  
Bioengineering Unit, University of Strathclyde  
Wolfson Centre, 106 Rottenrow, Glasgow G4 0NW, Scotland, UK.  
Tel: +44 (0) 7757 904107, Fax: +44 141 552 6098,  
E-Mail: [campbell.s.reid@gmail.com](mailto:campbell.s.reid@gmail.com)

# Appendix D

## Participant Consent Form

**University of Strathclyde**  
**Bioengineering Unit**  
**Neurophysiology Lab**



**University of**  
**Strathclyde**  
**Glasgow**

**Title of the study**

Interactions between the pre-frontal cortex and temporal lobe in visual working memory: An EEG study

- I confirm that I have read and understood the information sheet for the above project and the researcher has answered any queries to my satisfaction.
- I understand that my participation is voluntary and that I am free to withdraw from the project at any time, without having to give a reason and without any consequences.
- I understand that I can withdraw my data from the study at any time.
- I understand that any information recorded in the investigation will remain confidential and no information that identifies me will be made publicly available.
- I consent to being a participant in the project

**Participant Signature:**

I, _____ (Print Name)	Hereby agree to take part in the above project
_____ (Signature)	_____ (Date)

**Witness Signature:**

I, _____ (Print Name)	
_____ (Signature)	_____ (Date)